VOL. 3 No. 3
JUNE 1961

UNIVERSITY OF HAWAII
LIBRARY
SEP 21 '61

JURNAL OF THE

LESS-COMMON METALS

AN INTERNATIONAL JOURNAL ON
THEIR CHEMISTRY AND METALLURGY

ORS:
CUTHBERTSON (Nottingham)
IRBROTHER (Manchester)

ORIAL ADVISORY BOARD:
NARD (Paris)
RICE COOK (Birmingham)
CROLY (Brussels)
DJINGHEUZIAN (Ottawa)
FLETCHER (Harwell)
GONSER (Columbus, Ohio)
ANSEN (Frankfurt a.M.)
NDELLI (Genoa)
LEMM (Münster)
KROLL (Corvallis, Ore.)
URRAY (Harwell)
WOTNY (Vienna)
PIDGEON (Toronto)
POWELL (Wembley)
RALSTON (Hyattsville, Md.)
VAN ARKEL (Leyden)
WORNER (Melbourne)
YNTEMA (Menlo Park, Calif.)

ELSEVIER

GENERAL INFORMATION

Types of contributions

(a) Original research work not previously published in other periodicals.
(b) Reviews on recent developments in various fields.
(c) Short communications.
(d) Bibliographical notes and book reviews.

Languages

Papers will be published in English, French or German.

Submission of papers

Papers should be sent to one of the following Editors:

Professor J. W. CUTHBERTSON (*Metallurgy*), Department of Metallurgy, The University, University Park, Nottingham, England.
Professor F. FAIRBROTHER (*Chemistry*), The University of Manchester, Department of Chemistry, Manchester 13, England.

Authors should preferably submit two copies in double-spaced typing on pages of uniform size. Legends for figures should be typed on a separate page. The figures should be in a form suitable for reproduction, drawn in Indian ink on drawing paper or tracing paper, with lettering etc. in thin pencil. The sheets of drawing or tracing paper should preferably be of the same dimensions as those on which the article is typed. Photographs should be submitted as clear black and white prints on glossy paper.
All references should be given at the end of the paper. They should be numbered and the numbers should appear in the text at the appropriate places.
A summary of 50 to 200 words should be included. Authors of papers in French or German are encouraged to supply also a translation of the summary in English.

Reprints

Twenty-five reprints will be supplied free of charge. Additional reprints can be ordered at quoted prices. They must be ordered on order forms which are sent together with the proofs.

Publication

The *Journal of the Less-Common Metals* will have six issues to the volume, approx. 500 pages per volume.
Subscription price: £ 5.7.6 or Dfl. 57.— per volume (post free).
Additional cost for copies by air mail available on request.
For advertising rates apply to the publishers.

Subscriptions

Subscriptions should be sent to:

ELSEVIER PUBLISHING COMPANY, P.O. Box 211, Spuistraat 110-112, Amsterdam-C., The Netherlands.

AMMONOLYSIS OF MOLYBDENUM(V) CHLORIDE

D. A. EDWARDS AND G. W. A. FOWLES

Dept. of Chemistry, The University of Southampton (Great Britain)

(Received December 12th, 1960)

SUMMARY

The ammonolysis of molybdenum(V) chloride has been studied at —36°C and at room temperature, when two and four molybdenum–chlorine bonds are ammonolysed respectively. The solubility of the products in concentrated solutions of ammonium salts in liquid ammonia is attributed to the formation of complex anionic species. The thermal decomposition of the reaction products has been studied up to 800°C.

INTRODUCTION

The reaction of ammonia with some of the higher halides of Group VIA has recently been studied in detail; the ammonolysis of tungsten(VI) chloride has already been reported[1]. Little work has, however, been done on the analogous reaction of molybdenum(V) chloride, apart from that of UHRLAUB[2], who obtained mixtures containing molybdenum, nitrogen and hydrogen only by heating molybdenum(V) chloride in a stream of ammonia gas, and of BERGSTRÖM[3], who found that molybdenum(V) chloride absorbed nearly eight moles of ammonia when the reaction was so controlled to prevent the loss of ammonium chloride by volatilisation. He suggested that the products were ammonium chloride and a molybdenum derivative and gave the equations:

$$MoCl_5 + 8\ NH_3 = Mo(NH)_2(NH_2) + 5\ NH_4Cl \quad (1)$$

$$MoCl_5 + 8\ NH_3 = Mo(NH_2)_4Cl + 4\ NH_4Cl \quad (2)$$

In view of the sparsity of information available we have studied this reaction again by removing soluble compounds by filtration and washing of products formed at both —33.5°C and at room temperature (Carius tube), and by tensimetric studies at —36°C.

EXPERIMENTAL

Materials

Molybdenum(V) chloride (Climax Molybdenum Co.) was resublimed before use. Found: Mo, 35.1; Cl, 64.6%. Calculated for $MoCl_5$: Mo, 35.1; Cl, 64.9%. Liquid ammonia (Imperial Chemical Industries) was dried with sodium before distillation *in vacuo* into the apparatus.

Analyses

Nitrogen and chlorine were determined as previously[4]. Molybdenum was deter-

mined by oxidation to the sexavalent state, followed by reduction to Mo(V) with mercury[5] and titration with standard cerium(IV) sulphate.

Magnetic moment measurements

These were made on a Gouy-type balance at room temperature, normally at a field strength of 8000 gauss.

Reactions and tensimetric studies

These were carried out in the usual type of all-glass closed vacuum system[4], as all reactants and products were easily hydrolysed.

Washing procedure

Ammonia was condensed onto the chloride and allowed to liquefy. The subsequent reaction gave a deep wine-red solution and an orange solid. The solution was filtered off through a filter pad and the ammonia then condensed back on the solid product; the solution was then filtered again. The second filtrate was paler in colour than the original solution and subsequent filtrates were paler still, until after five washes they were colourless. The insoluble product, which contained about 40% of the original molybdenum, was normally pumped between washings to break up the lumps and make subsequent washings more efficient (Table I). If the insoluble product was

TABLE I

INSOLUBLE PRODUCT

Run No.	Analyses (%)			Mol. Ratio	μ	Comments
	Mo	Cl	N	Mo : Cl : N	(B.M.)	
1	39.1	40.4	17.3	1.00 : 2.79 : 3.02	1.84	Pumped at room temp. between washes and at 40°C for 16 h after final wash
2	38.7	40.6	17.1	1.00 : 2.84 : 3.03	—	As run 1
3	37.7	44.1	16.1	1.00 : 3.16 : 2.93	—	As run 1
4	37.7	42.8	16.7	1.00 : 3.08 : 3.03	—	As run 1
5	43.3	36.0	15.6	1.00 : 2.25 : 2.46	2.06	Pumped at 100°C after washes 2 and 4, and finally at 40°C for 16 h
6	45.7	37.9	14.3	1.00 : 2.24 : 2.15	—	As run 5

TABLE II

SOLUBLE PRODUCT

Run No.	Analyses (%)			Mol. Ratio	Soluble Mo	N : Cl*
	Mo	Cl	N	Mo : Cl : N	Total Mo	
1	23.0	51.7	20.4	1.00 : 6.09 : 6.09	0.61	1.00 : 1.00
2	23.3	52.4	19.5	1.00 : 6.08 : 5.71	0.50	1.00 : 1.13
3	20.4	52.5	21.8	1.00 : 6.96 : 7.30	—	1.00 : 0.92
4**	24.5	50.7	20.1	1.00 : 5.60 : 5.62	0.72	1.00 : 0.99
5**	23.7	50.1	19.6	1.00 : 5.76 : 5.66	0.81	1.00 : 1.04

* Mo assumed to be present as $MoCl_3(NH_2)_2 \cdot NH_3$.
** Pumped at 100°C.

heated to 100°C between washings it became almost black and a larger proportion of soluble product resulted (*cf.* runs 4 and 5, Table II).

The ammonobasic molybdenum(V) chloride formed was insoluble in all solvents tried (*e.g.* benzene, chlorobenzene, cyclohexane and ethylene glycol dimethyl ether), so that molecular weight and spectroscopic studies could not be made.

When excess of ammonia was evaporated from the filtrate a heterogeneous solid remained, which after pumping for several hours was analysed (see Table II).

Effect of added salts on the solubility of the ammonobasic molybdenum(V) chloride in liquid ammonia. Samples of various ammonia-soluble salts were added to the orange ammonobasic molybdenum(V) chloride and liquid ammonia condensed onto the mixture. The orange solid largely dissolved in liquid ammonia when ammonium chloride, ammonium bromide or ammonium nitrate was added, but was less soluble in a potassium iodide–liquid ammonia solution and almost insoluble in the presence of sodium nitrate.

Thermal decomposition of the ammonobasic molybdenum(V) chloride. When heated *in vacuo* the product liberated only 0.26 mol of free ammonia between 20° and 200°C, but from 130°C upwards ammonium chloride was found on the cold parts of the reaction vessel, and free hydrogen chloride was liberated at 300°C. The product remaining was black and had the composition: Mo, 59.0; Cl, 21.5; N, 18.0%. $MoClN_2H_2$ requires: Mo, 59.4; Cl, 22.0; N, 17.4%.

When the product was heated to 800°C in a quartz tube a mirror of molybdenum metal was formed, leaving a black residue which contained no chlorine and which was soluble only with difficulty in concentrated nitric acid. Analysis gave: Mo, 92.1; Cl, 0.0; N (by difference), 7.9% corresponding to Mo : N = 2.00 : 1.17.

Reaction in a sealed Carius tube followed by washing with liquid ammonia

In an attempt to force further replacement of chlorine atoms, molybdenum(V) chloride and ammonia were sealed in a Carius tube and allowed to react for two weeks at room temperature. The tube was then cooled to below —33°C, the tip hot-spotted, and the contents quickly poured through a suitable adaptor onto the filter pad. After excess of ammonia had been distilled away, the product was pumped and then washed six times with liquid ammonia with the usual intermediate pumping at room temperature. The analyses of the products are shown in Tables III and IV. The insoluble product was a dark grey–brown solid and contained about 85% of the original molybdenum. After excess of NH_3 had been pumped away from the soluble portion, a light grey solid remained.

TABLE III

INSOLUBLE PRODUCT (CARIUS TUBE)

Run No.	Analysis (%)			Mol. ratio	μ
	Mo	Cl	N	Mo : Cl : N	(B.M.)
1	49.0	21.6	21.7	1.00 : 1.19 : 3.03	—
2	52.8	23.2	21.2	1.00 : 1.19 : 2.75	—
3	50.0	21.8	22.6	1.00 : 1.18 : 3.09	0.74
4	50.8	23.1	21.0	1.00 : 1.23 : 2.83	0.84*

* Constant over a range of field strengths.

TABLE IV

SOLUBLE PRODUCT (CARIUS TUBE)

Run No.	Analysis (%)			Mol. Ratio	Soluble Mo
	Mo	Cl	N	Mo : Cl : N	Total Mo
1	8.51	61.1	23.6	1.00 : 22.0 : 21.5	0.17
2	5.37	64.0	24.7	1.00 : 32.2 : 31.5	0.13
3	8.05	63.5	23.5	1.00 : 21.3 : 20.4	0.10

Tensimetric studies of the molybdenum(V) chloride–ammonia system

A known excess of ammonia was condensed onto a known weight of molybdenum-(V) chloride (using liquid oxygen), the reaction vessel was then surrounded with an ethylene dichloride slush bath (—36°C) and the final equilibrium pressure of ammonia measured. Small amounts of ammonia were then successively removed and measured, and the new pressures measured after equilibrium had again been reached; these pressures were only fully attained after at least 24 h. The results of these experiments are shown graphically in Fig. 1.

When the product was heated in stages (*cf.* Fig. 2) a slow general loss of almost two moles of ammonia was observed over the range —36° to 180°C, and by 250°C, a total of 3.1 moles of ammonium chloride had sublimed away leaving a black residue.

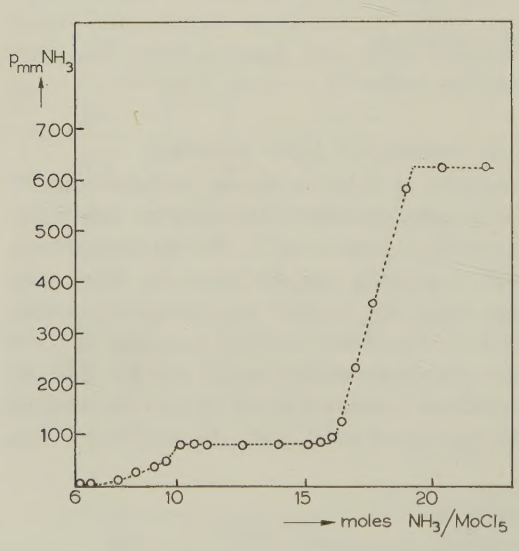

Fig. 1. $MoCl_5$–NH_3 system (tensimetric results).

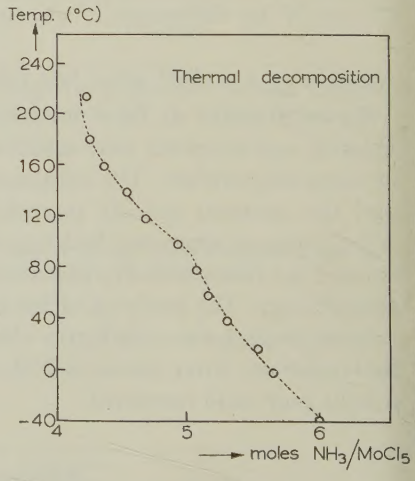

Fig. 2. Thermal decomposition of tensimetric mixture.

DISCUSSION

When molybdenum(V) chloride reacts with liquid ammonia two molybdenum–chlorine bonds are ammonolysed under normal conditions, and magnetic susceptibility measurements indicate that molybdenum remains in the quinquevalent state. Some

40% of the product is insoluble, and this has a composition close to $MoCl_3(NH_2)_2 \cdot NH_3$; it is insoluble in the usual organic solvents but dissolves in liquid ammonia upon the addition of ammonium salts or of potassium iodide. Analysis of the soluble portion of the reaction product suggests that it is a mixture of this same ammonobasic molybdenum(V) chloride with ammonium chloride.

The simplest interpretation of these observations is that the ammonolysis gives rise to a polymeric molybdenum product. This polymerisation could arise through elimination of hydrogen chloride between neighbouring molecules, or by condensation through chlorine or nitrogen bridges, or both,

e.g.

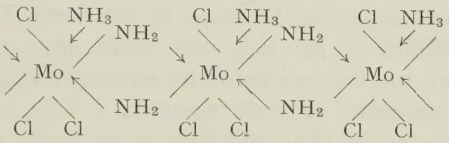

The analysis can give only the average composition of the product, and most likely the composition varies somewhat throughout the molecule, the degree of ammonolysis being above average at the extremities of the polymer. Ammonium chloride, which is produced in the reaction, may break down the polymer with the formation of soluble anionic species such as $[MoCl_4(NH_2)_2]^-$, analogous to those considered to be present in the titanium(IV) iodide–ammonia system[6]. Under our experimental conditions most of the ammonium chloride is removed in the first wash, and break-down of the polymer is incomplete, but the undissolved product can be taken into solution by the addition of ammonium salts or of potassium iodide. Complex anion formation also explains BERGSTRÖM's observation[3] that the product is entirely soluble in concentrated solutions, with the precipitation of an ammonobasic molybdenum(V) chloride on dilution, since complex formation will occur most readily in high concentrations of chloride ion.

Under the rather more drastic conditions of pumping at 100°C between washes, further reaction evidently occurs; over 70% of the molybdenum appears in the soluble portion, and the remaining insoluble material has a composition ratio in the region of $MoCl_{2.2}N_{2.1}$. Since magnetic susceptibility measurements show the insoluble product still to contain quinquevalent molybdenum, it may be that ammonolysis has gone one stage further, and the heating has decomposed the product to give an imide:

$$MoCl_3(NH_2)_2 \cdot NH_3 \xrightarrow{NH_3} MoCl_2(NH_2)_3 + NH_4Cl$$

$$\longrightarrow MoCl_2(:NH)(NH_2)$$

When this further ammonolysis takes place, the ammonium chloride formed will react with unchanged ammonobasic molybdenum(V) chloride with the formation of the soluble complex, thus increasing the percentage of the soluble molybdenum component.

The imide is less likely to be soluble, because the imide group makes complex formation more difficult.

When the reaction is carried out at room temperature in a sealed Carius tube, and the products subsequently washed free from ammonium chloride at low temperatures, four molybdenum–chlorine bonds are evidently ammonolysed since the insoluble product has an analysis close to $MoCl(:NH)(NH_2)_2$. In comparison with the ordinary washing runs at low temperature, very much less molybdenum is to be found in the soluble portion (only some 15%), and this we attribute to greater polymerisation and to the presence of the imide group.

We have assumed that molybdenum remains in the quinquevalent state throughout the reactions, and the magnetic susceptibility measurements support this assumption for the products formed in the normal washing runs. If any reduction were to take place, however, it should especially be found in the Carius tube reactions, but the susceptibility measurements do not help very much since values of 0.7–0.9 Bohr magnetons are obtained, whereas any reduction to quadrivalent molybdenum should give compounds with magnetic moments around 2.7 Bohr magnetons (*e.g.* 2.83 for $MoCl_4 \cdot 3\ C_5H_5N$)[7]. It is probable that the products are highly polymeric and 'magnetically concentrated'.

When the ammonobasic molybdenum(V) chloride $MoCl_3(NH_2)_2 \cdot NH_3$ is heated *in vacuo*, only a little ammonia is lost up to 130°C, but above this temperature a sublimate of ammonium chloride begins to form. Since there is no ammonium chloride in the product, it must be formed in the decomposition, presumably through the simultaneous liberation of ammonia and hydrogen chloride.

$$\left.\begin{aligned} MoCl_3(NH_2)_2 \cdot NH_3 &\rightarrow MoCl_3(NH_2)_2 + NH_3 \\ MoCl_3(NH_2)_2 &\rightarrow MoCl_2(:NH)(NH_2) + HCl \end{aligned}\right\} \rightarrow NH_4Cl$$

On further heating, hydrogen chloride is liberated at 300°C leaving $MoCl(:NH)_2$, which breaks down further to give the nitride Mo_2N at 800°C.

In the tensimetric studies, the amount of ammonium chloride present can be determined since it forms a triammoniate with a characteristic dissociation pressure. This method only detects 'free' ammonium chloride, however, and any that has taken part in complex formation will not be detected unless the complex is unstable under the experimental conditions and reverts to a mixture of ammonium chloride and the ammonobasic molybdenum(V) chloride. The experiments at —36°C detect an average of two moles of ammonium chloride from the ammonolysis of each mole of molybdenum(V) chloride. Since ammonolysis cannot be greater in the tensimetric experiments than in the washing runs (where removal of ammonium chloride favours increased ammonolysis), then it is apparent that all the ammonium chloride formed initially is 'free' and forms a triammoniate. Hence although a complex may form in the presence of liquid ammonia, it must be unstable in the solid; an analogous situation is found in the titanium(IV) halide–ammonia systems.[6]

When the ammonolysis mixture is heated *in vacuo* (*cf.* Fig. 2), it appears to break down in an analogous manner to that of the ammonobasic molybdenum(V) chloride isolated in the washing runs.

ACKNOWLEDGEMENTS

We greatly appreciate the provision of a maintenance grant (to D.A.E.) by the U.S. Department of Army, through its European Office, and by Laporte Titanium Ltd. and the gift of molybdenum(V) chloride from the Climax Molybdenum Company.

REFERENCES

1 G. W. A. Fowles and B. P. Osborne, *J. Chem. Soc.*, (1959) 2275.
2 E. Uhrlaub, *Poggendorfs Ann.*, 101 (1857) 605.
3 F. W. Bergström, *J. Am. Chem. Soc.*, 47 (1925) 2317.
4 G. W. A. Fowles and F. H. Pollard, *J. Chem. Soc.*, (1953) 2588.
5 N. H. Furman and W. M. Murray Jr., *J. Am. Chem. Soc.*, 58 (1936) 1689.
6 G. W. A. Fowles and D. Nicholls, *J. Chem. Soc.*, (1959) 990.
7 D. A. Edwards and G. W. A. Fowles, unpublished observations.

BROMIDE ALKOXIDES OF ZIRCONIUM

R. N. KAPOOR AND R. C. MEHROTRA

Department of Chemistry, University of Gorakhpur, Gorakhpur (India)

(Received January 11th, 1961)

SUMMARY

The reaction of zirconium isopropoxide and acetyl bromide has been studied and the compounds $ZrBr(OPr^i)_3 \cdot Pr^iOH$, $ZrBr_2(OPr^i)_2 \cdot Pr^iOH$ and $ZrBr_4 \cdot 2Pr^iOAc$ have been isolated. The first two are stable to heat, but the third decomposes on heating even under reduced pressure giving lower bromides. It has been shown for comparison that zirconium tetrachloride reacts with butyl acetate in a similar manner. $ZrBr_4 \cdot 2Pr^iOAc$ has been isolated by carrying out the reaction between $Zr(OPr^i)_4$ and AcBr under milder conditions and was found to react with isopropanol to give an equimolecular mixture of $ZrBr_2(OPr^i)_2$ and $ZrBr_3(OPr^i)$. The great ease with which these compounds exchange their radicals has been demonstrated by the reaction between dibromide and tetraisopropoxide when the monobromide compound crystallises out in quantitative yield. The mono and dibromide isopropoxide derivatives react with butanols or butyl acetates to give products in which the isopropoxy groups have been replaced. A number of new normal and secondary butoxide derivatives have been isolated, but side reactions occur in the case of tertiary butoxides.

Much work has been carried out on the chloride alkoxides of titanium[1,2] and zirconium[3,4,5] and on bromide alkoxides of titanium[6,7,8]. The only reference in the literature however concerning the zirconium bromide alkoxides is to the formation of zirconium monoisopropoxide tribromide[7] by the action of hydrogen bromide on zirconium isopropoxide in anhydrous benzene.

It was therefore considered of interest to find a more convenient and easily controllable method for the preparation of bromide alkoxides of zirconium and to study their properties. The reaction between zirconium isopropoxide and acetyl bromide was therefore investigated in detail. This exothermic reaction was found to be fast and straightforward leading to the formation of the dibromide diisopropoxide of zirconium. The products indicated by the following equations could be isolated in quantitative yield by using the required molecular ratios in boiling benzene:

$$Zr(OPr^i)_4 \cdot Pr^iOH + CH_3COBr \rightarrow ZrBr(OPr^i)_3 \cdot Pr^iOH + Pr^iOAc$$

$$Zr(OPr^i)_4 \cdot Pr^iOH + 2\ CH_3COBr \rightarrow ZrBr_2(OPr^i)_2 \cdot Pr^iOH + 2Pr^iOAc$$

As in the case of the zirconium isopropoxide–acetyl chloride reaction, the stoichiometric nature of the above rapid reactions indicated that radical interchange might occur between bromide alkoxides also. This has been proved by refluxing together zirconium dibromide diisopropoxide and zirconium isopropoxide in isopropanol in the

molar ratio 1 : 1 when the monobromide compound crystallised out on cooling the solution.

$$ZrBr_2(OPr^i)_2{\cdot}Pr^iOH + Zr(OPr^i)_4{\cdot}Pr^iOH \rightarrow 2\ ZrBr(OPr^i)_3{\cdot}Pr^iOH$$

It is interesting to observe that the above mono-, and dibromide derivatives of zirconium are stable to refluxing in benzene, whereas the corresponding acetate derivatives[9] obtained by the reaction of zirconium isopropoxide with acetic anhydride are unstable and decompose as follows:

$$Zr(OPr^i)_3(OAc) \rightarrow ZrO(OPr^i)_2 + Pr^iOAc$$

The reaction of zirconium isopropoxide with more than 2 moles of acetyl bromide appeared to be comparatively slower and the product obtained by refluxing together zirconium isopropoxide and acetyl bromide (molar ratio 1 : 4) in benzene was found to have a bromine: zirconium ratio of 3.14 : 1. On recrystallisation from benzene, the above product yields a crystalline material with a Br : Zr ratio equal to 3.02. Even when a larger excess of acetyl bromide was taken, the product had almost the same analysis as obtained initially in the 1 : 4 reaction. With a view to completing the reaction, the above bromide product was dissolved in benzene and was refluxed with more acetyl bromide. However, the bromide : zirconium ratio remained almost unchanged at 3.2 : 1. When this product was heated to 100°C under reduced pressure, the bromine : zirconium ratio was further reduced to 2.1 : 1. These results indicated that in contrast to dibromide derivatives, higher bromide products are unstable and react with the added isopropyl acetate to give decomposition products. The correctness of this supposition has been demonstrated by the reaction between zirconium tetrabromide (and also tetrachloride for comparison)and butyl acetate, when an exothermic reaction occurred and acetyl bromide (or chloride) could be distilled out leaving a product with a halogen: zirconium ratio about 2.1–2.4. These reactions may be compared with the stable nature of $TiBr_4{\cdot}CH_3COOPr^i$ which can be sublimed unchanged under reduced pressure.

The tetrabromide derivative, $ZrBr_4{\cdot}2Pr^iOAc$ could, however, be isolated by carrying out the reaction between zirconium isopropoxide and excess acetyl bromide in the cold:

$$Zr(OPr^i)_4{\cdot}Pr^iOH + 4\ AcBr \rightarrow ZrBr_4{\cdot}2Pr^iOAc + 2\ Pr^iOAc + Pr^iOH$$

This product also when heated even under reduced pressure undergoes decomposition as indicated above. The tetrabromide product was further found to react with isopropanol according to the reaction:

$$2\ ZrBr_4{\cdot}2Pr^iOAc + 3\ Pr^iOH \rightarrow ZrBr_3(OPr^i) + ZrBr_2(OPr^i)_2 + 4\ Pr^iOAc + 3\ HBr$$

The above reaction is of interest in view of the analogous reaction between zirconium tetrachloride and ethyl alcohol[3] and also of the reverse reaction of zirconium isopropoxide with hydrogen bromide[7].

Further, the reactions of mono- and dibromide derivatives, prepared as above with higher alcohols[8,10] or esters[8,11], indicated a ready alcohol or ester interchangeability,

thus providing methods for preparing the corresponding derivatives containing higher alkoxy groups:

$$ZrBr_x(OPr^i)_{4-x} + (4-x)\ ROH \rightarrow ZrBr_x(OR)_{4-x} + (4-x)\ Pr^iOH$$

$$ZrBr_x(OPr^i)_{4-x} + (4-x)\ ROAc \rightarrow ZrBr_x(OR)_4 + (4-x)\ Pr^iOAc$$

(where $x = 1$ or 2)

As in the case of the corresponding titanium compounds, the interchange reactions are straightforward in the case of primary and secondary alcohols or their acetates, but side reactions occur with tertiary butanol or tertiary butyl acetate[4,8].

EXPERIMENTAL

Apparatus

All glass apparatus was used with rigid exclusion of moisture[8].

Materials

Zirconium isopropoxide [$Zr(OPr^i)_4 \cdot Pr^iOH$] was prepared by the action of ammonia on a mixture of zirconium tetrachloride and isopropanol in benzene[11] and purified by crystallising from isopropanol five times. Found: Zr, 23.60; Pr^iO, 76.9%. Calculated for $Zr(OPr^i)_4 \cdot Pr^iOH$: Zr, 23.53; Pr^iO, 76.21%.

All other materials were treated as described in an earlier communication[8].

Analytical methods

Zirconium was estimated as its dioxide by ignition of the hydroxide obtained by precipitation with dilute ammonia.

Preparation of monobromide triisopropoxide of zirconium, $ZrBr(OPr^i)_3 \cdot Pr^iOH$. To zirconium isopropoxide [$Zr(OPr^i)_4 \cdot Pr^iOH$, 5.3 g] in benzene (16 g) was added acetyl bromide (1.68 g) (molar ratio of isopropoxide:acetyl bromide = 1 : 1). The mixture became quite hot and the clear solution was refluxed for about half an hour. The solvent was then removed by distillation and the yellowish mass obtained was dried under reduced pressure (1 mm) at a temperature not higher than 40°C for nearly 3 h. A yellowish white powder was obtained. Found: Zr, 22.72; Br, 17.99%; Br:Zr, 0.904. Calculated for $ZrBr(OPr^i)_3 \cdot Pr^iOH$: Zr, 22.34; Br, 19.57%.

About 60 ml of isopropyl alcohol was distilled onto the above powder and the mixture was refluxed for 20 min. From the clear solution, colourless crystals were deposited on cooling. The crystals were dried under reduced pressure (2 mm) at room temperature for nearly 6 h and were analysed. Found: Zr, 22.40; Br, 19.72%; Br:Zr, 1.0. Calculated for $ZrBr(OPr^i)_3 \cdot Pr^iOH$: Zr, 22.34; Br, 19.57%.

Preparation of the dibromide diisopropoxide of zirconium, $ZrBr_2(OPr^i)_2 \cdot Pr^iOH$. Acetyl bromide (3.41 g, 2 moles) was distilled onto a mixture of crystalline isopropoxide [$Zr(OPr^i)_4 \cdot Pr^iOH$, 5.46 g, 1 mole] in benzene (35 g). A considerable amount of heat was evolved in the reaction, but no liberation of hydrogen bromide could be detected. After allowing the mixture to stand overnight, it was refluxed at 100–110°C for 1 h. As nothing could be crystallised out on cooling, the volatile fractions were removed under reduced pressure (2 mm) at a temperature not higher than 40°C. 6.2 g of a

crystalline yellowish white solid was obtained. Found: Zr, 21.78; Br, 37.42%; Br:Zr, 1.97. Calculated for $ZrBr_2(OPr^i)_2 \cdot Pr^iOH$: Zr, 21.28; Br, 37.3%.

Reaction between acetyl bromide (4 moles) and zirconium isopropoxide (1 mole). To a mixture of zirconium isopropoxide [$Zr(OPr^i)_4 \cdot Pr^iOH$, 2.74 g] in benzene (20 g) was added acetyl bromide (3.6 g) drop by drop through the column, when the temperature rose to nearly 70°C. The yellowish coloured solution was refluxed for 3 h at 100°C. The volatile fractions were removed under reduced pressure at 40°C for 3 h. A yellowish syrupy liquid (4.1 g) was obtained which was analysed. Found: Zr, 16.98; Br, 46.86%; Br : Zr, 3.14.

To the above liquid was added benzene (5 ml) when a clear solution was obtained. A yellowish compound crystallised out after 4 days. It was decanted and dried under reduced pressure (2 mm) at 40°C for nearly 2 h. The yellowish product was analysed. Found : Zr, 16.7; Br, 44.36%; Br:Zr, 3.02.

Reaction between zirconium isopropoxide and excess acetyl bromide. Acetyl bromide (4.7 g, about 6 moles) was distilled onto zirconium isopropoxide (2.50 g, 1 mole) in benzene (14 g). The mixture became very hot as the acetyl bromide was distilled in and assumed a yellow colour. It was refluxed for 6 h at the bath temperature of 110°C. Excess acetyl bromide and some benzene were removed by distillation under reduced pressure (2 mm) at room temperature. A brownish viscous liquid was obtained, which was again dried at 40–50°C under reduced pressure (2 mm) for nearly 2 h. Found: Zr, 17.21; Br, 50.21%; Br:Zr, 3.2.

To the brown pasty mass obtained in this experiment was added acetyl bromide and the clear solution was refluxed for 1 h at 110°C. The volatile fractions were removed under reduced pressure (2 mm) at a bath temperature of nearly 40°C for nearly 2 h, when a pasty brown mass was obtained. Found : Zr, 17.98; Br, 50.23% Br:Zr, 3.19.

The above two experiments show that the reaction between zirconium isopropoxide and excess acetyl bromide in refluxing benzene does not give a tetrabromide derivative. This might be due to the reaction becoming slow towards the end, but the fact that a repeated refluxing with more acetyl bromide does not increase the Br:Zr ratio makes the above suggestion doubtful. It appears more probable that some side reactions take place due to which, the tetrabromide derivative, formed initially, gets decomposed. The correctness of the latter suggestion is proved by heating the above compound at 100°C for nearly 2 h, when a further loss in weight is noticed. The brown solid, thus obtained was analysed. Found : Zr, 23.84; Br, 44.21%; Br:Zr, 2.1.

The correctness of the suggestions is further confirmed by the isolation (next experiment) of a probable tetrabromide derivative by carrying out the reaction at a lower temperature.

Reaction between zirconium isopropoxide and acetyl bromide in cold. Acetyl bromide (8 g) was distilled onto the zirconium tetraisopropoxide [$Zr(OPr^i)_4$, 3.02 g]. The reaction mixture became hot and was allowed to cool down to room temperature. The excess acetyl bromide was then removed under reduced pressure (1 mm) at room temperature for nearly 3 h, when a yellowish solid was obtained. The yellowish solid was again dried under reduced pressure at 40°C for nearly 1 h. Found: Zr, 15.42; Br, 50.41%; Br:Zr, 3.74. $ZrBr_4 \cdot 2CH_3\text{-}COOPr^i$ requires Zr, 14.83%; Br, 51.97%.

Reaction between zirconium tetrachloride and butyl acetate. Zirconium tetrachloride (1.18 g) was added to dry *n*-butyl acetate (28 g). Heat was evolved and a clear solu-

tion was obtained. The solution was left overnight and then refluxed for 2 h and then the volatile fractions were distilled out, first at ordinary pressure (boiling range 90–110°C) and finally the product was dried for 3 h at 70–80°C under 2 mm pressure giving 2.35 g of a pasty mass. Found: Zr, 35.6; Cl. 33.9%; Cl:Zr = 2.45.

Reaction of $ZrBr_4 \cdot 2Pr^iOAc$ with isopropanol (excess). $ZrBr_4 \cdot 2Pr^iOAc$ (1.7 g) was added to isopropanol (8.2 g). The compound dissolved with evolution of a little heat. As nothing crystallised out even at 0°C, the volatile solvent was removed at 50–55°C under reduced pressure (1–2 mm) yielding a semi-solid yellow product. Found: Zr, 23.12; Br, 47.84%. Br:Zr, 2.59.

Reaction between dibromide diisopropoxide of zirconium, $ZrBr_2(OPr^i)_2 \cdot Pr^iOH$ and zirconium isopropoxide $Zr(OPr^i)_4 \cdot Pr^iOH$ in equimolecular proportions. A mixture of $ZrBr_2(OPr^i)_2 \cdot Pr^iOH$ (1.85 g, 1 mole) and $Zr(OPr^i)_4 \cdot Pr^iOH$ (1.02 g, 1 mole) in isopropyl alcohol (10 g) was refluxed for 20 min, when a clear solution was obtained. On cooling colourless crystals were obtained. The crystals were dried under reduced pressure. Found: Zr, 22.54; Br, 19.8%; Br:Zr, 1.0. Calculated for $ZrBr(OPr^i)_3 \cdot Pr^iOH$: Zr, 22.34; Br, 19.57%.

Alcohol and ester interchange experiments. For alcohol and ester interchange experiments (summarised in Tables I and II), the general procedure was the same as described earlier[8] for corresponding titanium compounds.

TABLE I

REACTIONS OF $ZrBr(OPr^i)_3 \cdot Pr^iOH$ WITH BUTANOL OR BUTYL ACETATE

$ZrBr(OPr^i)_3 \cdot Pr^iOH$ (g)	Butyl alcohol (n-, sec.- or tert.-) (g)	Benzene (g)	Butyl acetate (n-, sec.- or tert.-) (g)	Analysis* of products	
				Zr (%)	Br (%)
1.6	3.0(*n*)	30	—	23.3	20.4
1.7	1.8(*sec.*)	34	—	23.4	20.4
1.4	2.0(*tert.*)	36	—	25.2	18.7
1.5	—		15(*n*)	23.4	20.4
1.6	—		13(*sec.*)	23.3	20.4
1.5	—		12(*tert.*)	28.0	17.4

* $ZrBr(OBu)_3$ requires Zr; 23.36; Br, 20.46%.

TABLE II

REACTIONS OF $ZrBr_2(OPr^i)_2 \cdot Pr^iOH$ WITH BUTANOL OR BUTYL ACETATE

$ZrBr_2(OPr^i)_2 \cdot Pr^iOH$ (g)	Butyl alcohol (n-, sec.- or tert.-) (g)	Benzene (g)	Butyl acetate (n-, sec.- or tert.-) (g)	Analysis* of products	
				Zr %	Br %
1.8	3.2(*n*)	25	—	23.0	40.3
1.5	2.0(*sec.*)	27	—	23.1	40.1
1.9	1.9(*tert.*)	24	—	25.2	38.0
1.4	—	—	12(*n*)	23.1	40.1
1.6	—	—	16(*sec.*)	23.2	40.0
1.9	—	—	12(*tert.*)	30.1	36.3

* $ZrBr_2(OBu)_2$ requires Zr, 22.96; Br, 40.23%.

REFERENCES

1 D. C. Bradley, D. C. Hancock and W. Wardlaw, *J. Chem. Soc.*, (1952) 2773.
2 A. N. Nesmeyanov, R. K. Freidlina and O. V. Nogina, *Izvest. Akad. Nauk S.S.S.R., Otdel. Khim. Nauk*, (1951) 518.
3 D. C. Bradley, F. M. Abd-el Halim and W. Wardlaw, *J. Chem. Soc.*, (1950) 3450.
4 D. C. Bradley, F. M. Abd-el Halim, R. C. Mehrotra and W. Wardlaw, *J. Chem. Soc.*, (1952) 4609, 4960.
5 R. C. Mehrotra, *J. Indian Chem. Soc.*, 30 (1953) 731.
6 A. N. Nesmeyanov, E. M. Brainina and R. K. Freidlina, *Izvest. Akad. Nauk S.S.S.R., Otdel. Khim. Nauk*, (1955) 838.
7 R. C. Mehrotra, *J. Indian Chem. Soc.*, 32 (1955) 759.
8 I. D. Verma and R. C. Mehrotra, *J. Less-Common Metals*, 1 (1959) 263.
9 R. N. Kapoor and R. C. Mehrotra, *J. Chem. Soc.*, (1959) 422.
10 D. C. Bradley, R. C. Mehrotra and W. Wardlaw, *J. Chem. Soc.*, (1952) 2027, 4204, 5020.
11 R. C. Mehrotra, *J. Am. Chem. Soc.*, 76 (1954) 2266.

SOLID SOLUBILITY OF In_2Se_3 IN SOME COMPOUNDS OF ZINC BLENDE STRUCTURE

J. C. WOOLLEY AND P. N. KEATING*

Department of Physics, University of Nottingham (Great Britain)

(Received January 20th, 1961)

SUMMARY

The ranges of solid solubility of In_2Se_3 in the zinc blende type compounds InAs, InSb, In_2Te_3 and Ga_2Se_3 have been studied by X-ray methods. The solubility ranges are found to be appreciable in the cases of InAs, In_2Te_3 and Ga_2Se_3 and only in the case of InSb is the range limited to a few mol. percent. It is found that in most cases prolonged annealing is required before equilibrium is attained, this being particularly the case for the $A^{III}B^{V}$ compounds, InAs and InSb. Ordering effects have been observed in the InAs–In_2Se_3 system, where an undetermined ordered structure occurs, and in the In_2Te_3–In_2Se_3 system where ordering of lattice vacancies analogous to that in In_2Te_3 itself is found. In the Ga_2Se_3–In_2Se_3 system, blurring of X-ray powder lines is attributed to stacking faults occurring in the alloys and in Ga_2Se_3 itself.

INTRODUCTION

Considerable work has been carried out in the last few years on semiconductor alloys formed by solid solution between two intermetallic compounds. A group of compounds of particular interest because of their similarity to the Group IV elements are the $A^{III}B^{V}$ compounds (*e.g.* InSb, GaAs, etc.) and solid solution between various members of this group, which all possess zinc blende structures, has been studied in some detail. Other compounds which possess a similar structure and in which interest has recently increased are the $A_2^{III}B_3^{VI}$ compounds, *viz.*: In_2Te_3, Ga_2Te_3 and Ga_2Se_3. These compounds are reported[1,2] to have a defect zinc blende structure in that on the A sub-lattice, one lattice site in three is vacant, although as has been pointed out[3] the present X-ray data could be interpreted as a defect antifluorite structure, A_2B, with two lattice sites in every three on the A sub-lattice vacant. The presence of lattice vacancies in these compounds, which have semiconducting properties, could be of interest, particularly in thermoelectric applications. Hence, alloys of these compounds have been investigated and it is found that wide ranges of solid solution can be obtained for compounds of this type, not only between themselves[4,5] but also with the zinc blende type $A^{III}B^{V}$ and $A^{II}B^{VI}$ compounds[4,6 9]. These are of interest in that the number of lattice vacancies present in the material can be adjusted by varying the percentage composition of the alloy.

A problem which applies to most of the work on alloys of this type is the difficulty of determining initially the equilibrium condition. As a result of the low diffusion rates in the compounds, particularly of the $A^{III}B^{V}$ compounds, it is found in many

* Now at A.E.I. (Woolwich) Ltd., Harlow, Essex.

cases that alloys must be annealed for weeks at temperatures close to the solidus before equilibrium is attained[10]. As usually the solidus temperature cannot be determined until equilibrium has been attained the process can be very tedious. In most cases it has been found that compressed powder specimens reach an equilibrium within a shorter time of anneal than is required for solid ingots. The alloy systems already investigated which are of interest because they are analogous to the work described below are (a) InAs–In_2Te_3[4,7,11], (b) InSb–In_2Te_3[8], (c) Ga_2Te_3–In_2Te_3[4,5], and (d) Ga_2Te_3–Ga_2Se_3[4]. In systems (a), (c) and (d) single phase solid solution occurs throughout the whole composition range. In (b) solid solution of In_2Te_3 in InSb is limited to 15 mol.%* when alloys are annealed close to the solidus, but at lower temperatures the solid solution limit is reduced, being only about 8 mol.% at 450°C. In systems (b) and (c) equilibrium is attained rapidly and only a few hours annealing is required, but system (a) requires much longer annealing, especially at the InAs end of the diagram, and several months of annealing are required to give good equilibrium conditions for a specimen in solid ingot form. In system (d) the annealing times are shorter, but the determination of equilibrium conditions is complicated by the ordering which occurs in the system[4].

The compound In_2Se_3 is found to possess a structure of much lower symmetry than that shown by the $A_2^{III}B_3^{VI}$ compounds mentioned above. Because of its similarity to these, however, it seemed probable that solid solution of In_2Se_3 in other compounds of zinc blende structure should occur to a considerable extent. GORYUNOVA, RADAUTSAN AND DERYABINA[12–14] investigated the system InAs–In_2Se_3. Alloys were prepared by melting the elements together and then slow cooling at 50–60°C/h. These alloys were shown by X-ray work, photomicrograph and microhardness studies to be non-homogeneous, and were therefore annealed for up to 200 h at 600°C, the improvement in homogeneity being observed by the same techniques. It was found that annealing with an applied gaseous pressure of hydrogen of up to 820 kg/cm² enabled the homogenisation of the alloys to be achieved in a shorter time. In this work GORYUNOVA *et al.* found a limit of solid solution of In_2Se_3 in the zinc blende phase of approximately 80 mol.%. Extra X-ray lines were observed for specimens of composition 75 mol. % In_2Se_3 and these were attributed to ordering in the lattice, but no analysis of this was given.

Recently, HAHN AND THIELE[9] have also published results on the range of solid solution in the InAs–In_2Se_3 system. In this case specimens in compressed powder form were annealed for one week at 650°C. Lattice parameters were determined and the limit of solid solution was reported to be a little above 75 mol.% In_2Se_3. HAHN AND THIELE also report similar work on the solubility of In_2Se_3 in InP where the solid solution range in the zinc blende phase extends to 85 mol.% In_2Se_3.

The work described in this paper represents the initial step in an investigation of the semiconducting properties of alloys of In_2Se_3 with zinc blende type compounds. The zinc blende compounds chosen all had one element in common with In_2Se_3 and hence the systems investigated were sections of ternary diagrams. No previous data seemed available on the systems InSb–In_2Se_3, In_2Te_3–In_2Se_3 and Ga_2Se_3–In_2Se_3 while the fourth system InAs–In_2Se_3 was investigated to obtain more detailed results for

* In calculating mol. % in all systems composed of one $A^{III}B^{V}$ compound and one $A_2^{III}B_3^{IV}$ compound, the molecules have been taken as $A_3^{III}B_3^{V}$ and $A_2^{III}B_3^{VI}$, *i.e.* the percentage is strictly the percentage of B^{V} and B^{VI} atoms on the B sub-lattice.

the variation of lattice parameter with composition than those provided by GORYUNOVA *et al.*, the results of HAHN AND THIELE not being published when this work was carried out.

PREPARATION OF ALLOYS

In all cases the compounds were prepared directly from the elements, and then the alloys produced by melting together under vacuum the appropriate weights of the compounds required. In the initial work, the indium and gallium used were of 99.9% purity, but in the later work when the alloys were required for electrical and optical work indium of 99.999% and gallium of 99.99% purity were used. In all cases the antimony used was of 99.999% purity. The selenium, tellurium and arsenic used were normal commercial high purity materials which had been repeatedly distilled to give better purity. The InSb and InAs were further purified by normal zone refining methods.

In practically all cases alloys quenched from the melt were found to be in a non-equilibrium condition, showing considerable blurring of the lines of an X-ray photograph. In order to determine the equilibrium conditions samples were powdered and compressed and then annealed at a suitable temperature until the X-ray results indicated that an equilibrium condition had been attained. The required time and temperature of annealing varied from one system to another and will be listed below for the individual systems. When equilibrium conditions had been attained, lattice parameter values were determined from the X-ray photographs. In all cases copper $K\alpha$ radiation was used, and for all alloys except those of the InSb–In_2Se_3 system the powder photographs were obtained with 9 cm cameras.

In the case of the InSb–In_2Se_3 alloys 19 cm cameras were used to give greater accuracy.

RESULTS

InAs–In_2Se_3

Alloys in the quenched condition were found to give blurred lines and both compressed powder and solid ingot specimens were annealed at 720°C, X-ray photographs being taken after various times of annealing up to 240 h. In addition to causing

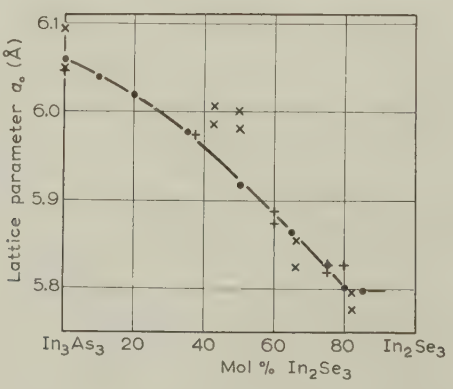

Fig. 1. Variation of lattice parameter with composition for InAs–In_2Se_3 system: ×, GORYUNOVA AND RADAUTSAN[12]; +, HAHN AND THIELE[9]; ●, present work.

the lines to sharpen, the effect of annealing was to cause the centre of the lines to shift towards positions corresponding to lower values of a_0. The equilibrium values of lattice parameter are shown in Fig. 1, together with those of GORYUNOVA *et al.* and HAHN AND THIELE. It is seen that there is good agreement on the range of solid solution in the zinc blende phase, a value of 82 mol.% In_2Se_3 being obtained. The agreement on lattice parameter is less good, for in the centre of the solid solution range the values of GORYUNOVA *et al.* are higher than those presented here. It is suggested that this may be due to incomplete equilibrium in the samples used by GORYUNOVA *et al.*, who annealed solid ingots at 600°C for 200 h or less. Solid ingots used in the present work gave similar high values of a_0 after a corresponding time of annealing and only agreed with the results on powdered specimens after annealing for 350 h at 720°C. This suggestion is supported by the fact that the results of HAHN AND THIELE, obtained with compressed powders annealed at 650°C for about 170 h, are in reasonable agreement with the results presented here.

This variation in lattice parameter with annealing has been observed with other alloys containing a defect structure compound, *e.g.* InAs–In_2Te_3[11]. It is suggested that the quenched specimens contain a non-equilibrium number of lattice vacancies and that the equilibrium number is only attained after long annealing. A simultaneous change in density was observed in the InAs–In_2Te_3 case[11].

The alloys containing 65, 75, 80 and 85 mol.% In_2Se_3 gave extra lines in the X-ray photograph in agreement with the previous observations. It would appear that this indicates the presence of ordering centred possibly on the 75 mol.% In_2Se_3 composition, but the determination of the ordered structure has not, as yet, been attempted.

Although the lattice parameter values indicate that the limit of solid solution is 82 mol.% In_2Se_3, no second phase lines were observed on the 85 mol.% sample. This however may be partly due to the presence of the ordering lines which have not been interpreted. The 90 mol.% alloy showed no observable zinc blende lines and so the two-phase miscibility gap would appear to be quite narrow in composition range. This is the reason for the absence in Fig. 1 of extra points in the two-phase region to give a more accurate determination of the limit of solid solution. The lines in the photograph of the 90 mol.% alloy did not appear to be those corresponding to In_2Se_3 itself and so probably another phase appears at the In_2Se_3 end of the diagram.

The mechanical condition of the ingots is important for the electrical measurements etc. The ingots of alloys containing less than 1 mol.% In_2Se_3, interesting for their electrical properties, were solid and mechanically good, containing no blow holes, etc. The condition of the ingots became worse as the In_2Se_3 content increased, particularly in the range 40–60 mol.%. The condition of the 75 mol.% alloys was very good, however.

InSb–In_2Se_3

Alloys in the quenched state gave slightly blurred X-ray lines and compressed powder and solid ingot specimens were annealed at 490°C. The powder specimens appeared to have reached equilibrium after 300 h of annealing, in this time the X-ray lines having sharpened and moved slightly in position towards larger lattice parameter values. Solid ingots appeared to need annealing for over 1,000 h at 490°C to give good X-ray photographs however. After this annealing the mechanical condition of the ingots was good and no blow holes, etc. occurred.

The X-ray photographs showed second phase lines in all alloys containing 5 mol.% In_2Se_3 or more and the lattice parameter values for the zinc blende phase when obtained from 9 cm camera photographs were all very similar to that for InSb. From 19 cm camera photographs the InSb parameter was determined as 6.4794 ± 0.0002 Å, and this value was reduced as In_2Se_3 was added, values within the range 6.478 ± 0.001 Å being obtained for all alloys containing between 2.5 and 30 mol.% In_2Se_3. The scatter in the parameter values did not allow the range of solid solution of In_2Se_3 in the zinc blende structure to be determined accurately, but this would appear to be about 2–2.5 mol.%. Thus the 19 cm photograph of the 3.5 mol.% alloy showed faint second phase lines, while specimens in solid ingot form and containing 2.5 mol.% In_2Se_3 or more showed different behaviour on etching in C.P.4 as compared with those containing less In_2Se_3. Finally the values of conductivity as a function of composition show a slight discontinuity at about 2.5 mol.% In_2Se_3.

Again the second phase lines in the photographs did not appear to correspond to those of In_2Se_3.

In_2Te_3–In_2Se_3

In this case, where alloys of two defect structure compounds were being investigated, the diffusion rates were considerably larger than when $A^{III}B^{V}$ compounds were involved. Thus the quenched alloys when X-rayed appeared to be in good equilibrium condition. The variation of lattice parameter shown in Fig. 2 indicates a limit of solid

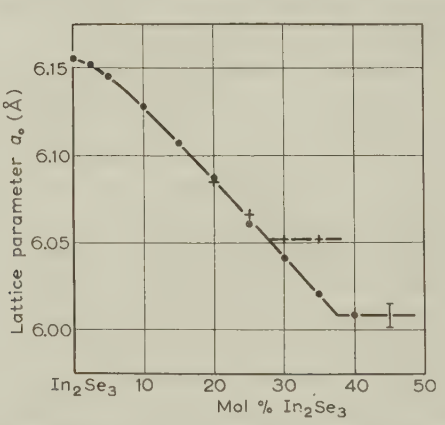

Fig. 2. Variation of lattice parameter with composition for In_2Te_3–In_2Se_3 system: •, quenched alloys; +, alloys annealed at 560°C.

solubility of In_2Se_3 in the zinc blende structure of 37–38 mol.%. After quenching, these alloys were annealed in compressed powder form for about 150 h at 560°C. The results of this annealing indicated a smaller range of solid solution at this temperature, *i.e.* 27–28 mol.% In_2Se_3 as shown in Fig. 2, but for In_2Se_3 content less than this, the lattice parameter was effectively unchanged from the value obtained with quenched material, except for the small effect due to ordering discussed below. Alloys containing respectively 30 and 35 mol.% In_2Se_3 were annealed at 600°C and 530°C, but the results indicated little change in the solid solubility range as compared with the value

at 560°C, the normal tendency for a slightly higher value at 600°C and a slightly lower value at 530°C being observed.

It has been shown previously that In_2Te_3 shows ordering of lattice vacancies in the indium sub-lattice[3,15,16] with an ordering temperature of 620°C. Even when samples of In_2Te_3 are annealed within 50°C of this temperature, it is found that normal annealing of powders or solid ingots must be carried on for many weeks before a good ordered condition is obtained, and directional freezing techniques have been used to obtain the ordered structure. However it was of interest to see whether such ordering occurred in this alloy system where the lattice vacancy density is unchanged by alloying. It was found that after suitable annealing all alloys in the solid solution range showed ordering lines and that the lines were identical with those observed with ordered In_2Te_3 indicating the same ordered structure. The ordering temperature was found to fall as the In_2Se_3 content was increased. Thus the alloy containing 10 mol.% In_2Se_3 showed relatively strong ordering lines after annealing at 530°C and faint lines after annealing at 560°C, indicating an ordering temperature a little above 560°C. The 20 mol.% In_2Se_3 alloy was ordered after annealing at 530°C but showed no ordering lines after an anneal at 560°C. The 35 mol.% In_2Se_3 alloy, which was two-phase and hence represented a zinc blende phase containing 28 mol.% In_2Se_3, showed no ordering lines after annealing at 560°C or 530°C, indicating that the ordering temperature has fallen below 530°C at the two-phase boundary. A further observation was that the annealing time required to produce definite ordering lines was less in the case of alloys containing appreciable In_2Se_3 content than for In_2Te_3 itself, when annealed at corresponding values below the ordering temperature.

In In_2Te_3 the ordering causes a change in lattice parameter from 6.150 Å in the disordered material to 6.165 Å in the ordered[17]. It was found that the difference between the parameters for the two conditions rapidly decreased as the In_2Se_3 content increased and that over much of the range of composition the difference was within the limits of experimental error in determining the parameters (only 9 cm cameras were used with these alloys). It has been shown however in the case of In_2Te_3 that the lattice parameter obtained depends upon the degree of ordering, and hence the small difference observed in the alloys may indicate that only partial ordering occurs.

Powdered alloys containing respectively 40 and 50 mol.% In_2Se_3, *i.e.* well within the two-phase range, were found to show signs of melting when heated to temperatures above 630°C. It then appears that the eutectic or peritectic horizontal corresponding to the two-phase field occurs at about 630°C. The X-ray photographs of alloys in this two-phase range were very much more complicated than that of In_2Se_3, and again appear to indicate some intermediate phase occurring in the diagram.

Ga_2Se_3–In_2Se_3

Alloys of this system when quenched and X-ray showed blurred lines apparently typical of the non-equilibrium conditions obtained in these types of alloy. The specimens were therefore powdered and annealed at 850°C, firstly for 300 h and then for a further 700 h. It was found that although the first annealing gave some improvement in the X-ray photograph, the results were unchanged after the further 700 h of annealing and some blurred lines still remained at all Bragg angles in the X-ray photograph, while other lines were quite sharp. It was found that the odd order lines, *i.e. 111, 311, 331, 511, 531* and *533* were blurred, while the even order lines, *i.e. 220, 400,*

422, *440* and *444* were sharp. In an attempt to obtain lattice parameter values from such photographs, normal zinc blende lattice conditions were assumed and the effective values of lattice parameter a were determined for the various lines. When these were plotted against the function

$$\tfrac{1}{2}\left(\frac{\cos^2\theta}{\sin\theta} + \frac{\cos^2\theta}{\theta}\right)$$

in the normal method of extrapolation to determine a_0 it was found that two distinct graphs were obtained, one corresponding to the sharp lines and one to the diffuse lines in the X-ray photograph. From this analysis two values of a_0 were obtained for each alloy and these are plotted against alloy composition in Fig. 3, the smaller values of a_0 corresponding to the sharp X-ray lines.

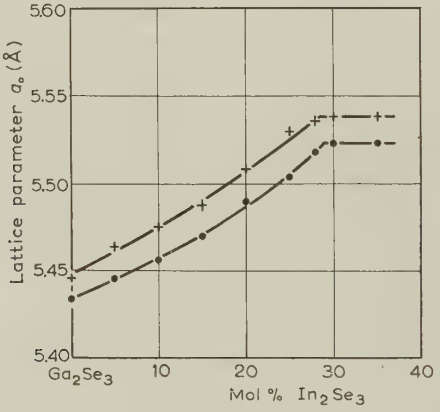

Fig. 3. Variation of lattice parameter with composition for Ga_2Se_3–In_2Se_3 system: ●, values from sharp lines in X-ray photograph; +, values from diffuse lines in X-ray photograph.

Results of this type had previously been observed in alloys of the Ga_2Se_3–Ga_2Te_3 system in the range 85–100 mol.% Ga_2Se_3[4], the blurring of the diffuse lines being greater in that case than in the present case of Ga_2Se_3–In_2Se_3 alloys. In the Ga_2Se_3–Ga_2Te_3 system however chalcopyrite type ordering is observed in the approximate composition range 65–80 mol.% Ga_2Se_3 and it had therefore been assumed that the sharp–diffuse effect was caused by partial ordering associated with the chalocpyrite type ordering in the system. In the present case, no such chalcopyrite ordering occurs and moreover the sharp–diffuse behaviour extends to Ga_2Se_3 itself, a result overlooked in the previous case. If, therefore, it is still assumed that the effect is due to partial ordering, in view of the Ga_2Se_3 result, the ordering would be of lattice vacancies rather than indium and gallium atoms. Another possibility however is that of stacking faults, for it has been shown[18] for the zinc blende structure that stacking faults on the {*111*} planes could produce blurring in some of the X-ray lines. Although the present results do not agree completely with the predictions for the particular case considered in the theoretical work, the general similarity would indicate stacking faults as a probable explanation of the observed behaviour in the case of Ga_2Se_3 and its alloys.

From the results in Fig. 3 an estimate of the limit of solubility of In_2Se_3 in Ga_2Se_3 can be made, giving a value of 28 mol.%. Only the zinc blende type phase could be observed in X-ray photographs for an alloy containing 28 mol.% In_2Se_3, but photographs for alloys containing 30 and 35 mol.% In_2Se_3 clearly showed a second phase to be present. Again this phase showed a different set of lines from those of In_2Se_3.

CONCLUSIONS

In_2Se_3 is found to show considerable solid solubility in three of the zinc blende type compounds investigated, and only in the case of InSb is the range of solid solution limited to a few mol.%. In comparison with the corresponding systems involving In_2Te_3, the results are similar in most respects, but the degree of solid solubility is less for In_2Se_3 than for In_2Te_3. In all four systems considered the new phase occurring at the limit of solid solution does not seem to be the In_2Se_3 phase, although no attempt has been made to identify these more complex phases.

In the alloys with other defect compounds, In_2Te_3 and Ga_2Se_3, where the lattice vacancy density remains constant, it is found that the crystallographic effects associated with the lattice vacancies, *i.e.* ordering in In_2Te_3 and possibly stacking faults in Ga_2Se_3, are also observed in the corresponding alloys.

ACKNOWLEDGEMENTS

We are indebted to Professor L. F. BATES for the facilities of his laboratory, and to Dr. M. E. HAINE of A.E.I. (Woolwich) for a maintenance grant to one of us (P.N.K.).

REFERENCES

1 H. HAHN AND W. KLINGLER, *Z. anorg. Chem.*, 260 (1949) 97.
2 H. HAHN AND W. KLINGLER, *Z. anorg. Chem.*, 260 (1949) 110.
3 J. C. WOOLLEY, B. R. PAMPLIN AND P. J. HOLMES, *J. Less-Common Metals*, 1 (1959) 362.
4 J. C. WOOLLEY AND B. A. SMITH, *Proc. Phys. Soc.*, 72 (1958) 867.
5 V. S. GRIGOR'EVA, *Soviet Phys.-Tech. Phys.*, 3 (1958) 1539.
6 N. A. GORYUNOVA AND V. S. GRIGOR'EVA, *Soviet Phys.-Tech. Phys.*, 1 (1957) 2094.
7 N. A. GORYUNOVA AND S. I. RADAUTSAN, *Soviet Phys. Doklady*, 3 (1958) 854.
8 J. C. WOOLLEY, C. M. GILLETT AND J. A. EVANS, *Phys. Chem. Solids*, 16 (1960) 138.
9 H. HAHN AND D. THIELE, *Z. anorg. Chem.*, 303 (1960) 147.
10 J. C. WOOLLEY AND B. A. SMITH, *Proc. Phys. Soc.*, 72 (1958) 214.
11 J. C. WOOLLEY, B. R. PAMPLIN AND J. A. EVANS, *Phys. Chem. Solids*, in the press.
12 N. A. GORYUNOVA AND S. I. RADAUTSAN, *Soviet Phys.-Tech. Phys.*, 3 (1958) 1762.
13 N. A. GORYUNOVA, S. I. RADAUTSAN AND V. I. DERYABINA, *Soviet Phys. Solid State*, 1 (1959–60) 460.
14 S. I. RADAUTSAN, *Russ. J. Inorg. Chem.*, 4 (1959) 510.
15 H. HAHN, *Angew. Chem.*, 64 (1952) 203.
16 H. INUZUKA AND S. SUGAIKE, *Proc. Japan Acad.*, 30 (1954) 383.
17 J. C. WOOLLEY AND B. R. PAMPLIN, in the press.
18 M. S. PATERSON, *J. Appl. Phys.*, 23 (1952) 805.

THE THERMAL AND ELECTRICAL CONDUCTIVITIES OF ZIRCONIUM AND OF SOME ZIRCONIUM ALLOYS

R. W. POWELL AND R. P. TYE

Basic Physics Division, National Physical Laboratory, Teddington, Middx. (Great Britain)

(Received January 27th, 1961)

SUMMARY

Three samples of zirconium and nine zirconium alloys have been studied, six with tin contents ranging from 0.84–6.7 wt. %, and alloys with 1.48% aluminium, 7.6% molybdenum and 9.79% niobium.

The thermal conductivity of zirconium has been measured to 780°C and the electrical resistivity to 970°C. The Lorenz function is found to decrease from about $3.10 \cdot 10^{-8}$ to $2.63 \cdot 10^{-8}$ J ohm/sec °C °Abs. over the range 50–750°C.

For these alloys the thermal conductivity determinations were mainly restricted to the range 50–250°C, and the electrical resistivity determinations mainly covered the range 20–600°C. Higher temperatures were reached in a few cases and the molybdenum and niobium alloys were found to undergo considerable changes in both properties after heat treatment, presumably due to the occurrence of phase changes when held at temperatures above 400°C. In two instances, for a 1.65% tin alloy and the heat-treated niobium alloy the thermal conductivity determinations were extended to over 600°C.

Using the values at 50°, 150° and 250°C the line $K = 2.503 \cdot 10^{-8}\ T/\varrho + 0.0223$ is obtained from a plot of thermal conductivity, K, expressed in J cm/cm² sec °C, against absolute temperature, T, divided by electrical resistivity, ϱ, ohm cm²/cm. All points are within 11% of this line and all but three within 5%. Results of other workers are discussed and examined in a similar way.

INTRODUCTION

During the period 1950 to 1957 thermal and electrical conductivity determinations were undertaken by the National Physical Laboratory on behalf of the Atomic Energy Research Establishment, Harwell, on three samples of zirconium and on nine zirconium alloys, and the results have been included in various reports on the progress of the work. The purpose of the present paper is to describe the results obtained for this group of metals and to discuss the results in the light of other conductivity determinations on zirconium and its alloys[1–6].

DETAILS OF SPECIMENS

The first sample of zirconium to be received and tested was in the form of a rod 9.7 cm long by 0.435 cm diameter. This was stated to have been cold swaged from a bar of about 0.5 cm diameter that had been prepared by the VAN ARKEL method. When deposited, the metal was stated to have consisted almost entirely of hexagonal crystals with their c-axes parallel to the axis of the bar, and considerable preferred orientation was believed to be present in the swaged bar. The density of this bar was 6.57 g/ml.

The other samples were each 1.27 cm in diameter and 10 cm long, and were supplied

in the "as-extruded" condition. One had been arc melted and the remainder melted in graphite. The reference numbers, descriptions and chemical compositions of these samples are given in Table I.

TABLE I

DETAILS OF ZIRCONIUM AND ZIRCONIUM-ALLOY SAMPLES[a]

Ref. No.	Description	Chemical composition (wt. %)							
		Fe	*C*	*Sn*	*Al*	*Nb*	*Mo*	N_2	O_2
—	Van Arkel Zr, cold-swaged	0.012	0.016	—	—	—	—	0.0025	0.3–0.6[b]
715	Graphite-melted Zr, extruded, 2 samples	0.018	0.043	—	0.007	0.007	—	0.0075	0.1–0.6[c]
050	Arc-melted low-carbon Zr, extruded	0.045	0.01	—	—	—	—	0.008	0.11
666	Graphite-melted Zr + 7% Mo, extruded	0.015	0.14	—	—	—	7.6	—	0.10
749	Graphite-melted Zr + 10% Nb, extruded	0.06	0.19	—	—	9.79	—	—	—
751	Graphite-melted Zr + 3% Al, extruded	0.11	0.14	—	1.48	—	—	0.0045	0.10
756	Graphite-melted Zr + 1% Sn, extruded	0.04	0.10	0.84	—	—	—	—	—
769	Graphite-melted Zr + 2% Sn, extruded	0.05	0.13	1.65	—	—	—	0.007	0.14
770	Graphite-melted Zr + 3% Sn, extruded	0.02	0.10	2.3	—	—	—	0.007	0.14
761	Graphite-melted Zr + 6% Sn, extruded	0.05	0.10	6.7	—	—	—	0.007	0.10
776	Graphite-melted Zr + 1½% Sn + Fe + Ni, extruded	0.14	0.13	1.37	*Cr* 0.09	*Ni* 0.07	*Ca* 0.008	—	0.098
771	Graphite-melted Zr + 3% Sn + Fe + Ni, extruded	0.12	0.14	2.38	~0.1	~0.05	—	—	0.14

[a] These details and chemical analyses were provided by the Atomic Energy Research Establishment.
[b] Analysis made after completion of tests. H_2 content, 0.016%. Range of values for O_2 represents local variations. Initial and final room temperature resistivities agreed.
[c] Analysis made after completion of tests. H_2 content, 0.0025%. Range of values for O_2 represents local variations. Increase in final room temperature resistivity suggests that oxidation had occurred during the tests.

EXPERIMENTAL METHODS

For the sample of Van Arkel zirconium first received electrical resistivity determinations were made to 600°C in an evacuated refractory tube placed in the central uniform temperature zone of a tubular furnace. Determinations to —180°C were also made by introducing the tube containing the sample into a flask of liquid oxygen. The customary method was used, thermo-couples attached towards each end of the rod serving for temperature measurement and as leads for the comparative potential drop method.

The heat treatment was found to cause little permanent change in the resistance of the sample, and thermal conductivity determinations were then made by the normal comparative longitudinal heat flow methods[7]. For mean temperatures to about 200°C a waterflow calorimeter was used to measure the outflowing energy, the energy inflow being derived from the gradient set up in a rod of Armco iron joined to the zirconium. For temperatures from 250° to 600°C vacuum conditions were used and the energy outflow was derived only from the Armco iron measurements.

The subsequent procedure with the other zirconium samples and alloys was generally similar. Owing, however, to the low thermal conductivities under investigation, a rod of Mcloy G steel was used instead of Armco iron as the comparison metal of known thermal conductivity[8]. Thermal conductivity measurements were first made over the lower temperature range, then electrical resistivity measurements to at least 600°C and then further thermal conductivity determinations over the lower range for the two alloys which had undergone changes as the result of the heat treatment, and to at least 600°C for two alloys, Nos. 749 and 769, which were considered typical of the tin and other alloys.

The resistivity measurements were extended to 970°C for one of the graphite-melted zirconium samples, so as to include the α to β transformation region, and to about 700° and 900°C for the 7.6% molybdenum and 9.79% niobium alloys, the two alloys which had been markedly affected by heating to 600°C.

EXPERIMENTAL RESULTS

Electrical resistivity of zirconium

The experimental results obtained for the electrical resistivities of the three samples of zirconium are shown in Fig. 1. At room temperature the resistivity of the sample prepared by the VAN ARKEL method is the lowest and that of the arc-melted sample

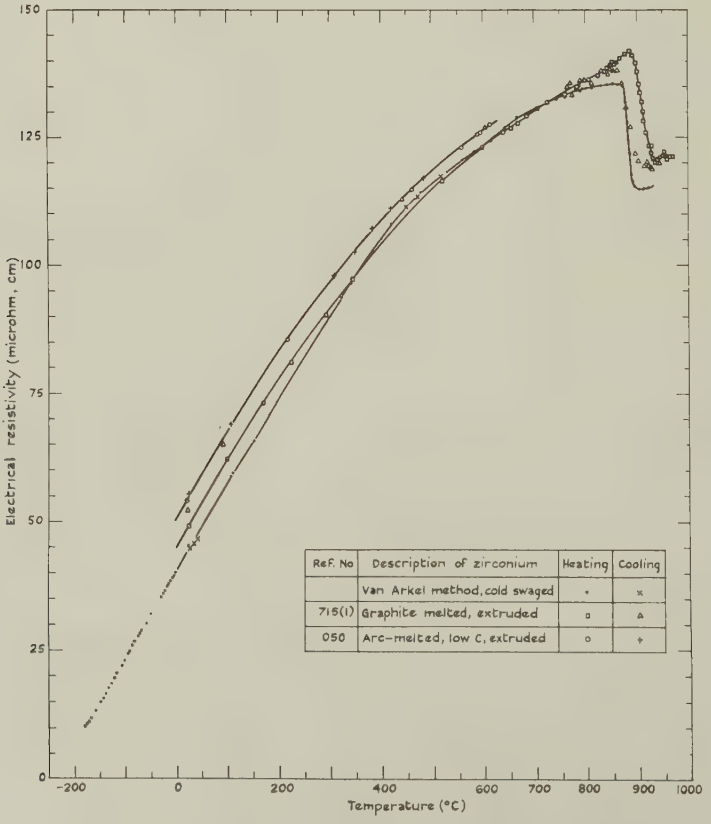

Fig. 1. Variation of electrical resistivity of zirconium with temperature.

is the highest. For the former the value at 0°C is 40.7 microhm cm, which agrees closely with a reported value of 41 microhm cm[9] but exceeds TRECO's value[4] of 38.8 microhm cm for an oxygen-free zirconium. The resistivity of the graphite-melted zirconium was almost mid-way between that of the other two samples at 0°C, but is seen to be comparable with that of the VAN ARKEL sample at 350°C and 600°C and a little lower between these two temperatures.

On heating to higher temperatures the resistivity shows a sharp drop at the $\alpha \rightarrow \beta$ transformation of zirconium. VAN ARKEL[10] had reported this transformation as occurring at 865 ± 10°C. For the sample prepared by the VAN ARKEL method a maximum resistivity of 135.4 microhm cm occurs at 855.4°C, followed by a gradual decrease to 135.1 microhm cm at 873.1°C, above which the sharp fall to 115.0 occurs and is complete by 904°C. The curve differs somewhat for the 715(1) sample, where the maximum of 142 microhm cm occurs at 886°C and the minimum of 120 is reached at 935°C. This less sharp fall and wider temperature range is consistent with the lower purity of sample 715. In some earlier experiments by ZWIKKER[11] the change occupied about 250°C.

On cooling the 715 sample, some hysteresis is noticeable, the change being displaced to temperatures some 35°C lower. Whilst held overnight at a temperature which decreased from 762 to 606°C the vacuum deteriorated and some oxidation occurred which presumably caused the higher resistivity values that will be noted on cooling from this last temperature.

Thermal conductivity of zirconium

Fig. 2 contains curves representing the variation with temperature of the thermal conductivity of the three samples of zirconium included in the present investigation, together with the results of other investigators. Owing to the small diameter of the VAN ARKEL sample and the low thermal conductivity the experimental points show a scatter of up to about ±5% from the smooth curve. For the larger diameter sample of graphite-melted zirconium the scatter was noticeably less and the thermal con-

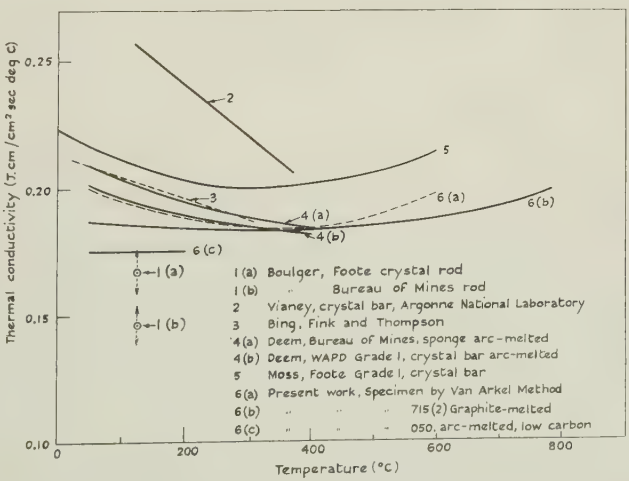

Fig. 2. Variation of thermal conductivity of zirconium with temperature.

ductivity value a little lower. The thermal conductivity of the arc-melted sample is the lowest, so the thermal and electrical conductivities are seen to behave similarly at the lower temperatures. Values for both conductivities of the VAN ARKEL and graphite-melted samples also tend to converge at about 300°C.

Regarding comparison with the results of other workers, it is likely that the low values of BOULGER[1] can be attributed to the use of less pure samples, whilst the high values of VIANEY[2] can be discounted since his results for austenitic steel, with which he checked the apparatus, are clearly in error in having a negative instead of a positive temperature coefficient. The remaining values of DEEM[5], BING *et al.*[3] and MOSS[6] are in good general agreement, and the differences of a few percent are probably due to variations in chemical composition. Only BING *et al.* reported electrical resistivity data as well. At 25°C the electrical resistivity of his arc-melted sample produced from crystal bar after heating at 600°C was 44.1 microhm cm; at 260°C it was 81.3 microhm cm. The corresponding values for our sample of lowest resistivity were 44.7 and 83.7 microhm cm. These values are consistent with the 3–5% higher thermal conductivities obtained by BING *et al.*

Lorenz function of zirconium

The relationship between the thermal conductivity and electrical resistivity of zirconium is treated further in Table II. This gives the data so far available for their product divided by the absolute temperature, that is for the Lorenz function. There is seen to be close agreement, each experiment commencing at 50°C with values

TABLE II

LORENZ FUNCTION OF ZIRCONIUM

K represents thermal conductivity expressed in J cm/cm² sec °C; ϱ represents electrical resistivity expressed in microhm cm²/cm; L represents 10^8 Lorenz function expressed in J ohm/sec °C °Abs.

Temperature (°C)	Bing et al.			Present work									Adjusted mean values
				Van Arkel method			Arc-melted method (050)			Graphite-melted (715)			
	K	ϱ	L	K	ϱ	L	K	ϱ	L	K	ϱ	L	(L)
50	0.209	48.1	3.11	0.199	49.2	3.03	0.175	59.5	3.22	0.187	53.5	3.10	3.10
150	0.200	63.9	3.02	0.191	65.6	2.96	0.175	75	3.10	0.185	70.0	3.06	3.03
250	0.192	79.7	2.93	0.186	82.1	2.92				0.183_5	85.0	2.98	2.95
350				0.183	97.8	2.87				0.183	98	2.88	2.88
450				0.185	111.2	2.85				0.184	110	2.80	2.83
550				0.193	119.7	2.80				0.186	119	2.69	2.73
650										0.189	127	2.60	2.68
750										0.196	133	2.55	2.63

within ±3% of the mean and the values showing similar decreases with increase in temperature. The adjusted mean values given in the last column of the table should serve for calculations of the thermal conductivity of zirconium to be made from electrical resistivity measurements, to within 5%. A lattice component of thermal conductivity of the order of 0.04 J cm/cm² sec °C at 50°C is indicated, decreasing to about half this value at 550°C.

Electrical resistivity of zirconium alloys

The full results obtained for the electrical resistivity of the various zirconium

alloys are plotted in Fig. 3. A smooth curve showing the temperature variation of the resistivity of one of the samples of graphite-melted zirconium on heating is included in order that comparison can readily be made. It is noteworthy that in the temperature region of 410–460°C this curve is crossed by those for two of the alloys and that at above this temperature region these alloys have much lower electrical

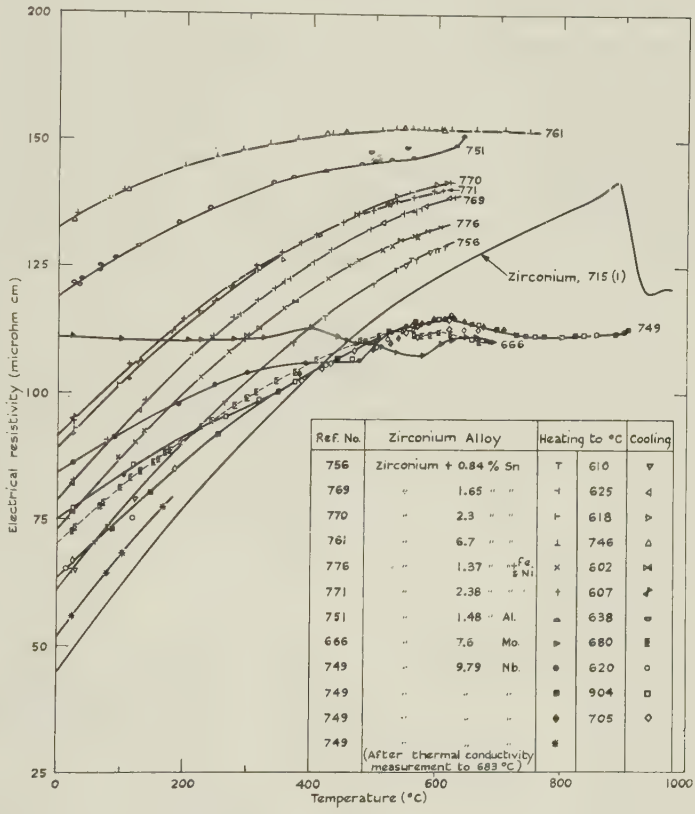
Electrical resistivity (microhm cm)
Temperature (°C)
761
751
770
771
769
776
756
Zirconium, 715 (I)
749
666
Ref. No. | Zirconium Alloy | Heating to °C | Cooling
756 | Zirconium + 0.84 % Sn | 610
769 | " 1.65 " " | 625
770 | " 2.3 " " | 618
761 | " 6.7 " " | 746
776 | " 1.37 " " Fe & Ni | 602
771 | " 2.38 " " " | 607
751 | " 1.48 " Al. | 638
666 | " 7.6 Mo. | 680
749 | " 9.79 Nb. | 620
749 | " " " | 904
749 | " " " | 705
749 | " " " | |
(After thermal conductivity measurement to 683 °C)

Fig. 3. Variation of electrical resistivity of zirconium alloys with temperature and heat treatment.

resistivities than the pure zirconium. The two alloys were those with 7.6% of molybdenum and with 9.79% niobium and it is significant that their resistivities differed from the other alloys in having an initial smaller change with temperature and in decreasing to much lower values on cooling to room temperature. For the molybdenum alloy the initial resistivity remained virtually independent of temperature on heating up to 320°C, had maxima at about 400° and 650° and a minimum at 570°C. From room temperature to 685°C, however, the value only differed from the initial value by about 3%. On cooling, the change is seen to be much greater, the final room-temperature resistivity being about 34% below the initial value.

In all, three heating runs were made on the niobium alloy. The first to 620°C gave a decrease of 14.3% on cooling back to room temperature. The second reached a maximum temperature of 904°C, in the course of which the specimen was held over-

night between the observations at 722° and 740°C, with no marked change in resistivity. Indeed, the points from 380° to 904°C and back lie on a smooth curve conforming to the upper points of the first run and having a small maximum at about 620°C and minimum at about 780°C. Below 380°C the return curve lies between the first and second heating curves. The third was to 705°C. Again the upper portion of the curve is in agreement with that of the earlier runs and this time the cooling curve agreed closely with that of the first run.

Following these measurements, a thermal conductivity determination was made on this sample to a maximum mean temperature of 683°C (extreme temperatures of 658° and 709°C), after which the room temperature resistivity was considerably lower, indeed, barely 15% greater than the resistivity of the zirconium curve of Fig. 3. The points for this condition shown for a limited temperature range were obtained during a final low temperature thermal conductivity determination made on the niobium alloy sample.

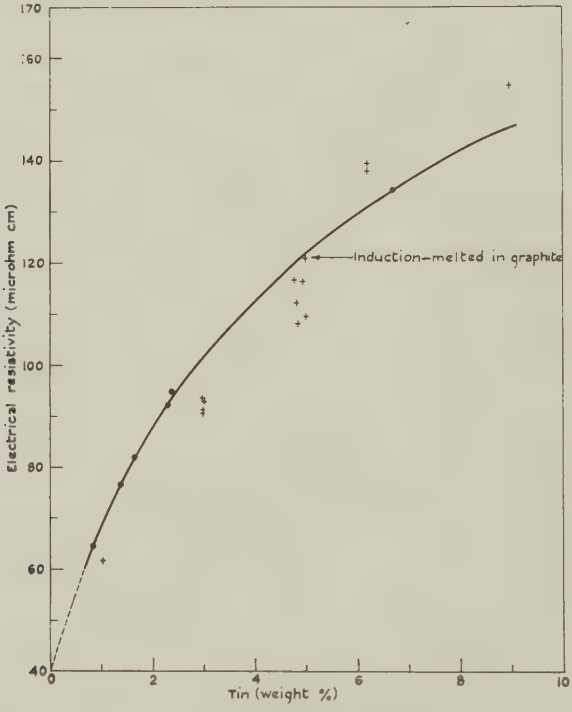

Fig. 4. Electrical resistivity of zirconium–tin alloys at 25°C against wt. % of tin. +, Bing, Fink and Thompson[3]; ●, present work.

The above resistivity changes would appear to be related to the occurrence of structural changes in the high-temperature region. These changes would appear to be rather sluggish and to have been partially suppressed for the condition in which these alloys were supplied.

The addition of 1.48% of aluminium is seen to cause a much greater increase in resistance than the corresponding weight percent of tin, indeed the increase in resistance at 25°C is of the order of two and a half times as great and so tends to be more

related to the volume effects of these added elements. For the aluminium alloy a change of between 1 and 2% in the room temperature resistivity was observed after heating to 640°C, but for the tin alloys no change of as much as 1% was observed.

In Fig. 4 a smooth curve has been drawn through the resistivity values at 25°C to show the variation of resistivity with weight percent of tin. These experimental points lie close to the curve, but the values of BING *et al.*[3], also included in the figure show much more scatter. This scatter no doubt reflects variations in the amount of other constituents present in their alloys. No detailed analysis was given for the uppermost point attributed to 5% tin, but this value of 121 microhm cm was for a sample stated to have been 'Induction melted in graphite from low-hafnium Bureau of Mines sponge', and is seen to be in good agreement with the curve for the present graphite-melted samples with 0.10–0.14% carbon. The carbon contents of the other samples reported by BING *et al.* were well under 0.1%. TRECO has shown that a gaseous impurity such as oxygen can appreciably affect the electrical resistivity of zirconium, and no figure has been given for the oxygen content of BING's samples, whereas the present samples contain about the same oxygen content as carbon.

Thermal conductivity of zirconium alloys

The experimental results obtained for the thermal conductivities of each zirconium alloy in its initial "as-extruded" condition are plotted in Fig. 5. The temperature

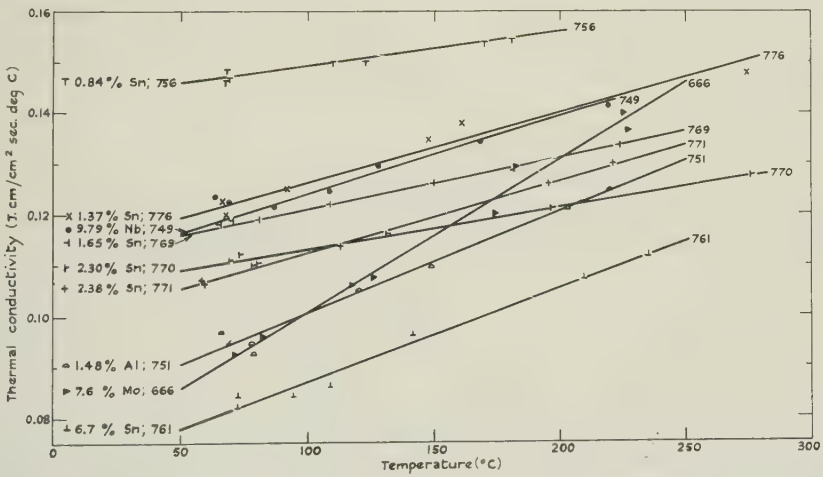

Fig. 5. Thermal conductivity of zirconium alloys in the "as-extruded" condition; range 50° to 250°C.

range covered was from about 50° to 250°C, for which the thermal conductivity of each alloy increases linearly with temperature. The maximum deviation of any experimental point from the straight lines drawn in the figure is 4%, whilst the majority of the points are within 2% of the lines.

The high-temperature phase retained in the 7.6% molybdenum alloy is seen to have by far the greatest temperature coefficient. The line for this alloy, as well as those for the 9.79% niobium and 1.65% tin alloys, are reproduced in Fig. 6, which contains

values to higher temperatures and includes the alloys for which the thermal conductivity is markedly affected by heat treatment. The curve for the graphite-melted zirconium is also included for comparison.

The thermal conductivity of the 1.65% tin alloy increases smoothly and at 600°C

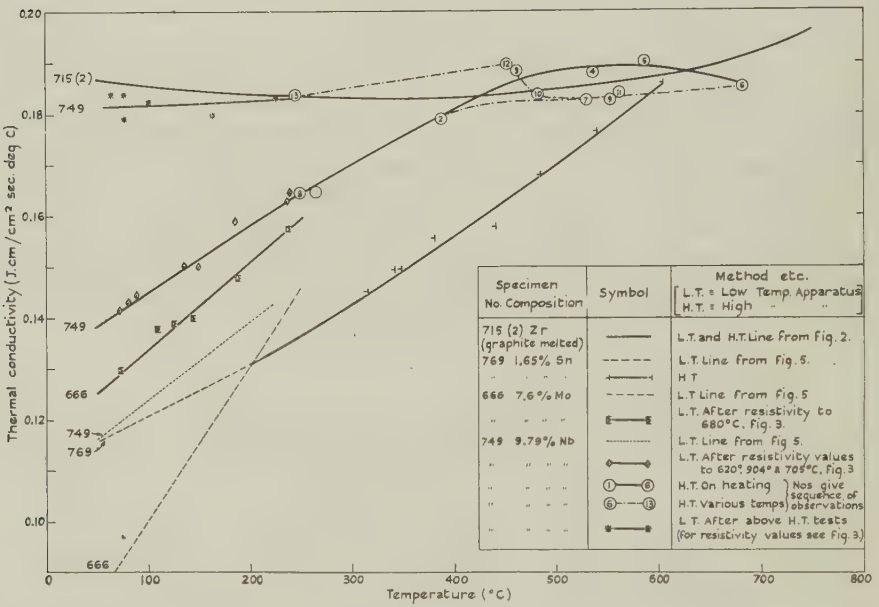
Thermal conductivity (J.cm/cm² sec. deg C)
Temperature (°C)
715 (2)
749
666
769
Specimen No. Composition
Symbol
Method etc.
L.T. = Low Temp. Apparatus
H.T. = High "
715 (2) Zr (graphite melted)
L.T. and H.T. Line from Fig. 2.
769 1.65% Sn
L.T. Line from Fig. 5.
H.T.
666 7.6% Mo
749 9.79% Nb
L.T. After resistivity to 680°C. Fig. 3.
L.T. After resistivity values to 620°, 904° & 705°C, Fig. 3
H.T. On heating
H.T. Various temps
Nos give sequence of observations
L.T. After above H.T. tests (for resistivity values see Fig. 3.)

Fig. 6. Thermal conductivity of zirconium alloys to over 600°C, and dependence on heat treatment.

its value is closely approaching that of the zirconium. The curve for the 9.79% niobium alloy is a little above that of zirconium over the range 400–630°C but falls to a 3% lower value at 685°C. Phase changes clearly occur in this alloy at temperatures above 400°C and the effects of time and temperature on its structure and properties need to be more fully investigated. In Fig. 6 the high-temperature points for this alloy have been numbered to indicate the sequence in which they were obtained. Two very different behaviours are indicated on cooling.

After cooling back and steadying at about 530°C for about 7 h the temperature was lowered to about 250°C and a point (8) obtained in good agreement with point (1). The temperature–time sequence 555°–17 h, 483°–7 h, 563°–14 h, 453–6 h and 245°C–16 h was then followed giving points (9) to (13). The value at 245°C is seen to be about 11% greater than the value first obtained on cooling back from 530°C and is comparable with the thermal conductivity of the zirconium.

Values of the thermal conductivity subsequently obtained for this sample in the low temperature apparatus are seen to confirm this value and to show but little dependence on temperature.

The thermal conductivities at 50°C of alloys of zirconium with tin are shown plotted against the weight percent of tin in Fig. 7. The points of the present investigation again lie reasonably close to a smooth curve. The value of the sample of BING *et al.* that had been induction-melted in graphite is also seen to be in good agreement

with this curve. All the other points lie above the curve and suggest that these samples, as well as those of DEEM[5], MOSS[6] and the Zircaloy 2 tested by THOMAS AND FORSCHER[12] contain less carbon and other additional elements than the alloys of the present investigation.

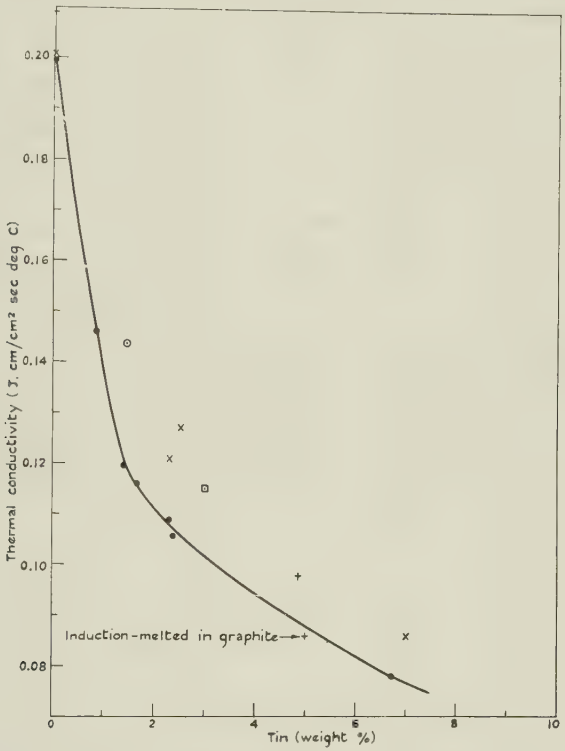

Fig. 7. Thermal conductivity of zirconium–tin alloys at 50°C against wt. % of tin. +, BING, FINK AND THOMPSON[3]; ×, DEEM[5]; ⊡, MOSS[6]; ⊙, THOMAS AND FORSCHER[12]; ●, present work.

Lorenz function of zirconium alloys

Table III contains for each alloy values of the thermal conductivity and electrical resistivity that have been read from Figs. 5 and 3 at temperatures of 50°, 150°and 250°C and a few values at 400° and 600°C read from Fig. 6. The table also includes derived values for the Lorenz function ($K\varrho/T$) and for the ratio T/ϱ.

Only for the 9.79% niobium alloy at 600°C is the Lorenz function comparable with the theoretical value of $2.45 \cdot 10^{-8}$. In all other instances it is much greater and indicates that these alloys possess a considerable lattice component of thermal conductivity. At 50°C this is greatest for the 1.48% aluminium alloy, where it amounts to about 40% of the electronic component, and least for two states of the 7.6% molybdenum alloy and the heat-treated to 705°C form of the 9.79% niobium alloy, where it is about half this value. The electronic component for this latter alloy is nearly doubled after the final heat treatment at about 450°C. The component for the 6.7% tin alloy is large at 50°C but is seen to decrease to about 20% of that of the electronic component at 600°C.

The Lorenz functions previously given in Table II for zirconium are comparable

TABLE III

THERMAL CONDUCTIVITY, ELECTRICAL RESISTIVITY AND LORENZ FUNCTION OF ZIRCONIUM ALLOYS AS READ FROM CURVES OR AS DERIVED FROM EQN. 1[a]

Alloy[a] (Ref. No.)	Temperature (°C)	Temperature °Abs (T)	Thermal conductivity J cm/cm² sec °C (K)	Electrical resistivity microhm cm²/cm (ϱ)	10^8 Lorenz function J ohm/sec °C °Abs (10^8 Kϱ/T)	10^6 T/ϱ
0.84% Sn	50	323	0.146	69.0	3.12	4.68
(756)	150	423	0.152$_5$	84.0	3.03	5.04
	250	523	0.159	96.8	2.94	5.40
	400	673	(0.170$_5$)	113.5	(2.88)	5.93
	600	873	(0.192)	128.6	(2.83)	6.78
1.37% Sn	50	323	0.119$_5$	80.4	2.97	4.02
(776)	150	423	0.133	94.3	2.97	4.49
	250	523	0.147	106.1	2.98	4.93
	400	673	(0.161$_5$)	120.7	(2.90)	5.57
	600	873	(0.186$_5$)	133.1	(2.84)	6.56
1.65% Sn	50	323	0.116	86.2	3.10	3.75
(769)	150	423	0.126	100.0	2.98	4.23
	250	523	0.136$_5$	111.8	2.92	4.68
	400	673	0.156	126.0	2.92	5.34
	600	873	0.185	138.0	2.93	6.32
2.3% Sn	50	323	0.109	95.8	3.23	3.37
(770)	150	423	0.117	107.8	2.98	3.93
	250	523	0.125	118.3	2.83	4.42
	400	673	(0.150)	131.5	(2.93)	5.12
	600	873	(0.176$_5$)	141.4	(2.86)	6.17
2.38% Sn	50	323	0.105$_5$	97.8	3.19	3.30
(771)	150	423	0.119$_5$	109.6	3.09	3.86
	250	523	0.133$_5$	119.6	3.05	4.37
	400	673	(0.150)	131.5	(2.93)	5.12
	600	873	(0.178)	140.2	(2.86)	6.22
6.7% Sn	50	323	0.078	136.3	3.29	2.37
(761)	150	423	0.096	142.4	3.23	2.97
	250	523	0.114	146.6	3.19	3.57
	400	673	(0.134)	150.7	(3.00)	4.46
	600	873	(0.167)	152.5	(2.92)	5.72
1.48% Al	50	323	0.090$_5$	123.4	3.46	2.62
(751)	150	423	0.110$_5$	130.8	3.40	3.23
	250	523	0.130	136.9	3.40	3.82
	400	673	(0.139)[b]	143.7	(2.97)[b]	4.68
	600	873	(0.169)[b]	148.0	(2.87)[b]	5.89
7.6% Mo	50	323	0.086	110.9	2.95	2.91
(666)	150	423	0.116	110.5	3.03	3.83
as-extruded	250	523	0.146	110.5	3.05	4.73
	400	673	(0.171)	113.0	(2.87)	5.96
7.6% Mo	50	323	0.125$_5$	76.0	2.95	4.25
(666)	150	423	0.142$_5$	86.0	2.90	4.92
heat-treated	250	523	0.159$_5$	95.3	2.92	5.49
to 680°C	400	673	(0.180$_5$)	106.4	(2.85)	6.33
9.79% Nb	50	323	0.116$_5$	88.3	3.18	3.66
(749)	150	423	0.131$_5$	95.5	2.97	4.43
as-extruded	250	523	0.146$_5$	102.0	2.86	5.12
	400	673	(0.181)	106.2	(2.86)	6.34

TABLE III (Continued)

Alloy (Ref. No.)	Temperature (°C)	Temperature °Abs (T)	Thermal conductivity J cm/cm² sec °C (K)	Electrical resistivity microhm cm²/cm (ϱ)	10⁸ Lorenz function J ohm/sec °C °Abs (10⁸ Kϱ/T)	10⁸ T/ϱ
9.79 Nb (749) heat-treated to 705°C	50	323	0.138	69.4	2.96	4.65
	150	423	0.151[5]	81.0	2.90	5.22
	250	523	0.164[5]	91.8	2.89	5.70
	400	673	0.181	104.5	2.82	6.44
	600	873	0.189	114.5	2.48	7.62
9.79 Nb (749) heat-treated at 453°C	50	323	0.181	60.5	3.39	5.34
	150	423	0.182	75.6	3.28	5.60
	250	523	0.183	89.0	3.12	5.88

[a] The values in brackets are derived from eqn. 1.
[b] These values are likely to be of the order of 10% low.

at 50°C, where the adjusted mean value indicates the lattice component to be 27% of the electronic component, but by 600°C the value has fallen to about 10%.

For groups of alloys previously investigated[7] a fair correlation has been obtained when the thermal conductivity is plotted against the ratio T/ϱ. The present zirconium alloys have been treated in this manner and the results are shown in Fig. 8. Use is

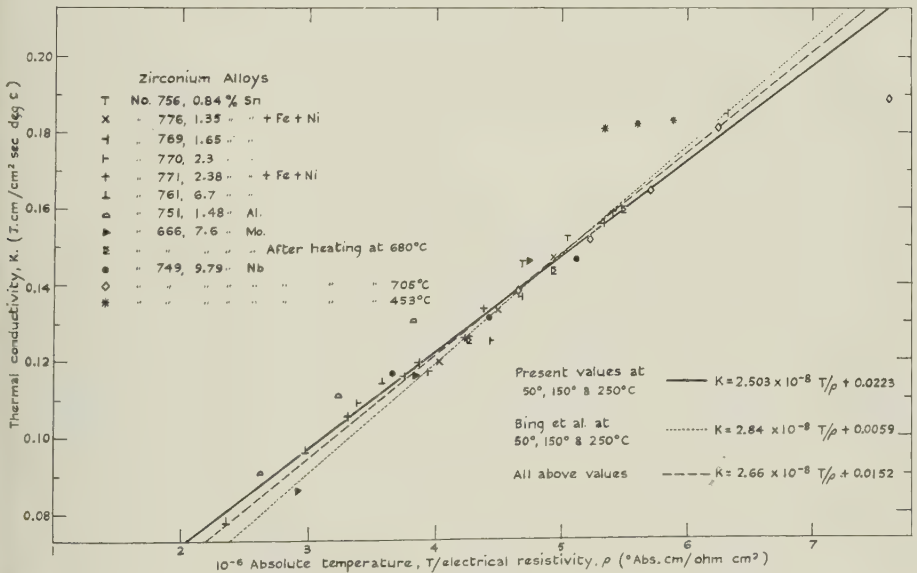
Zirconium Alloys
T No. 756, 0.84 % Sn
× " 776, 1.35 " " + Fe + Ni
H " 769, 1.65 " "
⊢ " 770, 2.3 " "
+ " 771, 2.38 " " + Fe + Ni
⊥ " 761, 6.7 " "
▲ " 751, 1.48 " Al.
▶ " 666, 7.6 " Mo.
" " " " After heating at 680°C
● " 749, 9.79 " Nb
◇ " " " " " " " " 705°C
✱ " " " " " " " " 453°C
Present values at 50°, 150° & 250°C K = 2.503 x 10⁻⁸ T/ϱ + 0.0223
Bing et al. at 50°, 150° & 250°C K = 2.84 x 10⁻⁸ T/ϱ + 0.0059
All above values K = 2.66 x 10⁻⁸ T/ϱ + 0.0152
Thermal conductivity, K. (J cm/cm² sec deg C)
10⁻⁶ Absolute temperature, T/electrical resistivity, ρ (°Abs. cm/ohm cm²)
0.20
0.18
0.16
0.14
0.12
0.10
0.08
1
2
3
4
5
6
7

Fig. 8. Zirconium alloys: thermal conductivity against absolute temperature divided by electrical resistivity.

made of the 50°, 150° and 250°C values of Table III for each alloy in the as-extruded states and for the 7.6% molybdenum and the 9.79% niobium alloys in their first heat-treated states. The heavy line drawn in the figure has been obtained by applying the method of least squares to these data. The equation of the line is

$$K = 2.503 \cdot 10^{-8}\, T/\varrho + 0.0223 \qquad (1)$$

The points for the aluminium alloy depart from this line by the greatest amount, about 11%. All but two of the remainder are within 5%, the 50°C point for the 7.6% molybdenum alloy being 9% low and the 250°C point for the 2.3% tin alloy 6% low. The 400° and 600°C points of Table III are also plotted in the figure. Those for the 1.65% tin alloy agree well with the line as does the 400°C point for the 9.79% niobium alloy. The 600°C point for this alloy is 11% low owing to the disappearance of the lattice component of thermal conductivity, whilst the 50°, 150° and 250° points for this alloy when in the β-phase are respectively 15, 12 and 8% high.

Since BING *et al.*[3] have published results for both conductivities of six zirconium alloys over the range 25–300°C it is tempting to include these values for the same three temperatures in Fig. 8. To do so, however, rather overcrowds the figure and so only the mean line obtained by applying the least-squares method to their data is included and is shown dotted. The points from the data of BING *et al.* do not conform so well to either line since they have a lower temperature coefficient of thermal conductivity and each set of three points tends to cross the line with a reduced slope, instead of progressing in the direction of the line as do most of the points of the present investigation. Due to this difference in behaviour, BING *et al.* had derived the line

$$K = 0.0308\ (1/\varrho - 0.00327)\ T + 0.0381 \qquad (2)$$

as giving the best fit to their data.

The line now shown dotted in Fig. 8 is represented by

$$K = 2.84 \cdot 10^{-8}\ T/\varrho + 0.0059 \qquad (3)$$

All their points lie within 9% of this line, but six are more than 5% above or below it.

On applying the method of least squares to the combined values at 50°, 150° and 250°C of BING *et al.* and of the present work the equation

$$K = 2.66 \cdot 10^{-8}\ T/\varrho + 0.0152 \qquad (4)$$

is obtained and this is shown as a broken line in Fig. 8.

This other investigation included zirconium alloys with 3 and 14% uranium and with 0.07 and 0.16% tantalum as well as the two with 5% tin. Thus a fairly comprehensive range of zirconium alloys has now been studied and it seems reasonable to conclude that eqn. 4 could be used to derive the thermal conductivity of most zirconium alloys to the order of 10% from electrical resistivity measurements. Alloys with aluminium and those in which the β-phase develops at high temperatures or is retained at lower temperatures are likely to involve the greatest uncertainty or to prove exceptions, but those included in this study all lie within 15%, as do all the points for zirconium derived from the data of Table II.

The bracketted thermal conductivity and Lorenz function values included in Table III at temperatures of 400° and 600°C have been derived from eqn. 1.

ACKNOWLEDGEMENTS

The authors wish to acknowledge the help of Mr. G. A. BAINBRIDGE, Mr. J. E. W. JONES AND Miss M. J. WOODMAN, who assisted with some of the experimental work at different periods during the investigation.

The investigation was undertaken at the National Physical Laboratory on behalf of the Atomic Energy Research Establishment and this account is published with their approval and with the permission of the Director of the Laboratory.

REFERENCES

1 F. W. Boulger, The properties of zirconium, *U.S.A.E.C. Rept. AECD-2726* (March 15, 1949).
2 L. R. Vianey, Thermal conductivity of 347 stainless steel and zirconium, *Mass. Inst. of Tech. Dept of Mech. Eng., D.I.C. Project 6627, ONR Contract N5-ori-07827 NR-035-267* (February 15, 1951).
3 G. Bing, F. W. Fink and H. B. Thompson, The thermal and electrical conductivities of zirconium and its alloys, *BMI-65 Contract No. W-7405-eng-92* (April 16, 1951).
4 R. M. Treco, Some properties of high purity zirconium and dilute alloys with oxygen, *A.S.M. Preprint No. 38* (1952).
5 H. W. Deem, Thermal conductivity of zirconium and zirconium-tin alloys, *BMI-849 Contract No. W-7405-eng-92* (July 10, 1953).
6 M. Moss, *Rev. Sci. Inst.* 26 (1955) 276.
7 R. W. Powell and R. P. Tye, *Engineer*, 209 (1960) 729.
8 R. W. Powell and R. P. Tye, *Brit. J. Appl. Phys.*, 11 (1960) 195.
9 *Metals Handbook*, Am. Soc. Metals, 1948, p. 21.
10 A. E. van Arkel, *Reine Metalle*, Springer Verlag, Berlin, 1939, p. 199.
11 C. Zwikker, *Physica*, 6 (1926) 361.
12 D. E. Thomas and F. Forscher, *J. Metals*, 8 (1956) 640.

HARDENING OF A MOLYBDENUM–ZIRCONIUM ALLOY BY NITRIDE DISPERSIONS

A. K. MUKHERJEE AND J. W. MARTIN

Department of Metallurgy, University of Oxford (Great Britain)

(Received February 8th, 1961)

SUMMARY

A 1% Zr–Mo alloy has been nitrided in the temperature range 1100–1500°C, producing a highly stable dispersion of ZrN in Mo. The effects of employing an atmosphere of nitrogen and of ammonia during the isothermal heat treatment have been compared. The dispersed phases have been studied metallographically, and microhardness traverses made of the diffusion layers. The results are discussed in terms of the relationship between hardness, particle sizes, and diffusion rates.

INTRODUCTION

The work described is a continuation of a general study of dispersion hardening in metals, with a view to improving high temperature mechanical properties.

The hardening of a dilute Mo–Ti alloy by nitride dispersions has been the subject of a previous paper[1]; the present work describes the extension of this study to the Mo–Zr system. With its exceptionally large negative free energy of formation, ZrN should form a stable second phase within Mo, and in order to produce such a precipitate the following conditions must be satisfied: (a) solubility of nitrogen in the alloy; (b) the rate of diffusion of nitrogen into the alloy at elevated temperatures should be greater than the rate of diffusion of solute outwards; (c) the stability of the solute metal nitride must be greater than that of the solvent nitride; (d) low solubility of the solute nitride in the matrix.

EXPERIMENTAL

Preparation of alloy

An alloy of 1% Zr in Mo was produced in an argon arc furnace, using a water-cooled copper hearth, a W electrode and 26 cm Hg argon pressure. The arc-cast molybdenum had a C content of 0.015% and the Hf-free zirconium had impurities: Si, 90–250 p.p.m.; Fe, 90–275 p.p.m.

Heat treatment

Two methods of effecting the nitriding have been studied. As in the case of the Mo–Ti alloys[1], a series of specimens were isothermally annealed in deoxidised nitrogen, but in an attempt to increase the rate of nitriding, a second series of heat treatments in ammonia was also carried out.

In each case the heating up and cooling down took place *in vacuo*, and during the

actual process of nitriding the nitrogen or ammonia was led through a previously evacuated glass tube to ensure no atmospheric contamination.

Metallography

After heat treatment, the specimens were mounted in plastic and sectioned for metallographic examination. Details of the mechanical polishing, and the etching for optical and electron metallography were given in the previous paper[1].

Examination of Mo–1% Zr specimens sectioned after nitriding in either nitrogen or ammonia showed microstructures of which Fig. 1 is representative. There was a relatively lighter etching outer rim (A) and beneath this was a darker etching zone (B) in the specimens nitrided at the higher temperature (1500°C). Beyond this there was

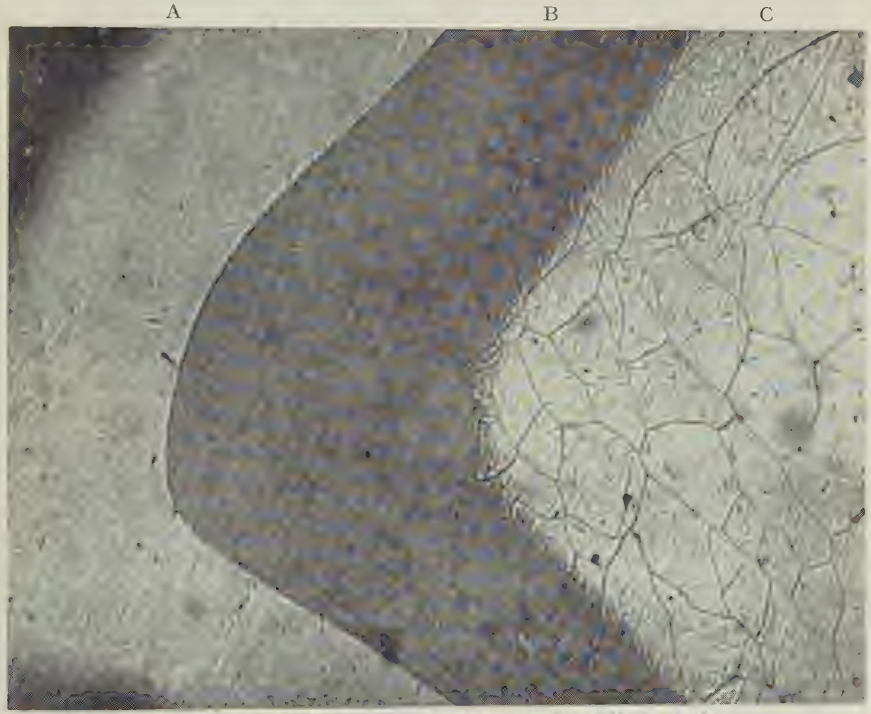

Fig. 1. Mo–1% Zr alloy nitrided in ammonia at 1500°C for 25 h; etched section. (× 150)

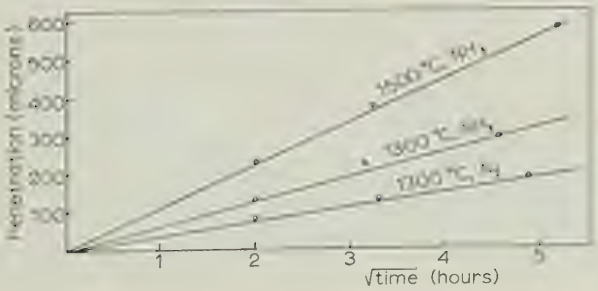

Fig. 2. Rate of nitriding of Mo–1% Zr alloy.

a zone of sub-boundary veining (C) followed by the unchanged matrix. In the zone (B) grain-boundary precipitation with adjacent denuded zones was observed.

The rate of formation of the continuous nitride layer is shown in the curves of Fig. 2. A parabolic law appears to be obeyed for the times and temperatures studied, and it is also evident that the rate of nitriding is greater when carried out in ammonia than in nitrogen. The experimental points were obtained from metallographic sections of nitrided specimens.

Microhardness traverses were made over all sectioned specimens, using a Reichert microhardness indenter and load of 20 g. Typical results appear in Fig. 3(a) and 3(b)

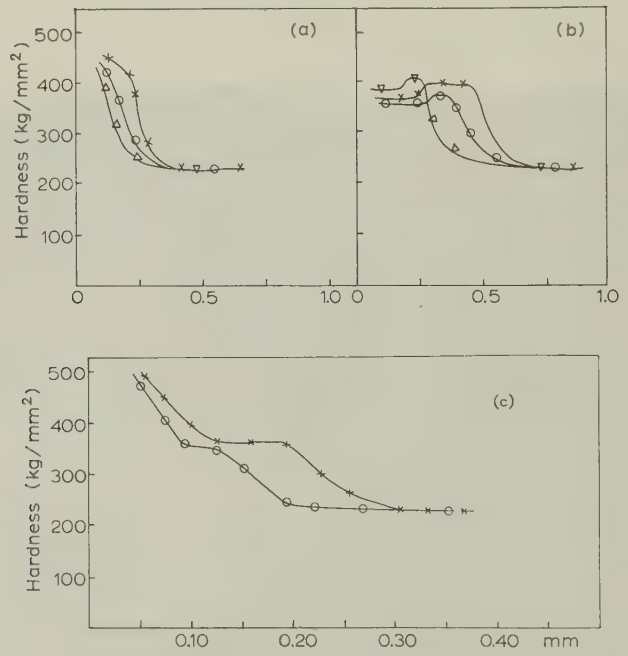

Fig. 3. Reichert microhardness traverses: load 20 g: (a) specimen nitrided at 1300°C; (b) specimen nitrided at 1500°C; △, nitrided for 4 h; O, nitrided for 10 h; ×, nitrided for 27 h; (c) specimens nitrided at 1400°C for 9 h in (i) ammonia and (ii) nitrogen: ×, nitrided in ammonia at 1400°C for 9 h; O, nitrided in nitrogen at 1400°C for 9 h.

for specimens nitrided at 1300°C and 1500°C respectively. It is evident that the lighter-etching outer rim is harder by a factor of more than 2 than the solid solution of Zr in Mo. The microhardness decreases on passing inwards from the surface, the zone of coarse sub-grain particles being unhardened. For the specimens nitrided at 1500°C there is an intermediate hardness peak corresponding to the darker-etching rim in the microstructure. The extent of this intermediate zone of higher hardness increases as the time of nitriding increases (Fig. 3(b)). In order to compare the hardening produced under identical conditions in atmospheres of nitrogen and of ammonia, specimens were given an isothermal anneal for 9 h at 1400°C in each gas. The resulting microhardness curves are shown in Fig. 3(c), and the greater depth of hardening after the ammonia treatment is apparent.

In the specimens nitrided at 1500°C, particles in the hardened zone could readily be resolved by the optical microscope, but they were only just resolvable in specimens nitrided at 1300°C. In both cases, however, the electron microscope readily resolved particles in carbon extraction replicas taken from the hardened zone. Fig. 4 is an electron micrograph showing typical precipitate distribution: there is a plate-like

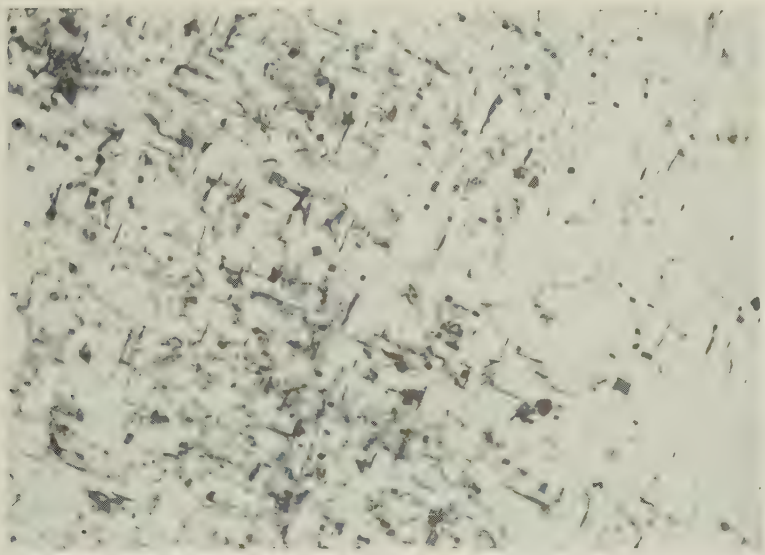

Fig. 4. Mo–1% Zr alloy nitrided in ammonia for 27 h at 1500°C: electron micrograph of carbon extraction replica. (× 9000)

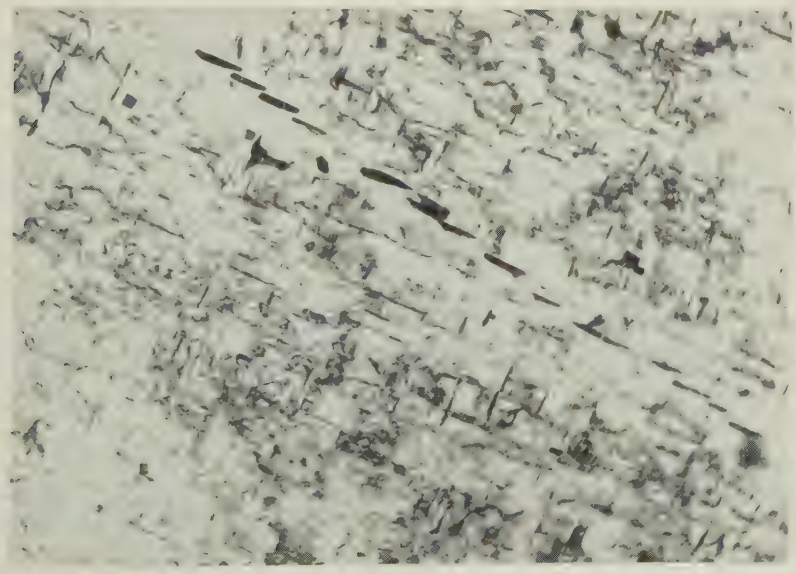

Fig. 5. Mo–1% Zr alloy nitrided in ammonia for 27 h at 1500°C: electron micrograph of carbon extraction replica. (× 9000)

precipitate arranged, apparently, on two mutually perpendicular crystallographic directions, in addition to small particles of square outline lying predominantly with their sides parallel to the directions of the precipitated plates. Fig. 5 shows precipitation along a sub-boundary, consisting of a series of plates lying parallel to one of the sets of precipitates in the lower sub-grain. Coarse precipitated particles along grain boundaries were also observed.

Powder X-ray diffraction techniques were used to identify particles collected by electrolysing a nitrided specimen within a semipermeable membrane. Debye–Scherrer photographs were taken using Cu $K\alpha$ radiation. The high angle reflections corresponded to a f.c.c. lattice with a lattice parameter closely resembling that of ZrN with $a = 4.567$ Å.

In view of the large negative free energy of formation of ZrN, a high stability of the precipitate would be expected. This was confirmed by isothermally annealing nitrided specimens at 1500°C for 11 h. No observable change in microstructure or microhardness resulted from this treatment.

DISCUSSION AND CONCLUSIONS

Since the diffusion mechanism is seen to obey a parabolic law, the coarsening of the structure with depth of penetration can be explained on the same basis: as the diffusion front slows down, the time available for dissociation, diffusion and growth of nitride is increased. The particle size appears also to become coarser with increase of nitriding temperature.

It has been demonstrated that the diffusion front moves at a faster rate when the nitriding is carried out in ammonia than when it is in nitrogen. This effect is presumably related to the ease of dissociation at the metal–gas interface of the NH_3 molecule and the N_2 molecule respectively at these temperatures. Since, in the case of a faster moving front, the time available for dissociation, diffusion and growth of nitride particles is decreased, a finer particle size should result, and this finer dispersion will produce a higher microhardness. Both of these conclusions are confirmed in Fig. 3(c).

The darker-etching layer in the specimens nitrided at 1500°C (Fig. 1) is similar to that observed in the nitriding of Mo–Ti alloys at this temperature[1]. The morphology of the dispersed phase, as revealed by electron microscopy of extraction replicas, differs from that of titanium nitride. In the former alloys, predominantly equiaxed particles were observed, whereas it appears that in the present system the nitrided structure consists of an array of thin rectangular plates precipitated on three mutually perpendicular crystallographic planes.

The present work indicates the possibility of producing dispersion hardening in Mo by means of ZrN particles, and their thermal stability has also been demonstrated. Their high-temperature mechanical properties should be of interest, and it is intended to examine them by creep, high-temperature tensile and hot hardness testing.

ACKNOWLEDGEMENT

The authors are grateful to Prof. W. HUME-ROTHERY, Isaac Wolfson Professor of Metallurgy at Oxford, for his encouragement and for the laboratory facilities made available.

REFERENCE

1 A. K. MUKHERJEE AND J. W. MARTIN, *J. Less-Common Metals*, 2 (1960) 392.

THE SOLID SOLUBILITY OF TANTALUM IN CHROMIUM

J. H. AULD AND N. E. RYAN

Aeronautical Research Laboratories, Department of Supply, Melbourne (Australia)

(Received February 11th, 1961)

SUMMARY

X-ray and metallographic examinations have shown that the solid solubility of tantalum in chromium increases from 1.5 wt.% at 1200°C to 8 wt.% at 1600°C. It has been confirmed that an allotropic modification occurs in the compound $TaCr_2$.

INTRODUCTION

In recent years, considerable attention has been directed to the possibilities of chromium-based alloys as improved gas turbine materials. Many of the alloys investigated have contained significant additions of refractory metals, such as molybdenum, tantalum and tungsten[1-3]. Of these three solute elements, molybdenum and tungsten are in the same group as chromium, and, as would be expected from Hume-Rothery's size-factor and "relative valency" effects, they exhibit extensive solid solubility in chromium. Tantalum, however, is a metal of the preceding group with

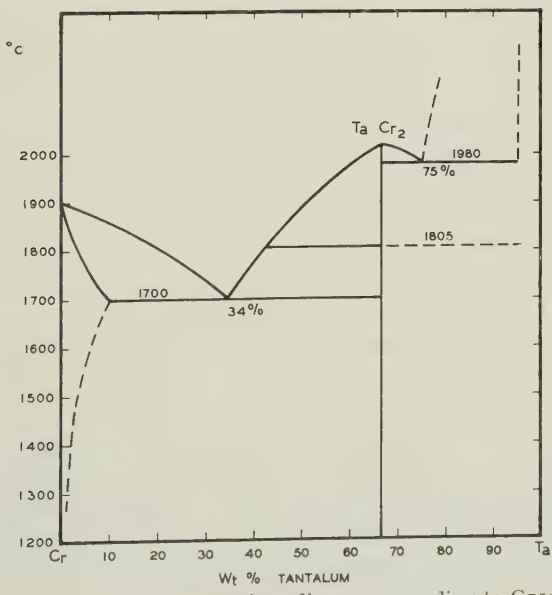

Fig. 1. Chromium–tantalum equilibrium diagram according to GRIGOR'EV *et al.*[5].

an atomic size factor considerably less favourable with respect to chromium. This points to a limited solid solution of tantalum in chromium, and the probability of a decreasing solubility with decreasing temperature. This paper describes the determination of the solubility line.

A preliminary study of the chromium–tantalum system was made by KUBASCHEWSKI AND SPEIDEL[4], and more recently, GRIGOR'EV *et al.*[5] published the diagram reproduced in Fig. 1. From this it is evident that only cursory attention has been paid to the chromium-rich solid solubility curve.

EXPERIMENTAL

The chromium used was an electrolytic product prepared under conditions conducive to very low impurity content[6] (~0.02 wt.% oxygen and less than 0.001 wt.% nitrogen with negligible metallic impurities). The tantalum was a 99.9% pure wire product of the Tantalum Defence Corporation.

The alloys were prepared in an atmosphere of purified argon by tungsten-arc melting on a water-cooled copper hearth. The initial melt was a chromium–30% tantalum master alloy, portions of which were used to make the tantalum additions in all subsequent melts. To ensure homogeneity, these were melted five times in the first furnace operation, removed, crushed, and remelted a further five times.

The 25 g alloy buttons were ground into the form of discs 0.875 in. dia. by 0.2 in. thick. Heat treatment was carried out in a small molybdenum resistance furnace using a purified argon atmosphere. Quenching was effected by shutting off the power to the furnace and applying a blast of cold argon. Measured quenching rate was of the order of 1000°C/min, which, in view of the slow diffusion rates in this alloy system, was found to be amply sufficient to retain the high temperature state. Annealing times are listed in Table I.

TABLE I

ANNEALING TIMES

Temperature (°C)	*Total time at temperature (h)*
1600	5
1500	10
1400	14
1350	14
1270	16
1200	52
1100	96

Metallographic methods were first used to obtain an indication of the solid solubility limit, as it had been reported[4] that the lattice parameter of chromium did not change with tantalum content. However, some X-ray diffraction measurements made to check this showed that reasonable lattice parameter changes were obtained and this was also found by GRIGOR'EV *et al.*[5]. The solubility line was then determined more accurately using the lattice parameter method.

The same specimens that had been used for the metallographic examination were mounted in a Philips X-ray goniometer using a specimen spinner which was also made to oscillate $\pm 7\frac{1}{2}^\circ$ through the focussing position. This latter modification[7] enabled quite smooth lines to be obtained from relatively coarse-grained specimens. A proportional counter was used to measure the 310 reflexion with cobalt radiation. In order to obtain absolute values of the lattice parameters from this single line a small constant correction was made to the calculated values to allow for absorption.

In addition, the application of microhardness measurements of solid solution phase to the determination of solubility limits was attempted, but found to be applicable only to alloys quenched from 1600° and 1500°C. At lower temperatures the distribution of the precipitated phase was such as to prevent measurements without interference from this compound. The results obtained at 1600°C and 1500°C agreed with those obtained by the other methods.

RESULTS

Solid solubility curve

The lattice parameter determinations are listed in Table II and plotted in Fig. 2. The resulting solid solubility curve together with the metallographic observations is shown in Fig. 3.

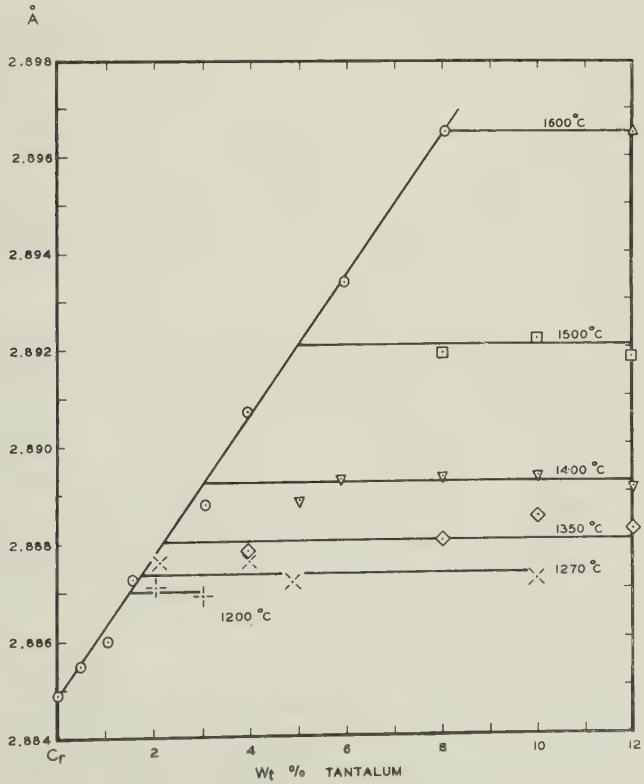

Fig. 2. Lattice parameter *vs.* composition determination.

TABLE II

COMPOSITION AND LATTICE DETERMINATIONS

Chemical composition		*Solid solution parameter*	*Lattice parameter (Å) quenched from*					
Nominal Ta (wt. %)	*Actual Ta (wt. %)*	*(Å ±.0001)*	*1200°C*	*1270°C*	*1350°C*	*1400°C*	*1500°C*	*1600°C*
0	0	2.8849						
0.5	0.48	2.8855						
1.0	1.04	2.8860						
1.5	1.55	2.8873						
2.0	2.05	—	2.8871	2.8876				
3.0	3.01	2.8888	2.8869	—		2.8888		
4.0	3.96	2.8907	—	2.8876	2.8878	—		
5.0	4.86	—	—	2.8872	—	—		
6.0	5.86	2.8934	—	—	—	2.8893		
8.0	8.04	2.8965	—	—	2.8880	2.8893	2.8919	
8.5	—	2.8972	—	—	—	—	—	
10.0	—	—	—	2.8872	2.8885	2.8893	2.8922	
12.0	—	—	—	—	2.8882	2.8890	2.8918	2.8965

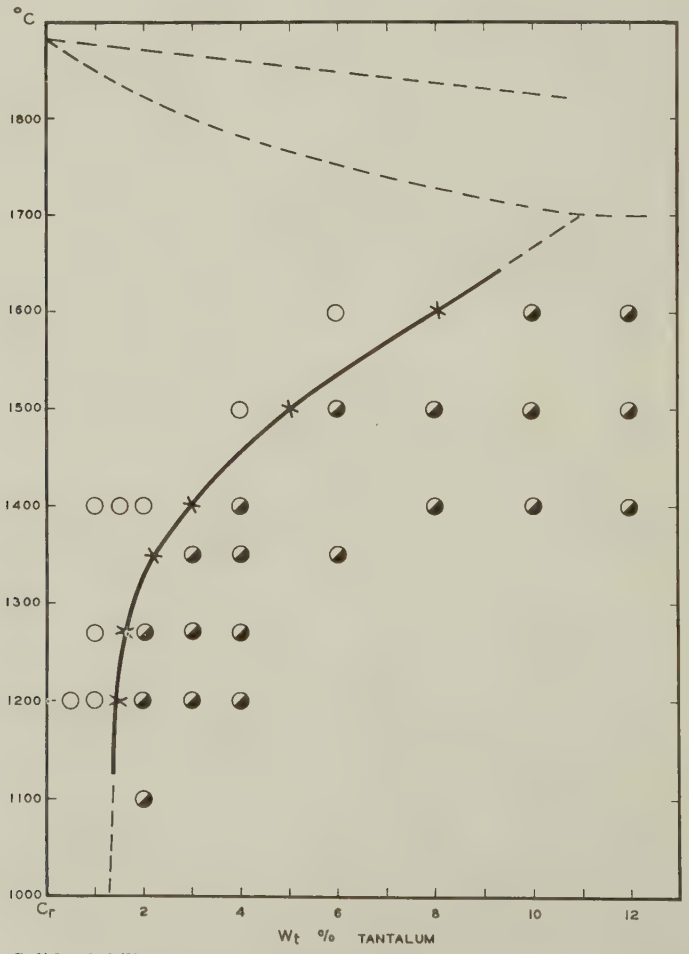

Fig. 3. Solid solubility curve for tantalum in chromium: ×, X-ray determination; metallography: ○, single phase; ◑, two phase.

Allotropy of $TaCr_2$

As indicated in Fig. 1, the phase which comes into equilibrium with the chromium-rich solid solution is the compound $TaCr_2$, and in the course of the X-ray analysis two modifications of this compound were identified. These were a high-temperature hexagonal form ($MgZn_2$ type) and a low-temperature cubic form ($MgCu_2$ type) as reported by DUWEZ AND MARTENS[8]. ELLIOTT[9] found no evidence of this change but this was probably due to too short annealing times at the lower temperatures. In the present investigations it was observed that the transformation at low temperatures was very sluggish and was only complete when the specimens could be worked or when the phase was precipitated from solid solution at temperatures below 1400°C. The behaviour of this compound is very similar to that reported recently for $TiCr_2$[10] and, as in that case, no evidence of a sharp transition temperature was obtained.

CONCLUSIONS

X-ray and metallographic examination have shown that the solid solubility of tantalum in chromium increases from 1.5 wt. % at 1200°C to 8 wt. % at 1600°C. The rate of increase in solubility with temperature rises markedly in the range 1300°C to 1400°C.

Contrary to a previous report[4], the solution of tantalum in chromium causes a significant change in the lattice dimensions, which though relatively small, is sufficient to permit successful application of the lattice parameter method to well-annealed samples.

It has been confirmed that an allotropic modification occurs in the compound $TaCr_2$.

ACKNOWLEDGEMENT

The authors wish to record their thanks to Mr. A. R. EDWARDS for his continued encouragement and to the Chief Scientist, Australian Defence Scientific Service, for permission to publish this paper.

REFERENCES

1 G. R. WILMS AND T. W. REA, *J. Inst. Metals*, 87 (1958–9) 77.
2 A. H. SULLY AND E. A. BRANDES, *J. Inst. Metals*, 81 (1952–3) 578.
3 C. S. LANDAU, H. T. GREENAWAY AND A. R. EDWARDS, *J. Inst. Metals*, 89 (1960–1) 97.
4 O. KUBASCHEWSKI AND H. SPEIDEL, *J. Inst. Metals*, 75 (1948–49) 418.
5 A. T. GRIGOR'EV, V. V. KUPRINA AND N. A. NEDUMOV, *Zhur. Neorg. Khim.*, (English Translation, 4 (1959) 296.
6 H. T. GREENAWAY, *J. Inst. Metals*, 83 (1954–55) 121.
7 R. A. COYLE, to be published.
8 P. DUWEZ AND H. MARTENS, *Trans. A.I.M.E.*, 194 (1952) 72.
9 R. P. ELLIOTT, *Armour Research Foundation Tech. Rept. 1, O.S.R. Tech. Note. O.S.R.-TN-247* (August, 1954).
10 K. A. GROSS AND I. R. LAMBORN, *J. Inst. Metals*, 88 (1959–60) 416.

THE THERMAL AND ELECTRICAL CONDUCTIVITY OF TITANIUM AND ITS ALLOYS

R. W. POWELL AND R. P. TYE

Basic Physics Division, National Physical Laboratory, Teddington, Middx. (Great Britain)

(Received February 15th, 1961)

SUMMARY

Values for the thermal conductivities of three samples of titanium metal and for four titanium alloys are presented, together with values by DEEM, WOOD AND LUCKS[10] for titanium and six titanium alloys.

The lattice component of thermal conductivity of titanium metal is relatively large, and for this reason it is considered preferable to omit the parent metal when correlating the thermal conductivity, K, with the absolute temperature, electrical resistivity ratio, T/ϱ, of titanium alloys.

The present results, expressed as J cm/cm^2 sec°C, are then represented by the equation, $K = 2.39 \cdot 10^{-8}\, T/\varrho + 0.0292$, and the present results, together with those of DEEM *et al.*, by $K = 2.435 \cdot 10^{-8}\, T/\varrho + 0.027$.

These properties are shown to be similar to those of zirconium and zirconium alloys.

INTRODUCTION

The measurements on titanium alloys included in the present paper were undertaken in 1957 and 1958 on behalf of William Jessop and Sons Ltd. (now Jessop-Saville Ltd.), for whom thermal conductivity determinations were reported for the alloys 'Hylite' 20, 30, 40 and 50 over the temperature range 50°–400°C. Electrical resistivity measurements were made at the same time from which it appeared that these alloys constituted another group for which the thermal conductivity could be derived to within 6% or so from a knowledge of the electrical resistivity[1–9].

With the thermal conductivity, K, expressed in J cm/cm^2 sec°C units, the electrical resistivity, ϱ, in ohm cm units and the temperature, T, in °K, the equation of the straight line obtained from these results by the method of least squares was

$$K = 2.39 \cdot 10^{-8}\, T/\varrho + 0.0292 \qquad (1)$$

DEEM *et al.*[10] have subsequently published thermal and electrical conductivity values for titanium and six titanium alloys over a rather wider range of temperature from which they derived an equation, which, converting to the same units is

$$K = 2.62 \cdot 10^{-8}\, T/\varrho + 0.0208 \qquad (2)$$

In these two sets of experiments T/ϱ has ranged from about $2 \cdot 10^6$ to $6 \cdot 10^6$ for which it will be seen that values of K derived from the two equations differ by only —5% and +3% respectively.

The greater slope of the line given by eqn. 2 is partly due to the inclusion by DEEM *et al.* of titanium metal in their correlation. The following account also presents values obtained by us for titanium metal and considers it preferable to omit titanium metal when treating the results in this manner.

In view of the exceptionally low thermal conductivity of titanium alloys, and the consequent increase in experimental uncertainty that is likely to result, the general agreement between these two independent investigations is regarded as very satisfactory, and a correlating equation based on these combined results is now proposed.

NEW DATA FOR TITANIUM ALLOYS

The following are the descriptions of the titanium alloys examined:

Jessop 'Hylite' 20, a 5% Al, 2½% Sn alloy with less than 0.015% H_2;
Jessop 'Hylite' 30, a 2% Al, 2% Mn alloy with less than 0.015% H_2;
Jessop 'Hylite' 40, a 4% Al, 4% Mn alloy with less than 0.015% H_2;
Jessop 'Hylite' 50, a 4% Al, 4% Mo, 2% Sn, 0.5% Si alloy with less than 0.015% H_2.

The alloys were supplied in the form of cylindrical bars 1 in. in diameter and 8 in. in length and their thermal conductivities were determined using the normal comparative longitudinal heat flow method[9] with Armco iron as the standard material. Electrical resistivity measurements were obtained in the course of these tests by passing a current through the rods and using the attached thermocouples to enable the potential drop established across a known length of the rod to be compared with that across a standard resistance carrying the same current. The thermal e.m.f.s developed on the specimen were large but were eliminated by reversing the current each time.

The titanium alloys considered by DEEM *et al.* had been:

A-55, commercially pure Ti;
A-110AT, Ti alloyed with 5% Al + 2½% Sn (similar to 'Hylite' 20);
C-110M, Ti alloyed with 8% Mn;
C-130AM, Ti alloyed with 4% Al + 4% Mn (similar to 'Hylite' 40);
Ti-6Al-4V, Ti alloyed with 6% Al + 4% V;
Ti-140A, Ti alloyed with 2.1% Cr, 2.2% Fe and 2.0% Mo;
Ti-155A, Ti alloyed with 5% Al, 1.4% Cr, 1.5% Fe and 1.2 %Mo.

Table I contains values of the thermal conductivity and electrical resistivity of the 'Hylite' alloys at 50°C temperature intervals over the range 50° to 450°C as read from smooth curves through the experimental points. Corresponding data for the two American alloys of nominally the same chemical compositions are also included. Values of the Lorenz function, $K\varrho/T$, are also presented and are seen to exceed the theoretical electronic value of $2.45 \cdot 10^{-8}$ J ohm/sec°C°K by from about 45 to 66% at 50°C and by about 20–30% at 450°C. The inference is that for these alloys the lattice component of the thermal conductivity is quite appreciable and amounts to the afore-mentioned percentages of the electronic component.

For another somewhat similar alloy RC-130-B manufactured by Rem-Cru Titanium Inc., and stated to contain 0.14% C, 3.99% Al and 4.7% Mn, TYLER *et al.*[11] have made conductivity measurements over the range 17° to 278°K. At this latter temperature, 5°C, their thermal conductivity value is 0.02 cal/cm sec°C (0.084 J cm/cm² sec°C) and the electrical resistivity is 166 microhm cm. These values lead to a still higher Lorenz function of about $5 \cdot 10^{-8}$ J ohm/sec°C°K.

TABLE I

THERMAL CONDUCTIVITY (J cm/cm² sec°C), ELECTRICAL RESISTIVITY (microhm cm) and LORENZ FUNCTION · 10^8 (J ohm/sec°C °K) OF TITANIUM ALLOYS

Mean temp. (°C)	*5% Al + 2.5% Sn*						*2% Al + 2% Mn*			*4% Al + 4% Mn*						*4% Al + 4% Mo + 2% Sn + 0.5% Si*		
	'Hylite' 20			*A–110AT*			*'Hylite' 30*			*'Hylite' 40*			*C–130AM*			*'Hylite' 50*		
	K	*ϱ*	*L*	*K*	*ϱ*	*L*	*K*	*ϱ*	*L*	*K*	*ϱ*	*L*	*K*	*ϱ*	*L*	*K*	*ϱ*	*L*
50	0.076_5	160.8	3.80	0.080	149	3.70	0.099	116.5	3.57	0.080_5	165.0	4.10	0.071_5	162	3.59	0.077_5	160.5	3.85
100	0.083	165.6	3.68	0.084	154.5	3.48	0.104_5	123.1	3.45	0.084_5	168.2	3.81	0.077_5	165.5	3.44	0.081_5	163.7	3.58
150	0.089	170.0	3.58	0.090	159	3.38	0.110_5	130.0	3.40	0.090	171.0	3.64	0.084	169	3.36	0.087	167	3.43
200	0.095	173.4	3.48	0.095_5	164	3.31	0.116	136.8	3.35	0.094_5	173.4	3.47	0.090	173	3.29	0.092_5	172.3	3.37
250	0.100_5	176.7	3.40	0.101	169	3.26	0.121_5	143	3.32	0.099_5	175.2	3.34	0.097	175.5	3.26	0.098	173.0	3.24
300	0.106	179.4	3.32	0.107	173	3.23	0.127_5	149.5	3.33	0.104_5	176.6	3.22	0.104	178	3.23	0.104	175.0	3.18
350	0.111	182	3.24	0.113_5	176	3.21	0.133	155	3.31	0.109	178.0	3.11	0.111	180.5	3.21	0.109	177.0	3.10
400	0.116	184	3.17	0.120	179	3.19	0.138	160.5	3.29	0.114	178.8	3.03	0.118	182	3.19	0.115	177.5	3.03
450	0.121	186	3.11	0.126	181	3.15	—	—	—	0.118_5	180	2.94	0.125_5	183.5	3.19	0.120	178.3	2.96

TABLE II

THERMAL CONDUCTIVITY *K* (J cm/cm² sec°C), ELECTRICAL RESISTIVITY, *ϱ*(microhm cm) and 10^8 · LORENZ FUNCTION, *L*, (J ohm/sec°C °K) FOR TITANIUM METAL

Mean temp. (°C)	*Sample A*			*Sample B*			*Sample C*			*A–55 (Deem et al.[10])*			*Mean L*
	K	*ϱ*	*L*	*K*	*ϱ*	*L*	*K*	*ϱ*	*L*	*K*	*ϱ*	*L*	
20	—	—	—	—	—	—	0.220	42.7	3.21	—	—	—	—
50	0.188_5	56.0	3.27	0.205	51.8	3.29				0.188	54.5	3.17	3.24
100	0.187_5	65.0	3.27	0.201	60.8	3.28				0.184_5	63.5	3.14	3.23
150	0.186_5	73.5	3.24	0.197	70.0	3.26				0.182	72.5	3.12	3.21
200	0.186	82.5	3.24	0.192_5	79.2	3.23				0.180	82.5	3.14	3.20
250	0.185	90.5	3.20	0.189	88.4	3.19				0.178_5	90.5	3.09	3.16
300	0.184	98.5	3.16	0.185_5	97.5	3.16				0.177	98.5	3.04_5	3.12
400	—	—	—	—	—	—				0.178_5	114	3.02	3.09
500	—	—	—	—	—	—				0.182_5	127.3	3.01	3.06

TITANIUM METAL

Tests have been made on three samples of titanium metal, *A*, a normal commercial grade, *B*, a high purity grade and, *C*, a very high purity grade. The last named was stated to have a DPN hardness of 58–62 and was on loan on the understanding that it would not be heated above 50°C. Thermal conductivity measurements on this sample could only be made at mean temperatures of 20° to 25°C.

The high purity sample was used in the first instance for electrical resistivity determinations to a temperature of the order of 1060°C. The *alpha* to *beta* transition occurred in the region 880° to 910°C over which the electrical resistivity decreased from 164.4 to 148.4 microhm cm. On cooling to room temperature the resistivity was observed to have increased, presumably as the result of oxygen pick-up despite an apparently good vacuum having been maintained during heating. The subsequent thermal conductivity determinations were therefore carried out for this sample after ϱ_{20} had risen from 42.9 to 46.5 microhm cm. The corresponding values of ϱ_{20} for samples *A* and *C* were 50.1 and 42.7 microhm cm respectively.

The thermal conductivity and electrical resistivity values obtained for these samples are given in Table II, together with the corresponding values of DEEM *et al.*[10] for their sample of commercial titanium.

The values of the Lorenz functions of these samples of titanium metal are all comparable and are rather lower than those of the alloys. At 50°C the lattice components of the thermal conductivity amount to about one third of the electronic components, whereas for the alloys it is about three fifths. Since the total thermal conductivity of titanium metal is over twice that of the alloys studied, both electronic and lattice components are considerably greater than those for the titanium alloys.

The data of DEEM *et al.* for the A–55 sample are seen to be in fair agreement with the present results. The lower Lorenz functions probably indicate an experimental difference of 3–4%, which should not be regarded as serious, in view of the relatively low thermal conductivity of titanium. An earlier communication[12] from the same laboratory had given slightly higher values for the thermal conductivity of an A–55 sample, which, assuming the same electrical resistivities gives Lorenz functions in closer agreement with those of the present work.

Other determinations of the thermal conductivity of titanium at temperatures above normal have been reported by SILVERMAN[13] and LOEWAN[14], but as electrical resistivity values were not included these values are of rather less interest in connection with the present work.

LOEWAN included three samples of commercially pure titanium for which the thermal conductivity values at 100°C, as read from published curves, range from 0.193 to 0.231 J cm/cm² sec°C. The sample of lowest conductivity was numbered RC–55, and presumably this should be comparable with the A–55 of DEEM *et al.*, which these workers state to have been formally designated RC–55. LOEWAN's values at 50°C are higher, 0.193 compared with 0.184_5, furthermore LOEWAN's thermal conductivity curve shows no minimum but continues to decrease to a value of about 0.174 at 500°C, compared with 0.182_5 of DEEM *et al.* The titanium contents of this sample and of that having the intermediate conductivity are given as 99.64 and 99.75% respectively. That of the sample with highest conductivity is not given.

SILVERMAN's thermal conductivity values for a titanium sample, stated to contain

99.81% of titanium, appear to be low, 0.154 J cm/cm² sec°C at 50°C decreasing linearily to 0.129 at 700°C. His values had previously been considered[15] as likely to err on the low side.

CORRELATION OF THERMAL AND ELECTRICAL CONDUCTIVITY

In Fig. 1 the results of Table I of the present work are shown with the thermal

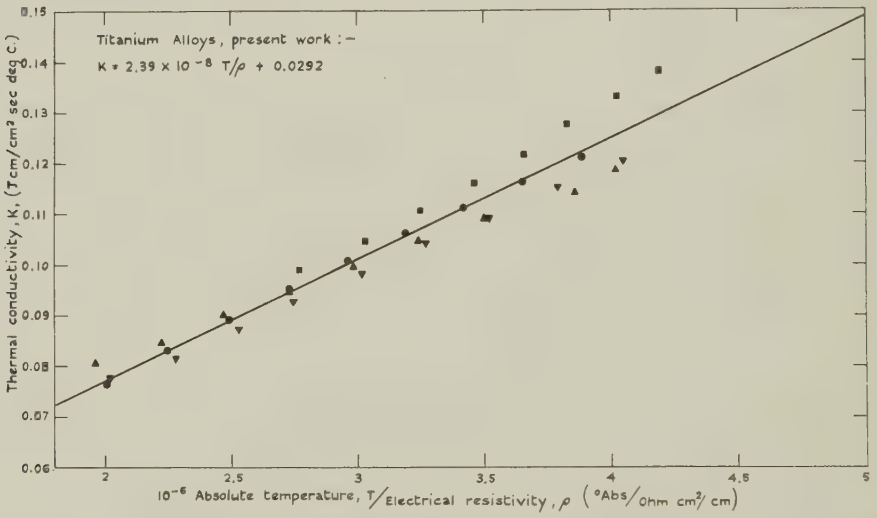

Fig. 1. Thermal conductivity, K, *vs.* ratio of absolute temperature, T, to the electrical resistivity, ϱ. Results obtained in present work for titanium alloys: ●, 5% Al, 2.5% Sn; ■, 2% Al, 2% Mn; ▲, 4% Al, 4% Mn; ▼, 4% Al, 4% Mo, 2% Sn, 0.5% Si.

conductivity plotted against the ratio of the absolute temperature to the electrical resistivity. The straight line

$$K = 2.39 \cdot 10^{-8}\, T/\varrho + 0.0292 \qquad (1)$$

was obtained by the method of least squares from these results.

The experimental points are all seen to lie within ± 7% of this line, whereas the points at 50°C (323°K) for the two samples of titanium metal, samples A and B are respectively 10 and 13% above the line.

The reason for this is apparent when it is recollected that in this equation the numerical coefficient of the first term is the true Lorenz constant, which should approximate to the theoretical value of $2.45 \cdot 10^{-8}$ J ohm/sec°C °K, whilst the constant term is the lattice component of the thermal conductivity. The lattice components for the four alloys derived from Table I, with assumed Lorenz constant of $2.45 \cdot 10^{-8}$, range from 0.027 to 0.036 J cm/cm² sec°C at 50°C and from 0.024 to 0.033 J cm/cm² sec°C at 300°C, and these assumed and derived numbers are comparable with those of eqn. 1. The lattice components of titanium derived in a similar way from the results of Table II, however, decrease from a value of about 0.05 to 0.04 J cm/cm² sec°C over the same temperature range. These lattice components are so much greater than

those of the alloys that the separate treatment of the pure metal and the alloys is justified.

DEEM *et al.* had represented their results for titanium and its alloys by the equation

$$K = 2.62 \cdot 10^{-8} T/\varrho + 0.0208 \qquad (2)$$

The inclusion of the titanium metal values has led to a line of increased slope and lower intercept. The departures of their experimental points from the line were tabulated; the worst percentage deviations are four points in the range 8.1 to 9.4 and two in the range —9.2 to —14.6.

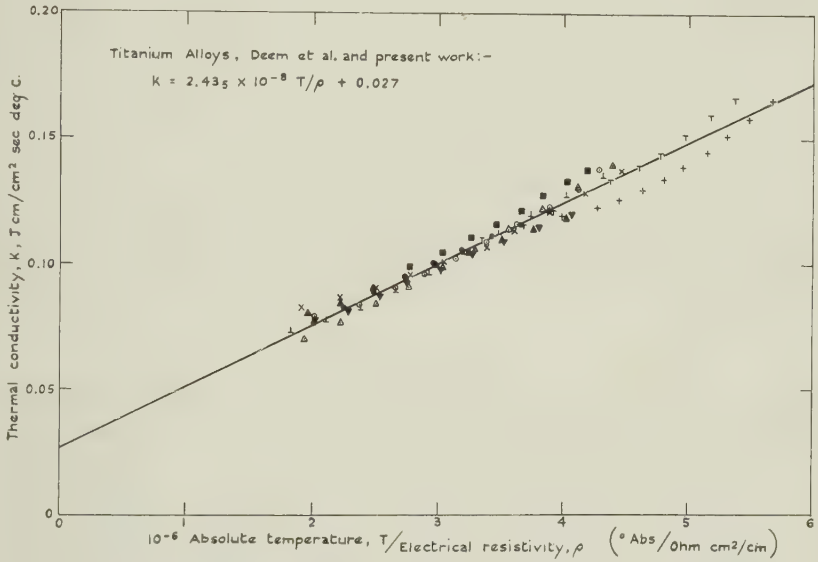

Fig. 2. Thermal conductivity, K, *vs.* ratio of absolute temperature, T, to the electrical resistivity, ρ. Comparison of results for titanium alloys obtained (a) by DEEM *et al.*: ⊙, 5% Al, 2.5% Sn; ⊔, 6% Al, 4% V; △, 4% Al, 4% Mn; ×, 5% Al, 1.4% Cr, 1.5% Fe, 1.2% Mn; +, 2.1% Cr, 2.2% Fe, 2% Mo; ⊤, 8% Mn, and (b) in present work: ●, 5% Al, 2.5% Sn; ■, 2% Al, 2% Mn; ▲, 4% Al, 4% Mn; ▼, 4% Al, 4% Mo, 2% Sn, 0.5% Si.

In Fig. 2 the two sets of data for the titanium alloys are plotted, those of the present work at 50°C intervals over the range 50° to 450°C, and those of DEEM *et al.* at 100°F (55.5°C) intervals over the range 100° to 1000°F (37.8° to 538°C). The equation of the line given by a least squares treatment is

$$K = 2.435 \cdot 10^{-8} T/\varrho + 0.027 \qquad (3)$$

This line has satisfactory numerical coefficients, one point is 12.5% above the line, but all the others are within ±7.5%.

It is suggested that this line can be adopted for deriving the thermal conductivities of titanium alloys, and should in most instances give values correct to within ±8%.

For titanium metal, use should be made of the mean Lorenz functions given in the last column of Table II.

COMPARISON WITH ZIRCONIUM

The elements titanium, zirconium and hafnium constitute one of the sub-groups of Group IV of the periodic table. The writers have recently made thermal and electrical conductivity measurements on zirconium and some zirconium alloys[16] and a comparison is considered of interest.

Both titanium and zirconium undergo transformations from the *alpha*- to *beta*-phase in the temperature range 850 900°C. At this transformation the electrical resistivity of titanium drops by about 10% and that of zirconium by about 16%. In each case the temperature coefficient for the *beta*-phase is very small. The thermal conductivities and electrical resistivities of both metals at normal temperatures are closely the same and both thermal conductivities appear to have minimum values at 300°–400°C. The lattice component K_1 of titanium is, however, greater, being about 0.052_2 J cm/cm² sec°C at 50°C compared with about 0.045 for zirconium. In both cases the lattice components are greater than those of the alloys, hence it is preferable to omit the data for the parent metal in correlations which enable the thermal conductivities of these alloys to be derived from their electrical resistivities.

DEEM[17] has made measurements on a sample of hafnium containing about 2% of zirconium as impurity, and conductivity values for the three metals are presented in Table III. The lattice component is seen to be only 0.038 J cm/cm² sec°C for hafnium despite its rather higher thermal conductivity.

TABLE III

THERMAL CONDUCTIVITY, ELECTRICAL RESISTIVITY AND LORENZ FUNCTION OF TITANIUM, ZIRCONIUM AND HAFNIUM AT 50°C

Metal	*Property, at 50°C*				
	K_{Total}	ϱ	$10^8 \cdot L$	K_{el}	K_1
Titanium	0.205	51.8	3.3	0.153	0.052
Zirconium	0.209	48.1	3.1	0.1645	0.0445
Hafnium*	0.223	40.6	2.8	0.185	0.038

* 2% zirconium as impurity.

On considering the alloys, a difference is at first apparent. Whereas for zirconium alloys the Lorenz function has usually been comparable or only a little greater than that for zirconium metal, for the present titanium alloys it is considerably greater. In view of their smaller lattice component the difference must arise from the relatively smaller electronic component of thermal conductivity in the case of the titanium alloys.

It appears likely, however, that this difference in behaviour can be attributed to the presence of aluminium rather than to a real difference between the main elements. This light element clearly causes a large increase in the resistance due to electrons, and the one zirconium alloy with aluminium had the highest Lorenz function of that series and showed most departure (11%) from the correlating equation

$$K = 2.503 \cdot 10^{-8} T/\varrho + 0.0223 \qquad (4)$$

for the zirconium alloys which we had examined.

Another equation

$$K = 2.66 \cdot 10^{-8}\, T/\varrho + 0.0152 \qquad (5)$$

was obtained when a set of American data was included.

In Table IV values derived for the thermal conductivity from these equations may be compared with the corresponding values for titanium alloys derived from eqns. 1 and 3 for two values of T/ϱ.

TABLE IV

THERMAL CONDUCTIVITY VALUES DERIVED FROM EQUATIONS FOR TITANIUM AND ZIRCONIUM ALLOYS

Equations	*Main element*	*Thermal conductivity* $T/\varrho = 2 \cdot 10^6$	$T/\varrho = 6 \cdot 10^6$
1	Titanium	0.0770	0.1726
3	Titanium	0.0757	0.1731
4	Zirconium	0.0724	0.1724
5	Zirconium	0.0682	0.1746

The results are seen to be very similar. The slightly better thermal conductivity indicated for the titanium alloys at the lower conductivity region may be due to the larger number of alloys of aluminium with titanium that have been included.

ACKNOWLEDGEMENTS

The authors wish to acknowledge the help of Miss M. J. WOODMAN, who assisted with the experimental work. They also wish to record the help given by Mrs. M. K. McQUILLAN, Research Dept., Imperial Chemical Industries Ltd., Kynoch Works, Witton, Birmingham 6, for the loan of the samples of titanium metal. The thermal conductivity determinations on the titanium (Hylite) alloys were undertaken at the National Physical Laboratory on behalf of Jessop-Saville Ltd., Sheffield, Yorkshire, and this account is published with their approval and with the permission of the Director of the Laboratory.

REFERENCES

1 C. S. SMITH AND E. W. PALMER, *Trans. A.I.M.E.*, 117 (1935) 225.
2 L. W. KEMPF, C. S. SMITH AND C. S. TAYLOR, *Trans. A.I.M.E.*, 124 (1937) 287.
3 R. W. POWELL, *Phil. Mag.*, 27 (1939) 677.
4 R. W. POWELL AND M. J. HICKMAN, *Metallurgia*, 41 (1949) 15.
5 M. E. FINE, *Trans. A.I.M.E.*, 188 (1950) 951; *J. Metals*, July (1950).
6 R. W. POWELL, *Iron Steel Inst. (London), Spec. Rept. No.* 43 (1952) 351.
7 R. W. POWELL, *Phil. Mag.*, 44 (1953) 645.
8 R. W. POWELL AND R. P. TYE, *J. Inst. Metals*, 85 (1957) 185.
9 R. W. POWELL AND R. P. TYE, *The Engineer*, 209 (1960) 729.
10 H. W. DEEM, W. D. WOOD AND C. F. LUCKS, *Trans. A.I.M.E.*, 212 (1958) 520.
11 W. W TYLER, L. B. NESBITT AND A. C. WILSON, JR., *Trans. A.I.M.E., Sect. 1*, 5 (1953) 1104.
12 J. W. HOLLADAY, *Memorandum on Thermal Conductivity of Titanium and Titanium Alloys*, Titanium Metallurgical Laboratory, Battelle Memorial Institute, (11th March, 1957).
13 L. SILVERMAN, *J. Metals*, 5 (1953) 631.
14 E. G. LOEWAN, *Trans. ASME*, 78 (1956) 667.
15 R. W. POWELL, *Research*, 7 (1954) 492.
16 R. W. POWELL AND R. P. TYE, *J. Less-Common Metals*, 3 (1961) 202.
17 H. W. DEEM, Thermal conductivity and electrical resistivity of hafnium, *Battelle Mem. Inst. Rept. No. 853*, (July 14, 1953), 12 p.

SCALING OF CHROMIUM IN A HOT GAS STREAM

G. R. WILMS AND T. W. REA

Australian Defence Scientific Service, Defence Standards Laboratories, Department of Supply, Maribyrnong, Victoria (Australia)

(Received February 20th, 1961)

SUMMARY

The scaling behaviour of chromium in a hot gas stream appears to depend on the type of flow over the metal surface, and there is evidence that the gas flow pattern could be a more important factor than the bulk gas composition. The oxide scale produced under certain conditions of gas flow provides some protection against further oxidation and nitriding.

INTRODUCTION

Previous work[1] on the high temperature behaviour of chromium showed that relatively small variations of air flow through a heating chamber at very low flow rates had a marked effect on oxidation behaviour. This observation was considered to be of particular importance, since chromium-base alloys are being developed primarily for use in gas turbine rotor-blading, wherein the metal will be subjected to high-velocity gas streams.

The object of the present work was to examine the scaling behaviour of chromium under conditions simulating those of an aircraft gas turbine engine, and to compare this with the scaling behaviour obtained in a "static" air atmosphere. Although chromium itself is not likely to be used in gas turbine engines, it is necessary to study first the effect of external physical and chemical variables on the basis metal, so that the influence of alloy additions on scaling behaviour under various conditions can subsequently be determined.

EXPERIMENTAL PROCEDURE

Electrolytic chromium, containing 0.0005–0.001% nitrogen, 0.01–0.02% oxygen, and total metallics <0.01 wt.%, was arc melted to give ingots 1½ in diam. 4 in. long. The ingots were extruded to ½ in. diam. bar, care being taken at all stages to avoid pickup of impurities. Cylindrical specimens, 0.4 in. diam. 2 in. long, were then machined from the extruded bars.

The hot gas stream was generated by burning a kerosene (Aviation grade)–air mixture in a large combustion tube*. The specimens were mounted externally near the mouth of the tube in a Nimonic holding block, five specimens being accommodated at the one time. The specimens were spaced 1.5 diam. apart, each specimen being

* The tests were carried out at the Aeronautical Research Laboratories, Department of Supply, Melbourne, Australia.

exposed to the gas stream over a $1\frac{1}{2}$ in. length. Since chromium alloys, with very interesting creep properties at 1038°C (1900°F), have been developed here[2], it was decided to adopt this temperature as standard for the initial study of scaling behaviour in a gas stream. Specimen temperature was measured by an optical pyrometer, the appropriate emissivity corrections being added to the readings. The composition of the gas stream for a specimen temperature of 1038°C was carbon dioxide 7.82%, oxygen 8.45%, water 7.82%, and nitrogen 75.85% by volume, and the gas velocity was of the order of 500 ft./sec. The specimens were heated in runs of $1\frac{1}{2}$ h average, the test being terminated after a total time of 50 h. For comparative tests carried out in a "static" air atmosphere at the same temperature, specimens were continuously heated for equivalent times in a small commercial electric furnace and air-cooled. In order to preserve the surface scales for subsequent metallographic examination, all specimens were first silvered by the Brashear process and then nickel plated[3]. Transverse sections along the length of the specimens were mechanically polished, and then electrolytically etched in a 10% oxalic acid solution.

RESULTS

There were considerable differences in scaling behaviour on each individual specimen, both around the circumference and along the length, this behaviour being common to all specimens. Since there was very little apparent change along the top two-thirds of the exposed length, the scaling behaviour around the circumference for the major part of the specimen length will be considered first.

Fig. 1. Upstream surface, showing thin oxide scale only. (× 500)

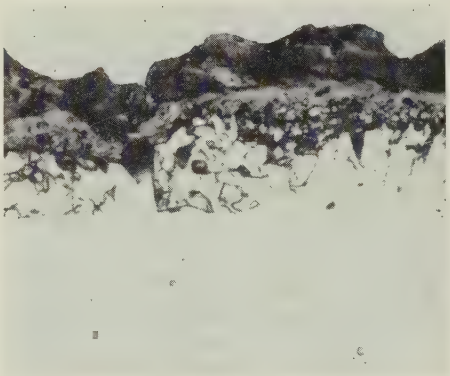

Fig. 2. Downstream surface, showing thick oxide scale and sub-scale nitride. (× 500)

Figs. 1–4. Chromium heated at 1038°C in a hot gas stream for 50 h.

The first feature was the marked difference between the oxide scale on the upstream surface and that on the downstream surface. The oxide on the upstream surface (Fig. 1) was relatively thin and very adherent, whereas the oxide on the downstream surface (Fig. 2) was substantially thicker and considerably less adherent. The second feature was the associated difference in the amount of sub-scale nitride formation. No nitride could be detected on the upstream surface (Fig. 1), whereas a thick nitride layer was present on the downstream surface (Fig. 2). The scaling behaviour at a side surface is shown in Fig. 3, where it will be noted that the oxide scale

is thicker than on the upstream surface (see Fig. 1), and also that there is a thin, discontinuous nitride layer. Between the side and downstream surfaces both the oxide scale and sub-scale nitride rapidly increased to the same order of thickness as that shown in Fig. 2. Between the side and upstream surfaces there was no appreciable change in the appearance of the oxide scale, although the occurrence of the sub-scale nitride was somewhat erratic in that thin discontinuous layers were observed, similar to that shown in Fig. 3, with occasional areas of much thicker nitride.

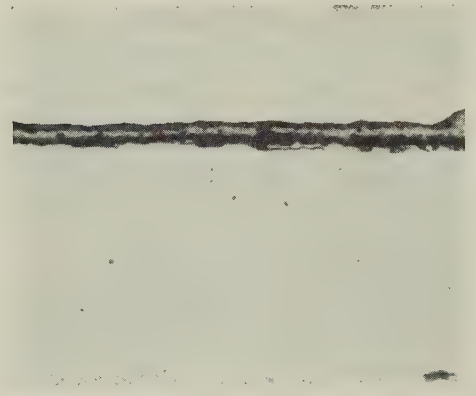

Fig. 3. Side surface, showing oxide scale and a thin discontinuous sub-scale nitride layer. (× 500)

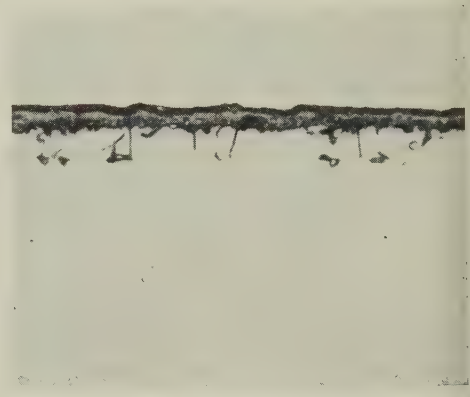

Fig. 4. Upstream surface on bottom portion of specimen, showing oxide scale and sub-scale nitride. (× 500)

Considering next the scaling behaviour around the circumference of the bottom one-third of the exposed length, the appearance of both the oxide scale and the sub-scale nitride on the downstream surface was similar to that previously described. However, certain relative differences in scaling behaviour were observed both on the upstream and side surfaces. The scaling behaviour on the upstream surface is shown in Fig. 4, where it will be noted that the oxide scale is somewhat thicker than in the previous case (see Fig. 1), and also that there is now a relatively thick nitride layer. The scaling behaviour on a side surface was similar to that shown in Fig. 1, which shows a thin oxide scale and no nitride, whereas in the previous case (see Fig. 3), a thicker oxide scale and some sub-scale nitride was observed.

Comparison specimens heated in air for 50 h developed a thick non-adherent oxide scale which completely spalled on cooling. In addition, there was a substantial nitride layer, as shown in Fig. 5, which was similar to that produced on the downstream surface of specimens heated in the hot gas stream (see Fig. 2). However, the scaling behaviour was quite different, in regard to both oxidation and nitriding, to that shown on the upstream or side surface of specimens heated in the hot gas stream (see Figs. 1 and 3).

It is of interest next to examine the effect of heating in air after exposure to the hot gas stream. Again, it is necessary to consider separately the subsequent scaling behaviour of the original upstream or side surface and the downstream surface. In the latter case, the oxide began to thicken and then spall, and the nitride progressively increased in thickness. After 50 h heating time (Fig. 6), the oxide had spalled in many areas, and the sub-scale nitride had increased in depth by nearly the same amount as

that produced by the heating in air alone (see Fig. 5). However, the subsequent scaling behaviour on the original upstream or side surface was substantially different. In this case, there was a gradual thickening of the oxide scale, and sub-scale nitride was only detected after heating for at least 10 h. After 50 h heating time (Fig. 7), the oxide scale had thickened appreciably, but it was still adherent over a large area,

Fig. 5. Chromium heated at 1038°C in air for 50 h, showing thick nitride layer. (× 500)

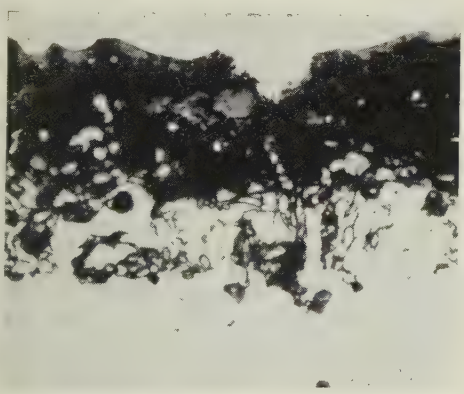

Fig. 6. Downstream surface, showing spalling of thick oxide scale and increase in thickness of the sub-scale nitride layer. (× 500)

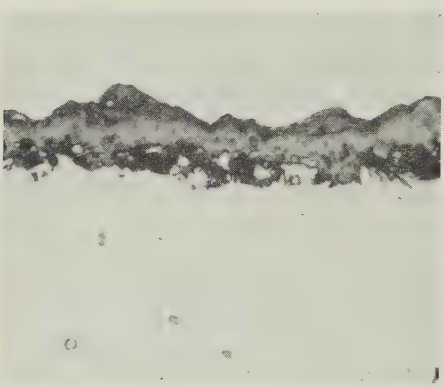

Fig. 7. Upstream surface, showing thickening of oxide scale and the appearance of sub-scale nitride. (× 500)

Figs. 6 and 7. Chromium heated at 1038°C in a hot gas stream for 50 h, and then heated at 1038°C in air for a further 50 h. (× 500)

whereas after merely heating in air for the same period most of the oxide had spalled. There was also some sub-scale nitride, but the depth of penetration was considerably less than that obtained by the heating in air alone (see Fig. 5).

Finally, all oxide scales and sub-scale nitrides were examined by X-ray diffraction methods. In every case the oxide was identified as chromic oxide (Cr_2O_3) and the nitride as β-Cr_2N.

DISCUSSION AND CONCLUSIONS

The essential points brought out by the investigation are as follows:

(1) The scaling behaviour of chromium in a hot gas stream appears to depend largely on the type of flow over the metal surface. Although the flow pattern around the specimens is not known for the particular set of conditions considered, the fact that there are such marked differences in scaling behaviour between the upstream and downstream surfaces over the major part of the exposed specimen length, strongly suggests that the gas flow over these surfaces is radically different. The relative change in scaling behaviour, on both the upstream and side surfaces over the bottom portion of the exposed length, indicates an alteration to the gas flow over these surfaces, possibly by an interference effect of the specimen holder. Since the scaling behaviour on the downstream surface is similar to that obtained by merely heating in air, and this was quite different to that on the upstream surface, it is evident that the type of gas flow over a metal surface could in fact be a more important factor than the bulk gas composition.

(2) The oxide scale formed on chromium in a hot gas stream under certain flow conditions appears to behave as a protective coating. It is significant that no subscale nitride could be detected over the major part of the upstream surface, despite the high nitrogen content of the gas. Since the oxide around the complete circumference of the specimen was found to be chemically the same, the implications are that the physical nature of the oxide scale can vary considerably. Moreover, the relative resistance to scaling of the upstream surface when subsequently heated in air is quite marked, and it appears likely that nitrogen can penetrate to the metal only after some change in the physical form of the oxide scale has occurred.

(3) In relation to more general issues, the need to consider the intended service conditions for a real assessment of high temperature properties is emphasized. The practice of studying the scaling behaviour of new high temperature materials under purely arbitrary conditions, has, in the past, been all too common.

ACKNOWLEDGEMENTS

The authors wish to thank Mr. P. F. WEINRICH for melting and extruding the chromium, Dr. T. MILLS of A.R.L. for his assistance with some of the tests, and Miss J. A. SHERIDAN for the metallographic preparation. The paper is published by permission of the Chief Scientist, Australian Defence Scientific Service, Department of Supply, Melbourne, Australia.

REFERENCES

1 G. R. WILMS AND T. W. REA, *J. Less-Common Metals*, 1 (1959) 411.
2 G. R. WILMS AND T. W. REA, to be published.
3 N. A. BURLEY AND J. J. DALE, to be published.

OXIDATION OF URANIUM ALLOYS IN CARBON DIOXIDE AND AIR

J. E. ANTILL AND K. A. PEAKALL

Atomic Energy Research Establishment, Harwell, Berks. (Great Britain)

(Received February 25th, 1961)

SUMMARY

Weight gain–time curves have been obtained for alloys of uranium containing up to 7.3% silicon, 10% titanium, 5% vanadium, 10% zirconium, 15% molybdenum, 10% niobium and 1% copper in carbon dioxide at 500–1000°C and in air at 500°C.

Additions of titanium, molybdenum, niobium and copper reduced the attack by carbon dioxide at 680–1000°C by factors up to 500. None of the elements was found to be markedly beneficial in carbon dioxide at 500°C and the silicon alloys had a high rate of attack in carbon dioxide at most temperatures.

Additions of molybdenum, titanium and niobium reduced the attack in air at 500°C by factors up to 200.

INTRODUCTION

The existence of an atomic energy power programme in the United Kingdom based upon gas-cooled reactors has necessitated knowledge of the stability of uranium compounds in carbon dioxide and air. Previous work has shown that uranium has little resistance to carbon dioxide, air and water at elevated temperatures whilst indirect evidence during the fabrication of alloys indicates that molybdenum additions are beneficial in air, and American workers have found additions of molybdenum, niobium, zirconium and silicon beneficial in water. However, few systematic investigations have been reported for uranium alloys in gaseous environments, and the present work was therefore undertaken to determine the behaviour of some of the more interesting binary uranium alloys in carbon dioxide and air.

EXPERIMENTAL

Materials

The alloys studied contained 3.8 and 7.3 wt.% silicon, 5 and 10 wt.% titanium, 1 and 5 wt.% vanadium, 3, 6 and 10 wt.% zirconium, 5, 10 and 15 wt.% molybdenum, 5 and 10 wt.% niobium and 1 wt.% copper. They were prepared by arc-melting and were subsequently heat treated for fourteen days at 900°C to homogenize them, followed by a further fourteen days at the test temperature to stabilize the structure. The results could therefore not be affected by changes in the substrate during the experiments. The 5 and 10% niobium alloys contained 400 700 p.p.m. aluminium, 200–300 p.p.m. iron and 300 p.p.m. carbon as the major impurities, whilst the remaining alloys contained only 20 p.p.m. aluminium, 40 p.p.m. iron and 300 p.p.m. carbon. With the exception of the 7.3% silicon alloy the specimens were ma-

chined cylinders approximately 1 cm diameter which were degreased in acetone before use. The 7.3% silicon alloy could not be machined and was therefore used as small round ingots weighing 10 g.

The carbon dioxide was obtained from a solid carbon dioxide ("Cardice") converter and was dried by a bed of magnesium perchlorate so that it contained <20 v.p.m. water vapour. The air was from a laboratory compressed air supply and contained 0.5 vol.% water vapour.

METHOD

The reactions were followed by continuously weighing the samples in a stream of the oxidizing gas on a thermal balance. The specimens were contained in an alumina crucible to retain the non-adherent product and were brought to the test temperature in argon before admitting the oxidizing gas. The temperature of the gas was measured by means of a thermocouple in a silica pocket adjacent to the crucible. The gas was at atmospheric pressure, flowed at 500 ml/min and was preheated before reaching the specimens.

RESULTS

Weight gain *versus* time graphs were obtained for each alloy in carbon dioxide at 500, 680, 800, 900 or 1000°C and in air at 500°C. A selection of the graphs is shown in Figs. 1–4. The time of exposure and extent of the reaction varied with the reactivity

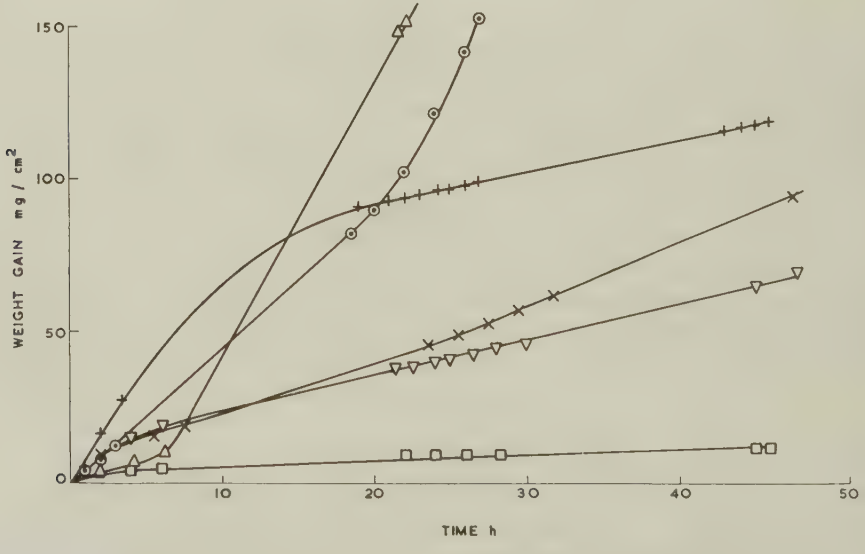

Fig. 1. Weight gain–time curves for uranium alloys in carbon dioxide at 680°C: ⊙, uranium; □, 10% Ti; ×, 10% Mo; +, 15% Mo; △, 10% Nb; ▽, 1% Cu.

of the specimens from 6% oxidation of the available metal during 240 h for the most resistant specimens to 50% oxidation over 12 min for the least resistant. Most of the graphs were linear after an initial period during which the rate either continuously increased or decreased with time. The final linear rates are summarized in Table I;

TABLE I

SUMMARY OF THE OXIDATION RATES OF URANIUM ALLOYS IN CARBON DIOXIDE AND AIR

Alloy	*Rate of weight gain (mg/cm² h) Carbon dioxide*					*Air*
	500°C	*680°C*	*800°C*	*900°C*	*1000°C*	*500°C*
Base uranium	0.1–0.3	3–10	250–330	—	⩽100	90
3.8% Si	7.7	170	1500	1050	—	126
7.3% Si	0.1	140	2500	⩾3000	—	110
5% Ti	15.7	6.2	105	—	10.8	22
10% Ti	1.7(P)	0.2(P)	0.56(P)	—	3.9(P)	50
1% V	0.24	5.9(P)	230	157	—	100
5% V	0.05	5.6	190	95	—	100
3% Zr	0.05	53	340	180	—	80
6% Zr	0.23	25(P)	400	250	—	70
10% Zr	0.2	26(P)	400(P)	230	—	45
5% Mo	0.3	5.1(P)	95(P)	—	21.4	0.66
10% Mo	0.2	2(P)	15(P)	—	19.7	0.48
15% Mo	1 → 8*(P)	1 → 2.5*(P)	0.9 → 3.5*(P)	—	13.7	2
5% Nb	0.15	17	90	—	~20(P)	18
10% Nb	0.23(P)	9(P)	6 → 25*(P)	—	⩽ 5.5(P)	21
1% Cu	0.16	1.2	5.9	—	12.2	64

(P) The surface of the oxidized metal was pitted.
* The rate continuously increased with time due to the formation of deep pits in the metal.

the few cases in which the rate continuously decreased with time are distinguished by less than or equal signs. The results for the unalloyed base metal from which the alloys were made are included for comparison purposes; the rates in carbon dioxide lay at the bottom of the scatter band reported in a previous investigation[1] and there was little or no difference observed between the batches of metal containing different amounts of iron and aluminium.

Preferred areas of attack appeared to exist for some of the titanium, vanadium,

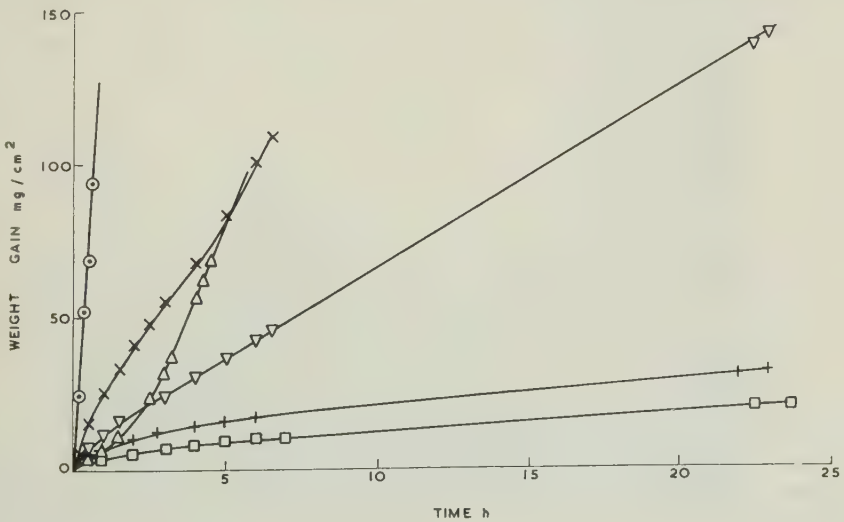

Fig. 2. Weight gain–time curves for uranium alloys in carbon dioxide at 800°C: ⊙, uranium; □, 10% Ti; ×, 10% Mo; +, 15% Mo; △, 10% Nb; ▽, 1% Cu.

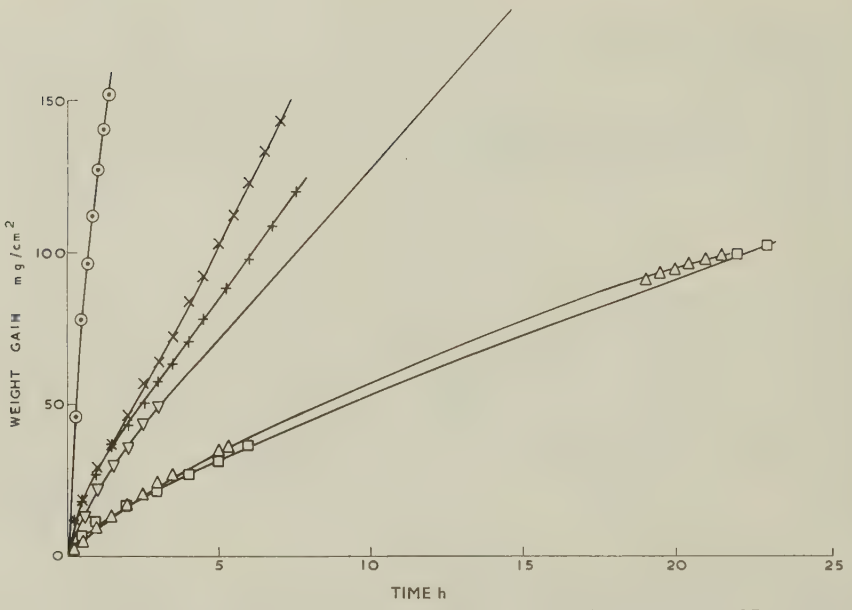

Fig. 3. Weight gain–time curves for uranium alloys in carbon dioxide at 1000°C: ⊙, uranium; □, 10% Ti; ×, 10% Mo; +, 15% Mo; △, 10% Nb; ▽, 1% Cu.

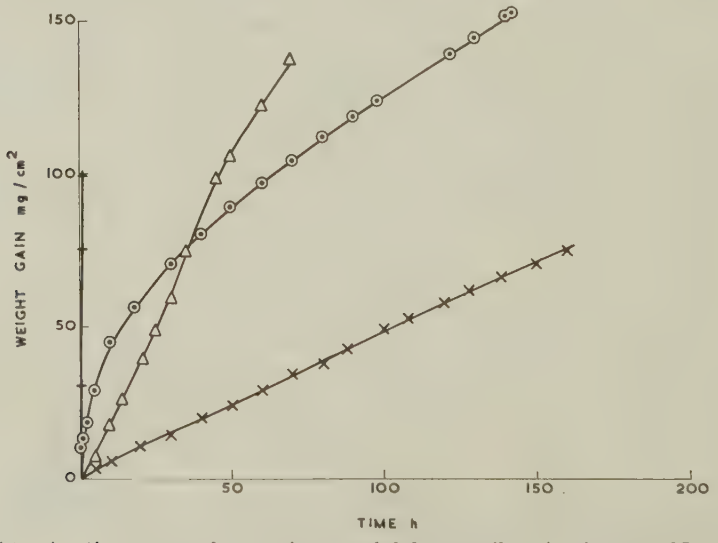

Fig. 4. Weight gain–time curves for uranium–molybdenum alloys in air at 500°C: +, uranium; ⊙, 5% Mo; ×, 10% Mo; △, 15% Mo.

zirconium, molybdenum and niobium alloys in carbon dioxide as they developed pits (Figs. 5 and 6) during some of the tests; the effect was so pronounced in some instances that the reaction rate continuously increased with time. Removal of the oxide on the 15% molybdenum alloy by pickling did not inhibit the growth of the pits, whilst an artificial pit produced by a punch did not grow during subsequent oxidation, indicating that the phenomenon was not associated with the structure of the oxide or the

contours of the surface. Work with an electron probe analyser revealed no gross inhomogeneity in the metal near the pits and metallographic examination showed no preferential attack at grain boundaries or inclusions.

Fig. 5. Gross pitting of a uranium–5% molybdenum alloy in carbon dioxide at 680°C.

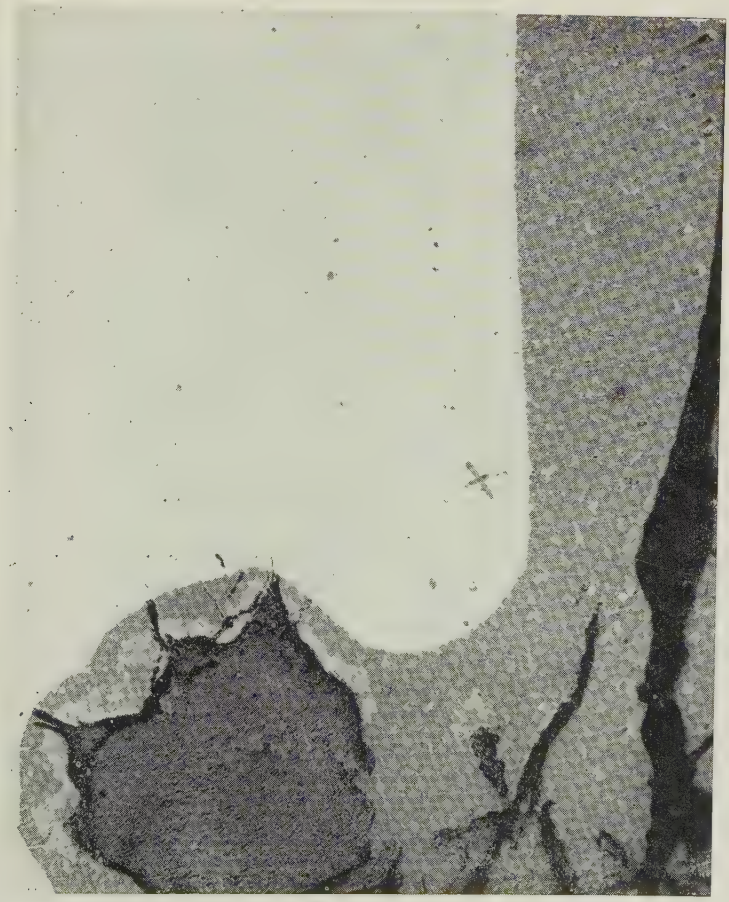

Fig. 6. Section of a pit in a uranium–10% niobium alloy after exposure to carbon dioxide at 800°C. (×750)

Previous experiments have indicated that with a reaction rate of 100 mg/cm^2 h in air the reaction is controlled by the supply of oxygen to the surface of the specimen whilst an equivalent situation does not appear to be reached with carbon dioxide until the rate is $\geqslant$3000 mg/cm^2 h. It follows that the rates obtained for the silicon and vanadium alloys in air are minimum values and might be considerably less than those obtained with a different apparatus providing better access for the oxygen to the metal.

DISCUSSION

The attack of a metal is normally inhibited and controlled by diffusion of ions through an adherent film of the product and hence the nature of the product is important. Unfortunately a discussion of these results is complicated by the fact that the structures and compositions of the oxides formed from most of the alloys are not known with certainty. For unalloyed uranium the final products in carbon dioxide and air are UO_2 and U_3O_8 respectively. Phase data exist only for the two systems of uranium dioxide with silica and zirconia; in the first case there is no solid solubility or compound formation[2] whilst in the second up to 8 mol.% zirconia may form a solid solution with uranium dioxide[3]. Chemical analysis and X-ray powder photographs of the products from the uranium–molybdenum alloys showed that there was no preferential attack or enrichment of one of the constituents in the oxide phase, and that molybdenum dioxide as well as uranium dioxide was formed in carbon dioxide; in air only U_3O_8 could be detected together with one extra line on the X-ray pattern, which was not characteristic of either U_3O_8 or the oxides of molybdenum.

Examination of Table I reveals that additions of vanadium and zirconium had little effect on the oxidation of uranium whilst the other alloy additions produced marked changes in some instances. The differences obtained depended upon the temperature and nature of the gas; the silicon alloys had high rates of attack at most temperatures in carbon dioxide whilst additions of titanium, molybdenum, niobium and copper reduced the attack in carbon dioxide at temperatures $\geqslant$680°C. Molybdenum and to a lesser extent titanium and niobium reduced the attack by air at 500°C. None of the alloys showed a significant improvement over uranium in carbon dioxide at 500°C. As different oxide phases form in air and carbon dioxide for uranium and some of the alloy additions, the differences in behaviour in the two gases are reasonable.

The changes produced by all the alloy additions cannot at the moment be explained satisfactorily although some of the effects may be attributed to changes in the plasticity of the product. The mechanism proposed for the oxidation of a metal which obeys a linear rate law is that a coherent film of oxide is first formed on the surface and that this cracks once the stresses in the oxide reach a critical value. The thickness of the uncracked part of the film next to the metal will vary with time for any particular part of the surface but may be given an average value which will determine the rate of attack, as diffusion of ions through this film should be the slowest stage in the oxidation. An improvement in the plasticity of the oxide produced by an increase in temperature or alloy addition may allow the stresses in the film to be relieved by deformation rather than cracking and may thereby result in a thicker uncracked film and a lower reaction rate. The particle size distributions of the products for the molybdenum alloys in air and the silicon and copper alloys in carbon dioxide

were consistent with a change in plasticity being responsible for the effects of the alloying elements as the particle size varied inversely with the reaction rate (Table II). Further, the products from the highly reactive silicon alloys were extremely brittle, small flakes violently flying off the specimens at the experimental temperature and on cooling.

TABLE II

PARTICLE SIZE DISTRIBUTIONS OF THE OXIDE PRODUCTS

Reaction	*Percentage of oxide in various size ranges*		
	>211 μ	*211–44 μ*	*<44 μ*
Uranium–CO_2 at 680°C	90	8	1.5
1% Cu–CO_2 at 680°C	96	3.3	0.5
3.8% Si–CO_2 at 680°C	72	23	5
Uranium–CO_2 at 800°C	80	19	1.4
1% Cu–CO_2 at 800°C	100	0.01	Nil
3.8% Si–CO_2 at 800°C	77	20	3
Uranium–CO_2 at 1000°C	98	1.7	0.3
1% Cu–CO_2 at 1000°C	100	Nil	Nil
Uranium–air at 500°C	29	49	22
5% Mo–air at 500°C	96	3.6	0.7
10% Mo–air at 500°C	91	7	1.6

The beneficial effects of titanium, niobium and molybdenum in carbon dioxide cannot be readily explained, as there is no obvious correlation between the reaction rate, particle size of the product and plasticity, and no alternative explanation appears consistent with all the results.

Arguments based upon altering the concentration of lattice defects in the oxide and hence the diffusion of ions by alloy additions are often used to explain the effects of alloying elements but objections may be raised to their application in the present work. The uranium dioxide film formed in carbon dioxide is believed to grow by the diffusion of interstitial oxygen ions through the film and hence the uniform distribution of cations with a valency less than four in the film should reduce the concentration of interstitials and the reaction rate. The beneficial effects of titanium, molybdenum, niobium and copper in carbon dioxide may therefore be explained upon this basis as all these elements may have a valency less than four. However, beneficial effects would be expected at the low as well as the high temperatures whilst none was in fact obtained at 500°C. Explanations for the difference in behaviour at different temperatures based upon differences in the metal structure are not convincing as the 10% titanium alloy has the same structure over the range 500–800°C. Further, if niobium and molybdenum are assumed to be beneficial on a lattice defect type argument, improvements should also be obtained with vanadium and zirconium, whilst in practice little effect was obtained with either of these elements. The objection is further supported by the fact that the zirconium ions may be uniformly dispersed as a solid solution in the oxide and hence be in their most effective form.

The pits obtained with the titanium, vanadium, zirconium, molybdenum and niobium alloys in carbon dioxide appear to be associated with impurities, the most important of which is believed to be carbon, because a 9% molybdenum alloy made with pure

uranium containing <50 p.p.m. carbon and <30 p.p.m. metallic impurities did not develop pits when oxidized in carbon dioxide at 680°C for 50 h. In addition, the linear rate of attack of the high purity alloy was only 0.44 mg/cm² h at 680°C, which is the lowest obtained for any molybdenum alloy under these conditions; this result is consistent with the fact that in earlier work[4] high rates of attack by carbon dioxide were obtained for molybdenum alloys high in carbon (0.1–0.16%) and carbide inclusions have been shown to enhance the attack of unalloyed uranium by carbon dioxide at 1 atmosphere and 450°C[5]. The mechanism by which the impurities lead to the formation of pits is not clear, preferential attack of inclusions could not be observed and there is no obvious reason why a pit should continue to grow when formed.

ACKNOWLEDGEMENTS

The authors gratefully acknowledge the assistance of J. W. ISAACS with some of the thermal balance work and F. R. CORLESS of the U.K.A.E.A. Culcheth Laboratories for the supply of the high purity 9% molybdenum alloy.

REFERENCES

1 J. E. ANTILL AND K. A. PEAKALL, *J. Less-Common Metals*, 1 (1959) 227.
2 S. M. LANG *et al.*, *NBS Circular 568*.
3 F. A. MUMPTON AND R. ROY, *J. Am. Ceram. Soc.*, 43 (1960) 234.
4 J. E. ANTILL *et al.*, *AERE M/R Rept. 2805*.
5 J. E. ANTILL AND K. A. PEAKALL, unpublished work.

DERIVATIVES OF TITANIUM WITH COMPOUNDS HAVING BIDENTATE LIGANDS

I. REACTIONS OF TITANIUM TETRACHLORIDE

D. M. PURI AND R. C. MEHROTRA

Dept. of Chemistry, University of Gorakhpur (India)

(Received January 30th, 1961)

SUMMARY

The reaction between titanium tetrachloride and acetyl acetone, ethyl acetoacetate, methyl acetoacetate and methyl salicylate has been studied and the compounds $TiCl_2(acac)_2$, $TiCl_2$(methyl acetoacetate)$_2$, $TiCl_2$(ethyl acetoacetate)$_2$ and $TiCl_2$(methyl salicylate)$_2$ have been isolated. The compound, $[Zr(acac)_3]Cl$, has also been prepared by the reaction between zirconium tetrachloride and acetyl acetone. By molecular weight measurements these compounds have been shown to be monomeric in nature rather than trimeric, as had been assumed by earlier workers.

INTRODUCTION

A derivative with the empirical formula, $TiCl_2(acac)_2$ was prepared by DILTHEY[1] by the reaction between titanium tetrachloride and acetyl acetone. A trimeric structure, based probably on the structures of the corresponding derivatives of silicon and zirconium, $[Si(acac)]_3Cl$ and $[Zr(acac)]_3Cl$, corresponding with the molecular formula, $[Ti(acac)_3]_2TiCl_6$, was also suggested for the above titanium derivative. Similar results were obtained by YOUNG[2]. The corresponding reaction between methyl salicylate[3] and titanium tetrachloride was found to yield a titanium dichloride derivative which was assigned a similar trimeric structure. The reaction between titanium tetrachloride and ethyl acetoacetate has been studied only recently by YU. N. VOL'NOV, GLEZER AND RAIKINA[4], who found that an addition product was obtained at —80°C which on blowing through it at 120°C yielded a titanium dichloride derivative.

Recently, YAMAMOTO AND KAMBARA[5] investigated the reaction between titanium tetraalkoxides and excess acetyl acetone and found that the highest substitution product obtained was titanium dialkoxy diacetylacetonate. By actual molecular weight measurements, these workers have shown that the compound was monomeric with the following plausible structure:

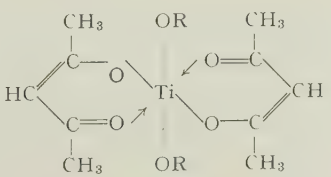

PANDE AND MEHROTRA[6] have shown that titanium dichloride diacetyl acetone can also be obtained by the reaction between titanium diethoxy diacetyl acetone and hydrogen chloride in benzene medium

$$Ti(OEt)_2(acac)_2 + 2\ HCl \rightleftharpoons TiCl_2(acac)_2 + 2\ EtOH$$

The reversible nature of the above reaction was demonstrated by these workers by carrying out the reaction between the titanium dichloride diacetyl acetone derivative and ethanol in the presence of anhydrous ammonia. The ready reversibility of the above reactions suggested a simple structure for titanium dichloride diacetyl acetone:

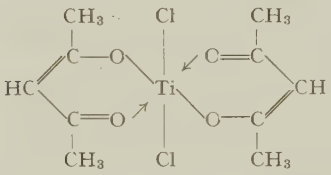

Repetition of the experiments of DILTHEY, ROSENHEIM *et al.* (*loc. cit.*) led to products with the empirical composition already described. However, a determination of the molecular weight in benzene showed them to be monomeric. The corresponding reaction between titanium tetrachloride and methyl acetoacetate also yielded the dichloride derivative, which is monomeric in benzene solution. The fact that this is not due to ionisation when benzene is employed as the solvent, has been confirmed by the determination of its molecular weight in a number of other solvents (acetone, chloroform and carbon disulphide), in all of which the compound is monomeric. Similarly, the corresponding zirconium compound, $[Zr(acac)]_3Cl$, prepared by the reaction of zirconium tetrachloride with acetyl acetone, is monomeric in benzene. This indicates that the molecular weight is not affected by ionisation effects, which might be expected to be more pronounced in the case of zirconium compounds as compared with the titanium compounds.

EXPERIMENTAL

Apparatus

Throughout all the work apparatus with interchangeable glass joints was used. Extreme care was taken to exclude moisture. Fractionations were carried out in a column 30 in. long packed with Raschig rings and fitted to a total condensation variable take-off still head. Molecular weights were determined by means of a semi-micro ebulliometer (Gallenkamp) specially adapted with interchangeable joints, as shown in Fig. 1, to avoid ingress of moisture during the determinations.

Materials

Titanium tetrachloride (b.p. 134°C, E. Merck product) was freshly distilled each time before use. Benzene (B.D.H.) was dried over sodium wire and finally dried azeotropically with ethanol. Acetyl acetone, ethyl acetoacetate (E. Merck) and methyl acetoacetate (May and Baker) were dried by refluxing over aluminium isopropoxide and purified by fractionation. Methyl salicylate was purified by distillation, b.p. 222°C. Acetone and chloroform (B.D.H.) were also dried with aluminium isopropoxide

and fractionally distilled. Carbon disulphide was shaken with a 0.5% solution of potassium permanganate for about 3 h, kept over anhydrous calcium chloride for 24 h, and then finally distilled, b.p. 46°C.

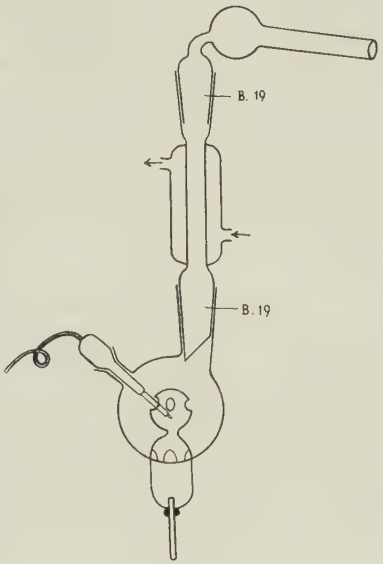

Fig. 1.

Analytical methods

Titanium and zirconium were estimated as dioxides by dissolving the compounds in water, precipitating as hydroxides and igniting. Chlorine was estimated in the filtrate as silver chloride.

REACTIONS

Reaction between titanium tetrachloride and acetyl acetone in benzene

17.5 g acetyl acetone was added to a cooled solution of 7.5 g titanium tetrachloride in 15 ml benzene. Hydrogen chloride gas was evolved as dense fumes and the reaction mixture became hot and gradually turned deep red in colour. After the reaction slowed down the solution was refluxed until all the hydrogen chloride gas was removed ($2\frac{1}{2}$ h). On cooling, yellow orange crystals separated. The supernatant liquid was decanted off and the crystals washed with benzene and dried under reduced pressure at room temperature. 11.68 g yellow-orange crystals were obtained. Found: Ti, 15.33; Cl, 22.64. Required for $TiCl_2(acac)_2$: Ti, 15.12; Cl, 22.40.

Reaction between titanium tetrachloride and methyl acetoacetate in benzene

8.5 g methyl acetoacetate was added to 6.5 g titanium tetrachloride in 30 ml benzene. Hydrogen chloride gas was evolved and the reaction mixture became hot and turned red in colour. After refluxing ($2\frac{1}{2}$ h) to remove HCl, the reaction mixture on standing overnight deposited 11.0 g orange-red crystals which were dried under

reduced pressure at room temperature. Found: Ti, 14.14; Cl, 20.34. Required for $TiCl_2$(methyl acetoacetate)$_2$: Ti, 13.75; Cl, 20.34.

Reaction between titanium tetrachloride and ethylacetoacetate in benzene

The reaction between 5.5 g titanium tetrachloride in 25 ml benzene and 8.5 g ethyl acetoacetate was similar to those described above. The orange crystals (10.5 g) obtained by drying at 60°–70°C under reduced pressure gave: Ti, 12.70; Cl, 18.59. Required for $TiCl_2$(ethyl acetoacetate)$_2$: Ti, 12.74; Cl, 18.84.

Reaction between titanium tetrachloride and methyl salicylate in benzene

The reaction between 10.78 g titanium tetrachloride in 50 ml benzene and 19.78 g methyl salicylate yielded 23.1 g orange crystals. Found: Ti, 11.6; Cl, 16.88. Required for $TiCl_2$(methyl salicylate)$_2$: Ti, 11.4; Cl, 16.87.

Reaction between zirconium tetrachloride and acetyl acetone in benzene

2.8 g acetyl acetone was added to 0.9 g zirconium tetrachloride in 15 ml benzene. The solution became slightly hot and some turbidity appeared which disappeared on refluxing. Hydrogen chloride gas was evolved but no change in colour took place. The mixture was refluxed for 4 h to remove all the hydrogen chloride gas produced. On cooling, a white crystalline compound (1.5 g) was obtained. The benzene was decanted off and the crystals were dried under reduced pressure at room temperature. Found: Zr, 21.58; Cl, 8.40. Required for $[Zr(acac)]_3Cl$: Zr, 21.40; Cl, 8.36.

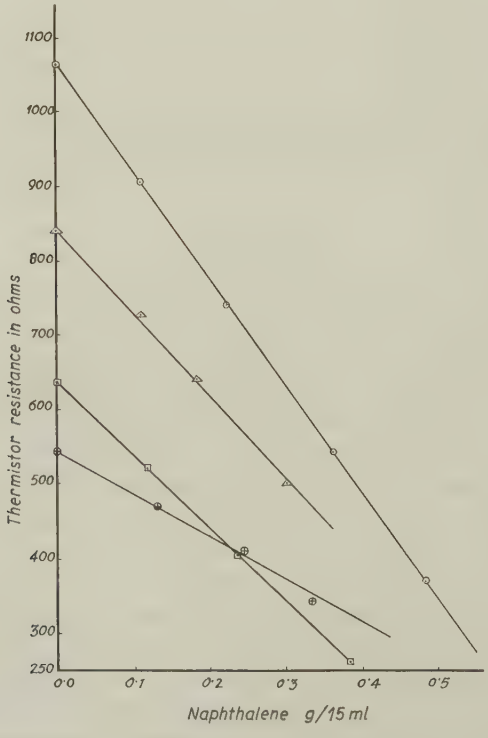

Fig. 2. ⊕, Benzene; △, acetone; ⊙, carbon disulphide; ⊡, chloroform.

Determination of molecular weights

Molecular weights were determined in a semi-micro ebulliometer (Gallenkamp), using thermistor sensing with the help of which the changes in the boiling points were recorded by the change in the resistance of the thermistor. The resistance of the thermistor, over the small range of temperature encountered in the present ebulliometric work, varies almost linearly with the temperature and hence its decrease can be taken as proportional to the increase in boiling point of the solution. This is shown in Fig. 2 in which naphthalene has been used as the calibration solute from which the appropriate "ebulliometric constants" in terms of the decrease of the resistance of the thermistor can be derived.

The solvents used in the determinations were benzene, chloroform, acetone and carbon disulphide (15 ml in each case). The constants of these solvents are given below:

benzene	77200
acetone	137700
chloroform	127400
carbon disulphide	186600

The following formula was applied for the determination of the molecular weights:

$$M = \frac{kw}{-\Delta R}$$

where M is the molecular weight of the unknown compound, k is the constant for the thermistor and solvent used, w is the weight of the compound added to the solvent, and $-\Delta R$ is the observed difference in resistance of the thermistor for the above quantities of solute and solvent.

RESULTS

The results of the determinations are shown in Tables I–V.

TABLE I

MOLECULAR WEIGHT OF TITANIUM DICHLORIDE DIACETYL ACETONE

Solvent (15 ml)	*Amount of substance used (g)*	*Observed mol. wt.*	*Average mol. wt.*	*Calc. mol. wt.*
Benzene	0.2482–0.5360	336.2, 337.9, 348.2, 338.8	340.2	316.8
Acetone	0.1232–0.3265	297.8, 291.2, 288.1, 284.7	290.4	
Chloroform	0.1289–0.3521	298.3, 335.3 314.6, 321.5	317.4	
Carbon disulphide	0.0326–0.0826	301.1, 302.2, 297.0	300.1	

TABLE II

MOLECULAR WEIGHT OF TITANIUM DICHLORIDE DIMETHYLACETOACETATE

Solvent (15 ml)	*Amount of substance used (g)*	*Observed mol. wt.*	*Average mol. wt.*	*Calc. mol. wt.*
Benzene	0.0719–0.3557	370.0, 367.4, 368.7, 379.2, 381.9	373.4	348.8

TABLE III

MOLECULAR WEIGHT OF TITANIUM DICHLORIDE DIETHYLACETOACETATE

Solvent (15 ml)	*Amount of substance used (g)*	*Observed mol. wt.*	*Average mol. wt.*	*Calc. mol. wt.*
Benzene	0.0861–0.2764	349.7, 351.0, 351.4, 349.8	350.4	376.8

TABLE IV

MOLECULAR WEIGHT OF TITANIUM DICHLORIDE DIMETHYL SALICYLATE

Solvent (15 ml)	*Amount of substance used (g)*	*Observed mol. wt.*	*Average mol. wt.*	*Calc. mol. wt.*
Benzene	0.1074–0.3390	427.4, 433.1 432.0, 436.9	432.1	420.8

TABLE V

MOLECULAR WEIGHT OF $Zr(acac)_3Cl$

Solvent (15 ml)	*Amount of substance used (g)*	*Observed mol. wt.*	*Average mol. wt.*	*Calc. mol. wt.*
Benzene	0.0505–0.2135	433.2, 463.5, 463.7, 449.1	452.3	423.6

REFERENCES

1 W. Dilthey, *Chem. Ber.*, 37 (1904) 588.
2 R. C. Young, *Inorg. Syntheses*, 20 (1946) 119.
3 A. Rosenheim, *Chem. Ber.*, 48 (1915) 447.
4 Yu. N. Vol'nov, P. M. Glezer and I. Ya. Raikina, *Sbornik Statei Obshcheĭ Khim. Akad. Nauk. S.S.S.R.*, 2 (1953) 976.
5 A. Yamamoto and S. Kambara, *J. Am. Chem. Soc.*, 79 (1957) 4344.
6 K. C. Pande and R. C. Mehrotra, *Chem. & Ind.*, (1958) 1198.

DERIVATIVES OF TITANIUM WITH COMPOUNDS HAVING BIDENTATE LIGANDS

II. REACTIONS OF TITANIUM ALKOXIDES WITH METHYL ACETOACETATE

D. M. PURI AND R. C. MEHROTRA

Dept. of Chemistry, University of Gorakhpur (India)

(Received February 27th, 1961)

SUMMARY

The reactions of titanium alkoxides (ethoxide, isopropoxide and butoxide) with methyl acetoacetate have been found to yield two types of derivatives — trialkoxy titanium monomethyl acetoacetate and dialkoxy titanium dimethyl acetoacetate; whereas the latter does not react with further amounts of methyl acetoacetate, both have been shown to interchange completely their alkoxide groups with higher alcohols and a number of new products have been isolated. The dialkoxy derivatives distil under reduced pressure with only slight decomposition but the trialkoxy derivatives also disproportionate to give the dialkoxy derivatives.

INTRODUCTION

The possibility of reaction between titanium alkoxides and bidentate chelating agents such as diacetone alcohol, acetyl acetone and ethyl acetoacetate was shown first by SCHMIDT[1] (1952) and later by REEVES AND MAZZENO[2] (1954). Although the reaction products were neither isolated nor analysed, these workers postulated the formation of hexa-coordinated compounds such as $(OR)_4Ti(acac)$ and $(OR)_2Ti(acac)_2$. The reactions of titanium alkoxides with acetyl acetone[3] and ethyl acetoacetate[3,4] have been investigated recently and products of the type $(OR)_3Ti(acac)$, $(OR)_2Ti(acac)_2$, $(OR)_3Ti(etac)$ and $(OR)_2Ti(etac)_2$ have been actually isolated.

The reactions between titanium alkoxides and methyl acetoacetate have not been investigated at all. This was of particular interest in view of a recent study by VARMA AND MEHROTRA[5] of the comparative reactivity of alkoxy groups OMe $\gg$ OEt $>$ OPr^i $>$ OBu^t in the alkoxides. It has been shown that the reaction between titanium alkoxides $Ti(OR)_4$ (R = Et, OPr^i or Bu) and methyl acetoacetate (meac) in the molar ratio of 1 : 1 and 1 : 2 can be represented by the following probable SN_2 type mechanism yielding derivatives represented by I and II:

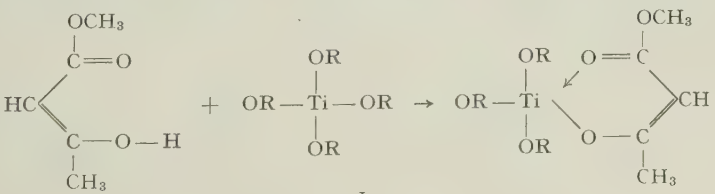

I

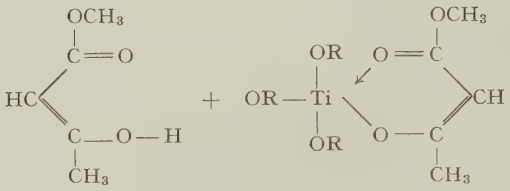

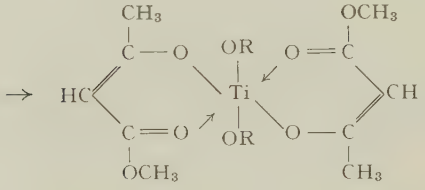

II

The reactions have been followed by estimating the alcohols produced in the reactions after their removal azeotropically with benzene; the products have been isolated and analysed. Further non-replacement of the alkoxy groups by methyl acetoacetate could be ascribed to the saturated coordination state of compound II. This appears to be confirmed by the observed approximately monomolecular state of the derivatives in the boiling benzene (Table III). However, a slight tendency towards dimerisation is present in all cases, the slight differences observed being explicable on the basis of the following observed molecular complexities of titanium alkoxides[6,7,8] themselves in benzene:

alkoxide:	$Ti(OEt)_4$	$Ti(OBu)_4$	$Ti(OPr^i)_4$	$Ti(OBu^t)_4$
molecular complexity:	2.4	1.4	1.4	1.0

On attempting to distil derivatives I and II, it was found that the dialkoxy dimethyl acetoacetate derivatives distil under vacuum with only very slight decomposition, whereas the trialkoxy monomethyl acetoacetate derivatives disproportionate into the dimethyl acetoacetate derivative and the tetra-alkoxide:

$$2\ (OR)_3Ti(meac) \rightarrow (OR)_2Ti(meac)_2 + Ti(OR)_4$$

Furthermore, it has been shown that the products I and II interchange their alkoxy groups with higher alcohols quantitatively, yielding new products (Table II). These reactions are of interest for synthetic purposes and also indicate that although II does not react with further methyl acetoacetate, the six-coordinate structure is sufficiently mobile to coordinate and react with a higher alcohol:

EXPERIMENTAL

Apparatus

The apparatus used for synthetic and ebulliometric work was described in part I[9].

Materials

Titanium ethoxide and isopropoxide (Peter & Spence) and butoxide (B.D.H.) were distilled and analysed before use. Methyl acetoacetate (May & Baker) was dried by refluxing over aluminium isopropoxide and fractionally distilled at 168–170°C. Benzene was dried over sodium wire and then azeotropically distilled with ethanol. Isopropanol, *n*-butanol and *tert*-butanol (B.D.H.) were also dried in the same way and fractionally distilled.

Analytical methods

Titanium was estimated as titanium dioxide by ignition of the product obtained on hydrolysis with one drop of ammonia. Ethanol and isopropanol were estimated oxidimetrically with normal $K_2Cr_2O_7$ solution in 12.5% sulphuric acid[10]. The excess of dichromate was titrated against sodium thiosulphate solution iodometrically.

REACTIONS

Reaction between titanium alkoxide and methyl acetoacetate in the molar ratio of 1 : 1 in benzene

Methyl acetoacetate was added to titanium alkoxide in benzene solution. Heat was produced and the colour changed to yellow. The reaction mixture was refluxed for $2\frac{1}{2}$ h over the column and then the benzene–alcohol azeotrope was removed at a bath temperature of 120–130°C. On cooling, a yellow solution was obtained. The volatile components were then removed from the product under reduced pressure at a bath temperature of 50–60°C. A yellow liquid or solid compound was obtained. The azeotrope contained the theoretical amount of one mole of alcohol. The compound was analysed and on distillation was found to decompose to a dialkoxy derivative. For brevity the results of the above type of reaction (1–3) are given in Table I.

Reaction between titanium alkoxide and methyl acetoacetate in the molar ratio of 1: > 4 in benzene

Excess methyl acetoacetate was added to titanium alkoxide in benzene solution. Heat was evolved and the colour changed to yellow. The mixture was then refluxed for 2–3 h over the column at a bath temperature of 120°C and then the azeotrope removed. After cooling the reaction mixture, the volatile fraction was removed under reduced pressure at a bath temperature of 60°C. A slight viscous orange–yellow liquid was obtained. The theoretical amount (2 moles) of alcohol was obtained. The compound was analysed before and after the distillation. The results of the above reactions are given (4–7) in Table I.

TABLE I

REACTIONS OF TITANIUM ALKOXIDES WITH METHYL ACETOACETATE

No.	Compound (g)		Methyl acetoacetate (meac) (g)	Product and state (g)	Amount of alcohol in azeotrope (g)		Analysis (% Ti)		Distillation
					Found	Calc.	Found	Calc.	
1	$Ti(OEt)_4$	3.82	1.94	$Ti(OEt)_3(meac)$ Light yellow solid (4.36)	0.76	0.77 (1 mole)	15.96	16.11	149 150°/2.5 mm Found: Ti, 13.4 Calc. for $Ti(OEt)_2(meac)_2$ Ti, 13.04
2	$Ti(OPr^i)_4$	4.04	1.85	$Ti(OPr^i)_3(meac)$ Light yellow liquid (4.97)	0.86	0.85 (1 mole)	13.99	14.10	
3	$Ti(OBu^n)_4$	3.23	1.14	$Ti(OBu^n)_3(meac)$ Yellow liquid (3.61)			12.71	12.56	159–160°/2 mm Found: Ti, 10.61 Calc. for $Ti(OBu^n)_2(meac)_2$ Ti, 11.34
4	$Ti(OEt)_4$	3.28	6.85	$Ti(OEt)_2(meac)_2$ Orange–yellow liquid (5.1)	1.13	1.32 (2 moles)	13.04	13.04	139–140°/0.1 mm Found: Ti, 12.45 Calc. for $Ti(OEt)_2(meac)_2$ Ti, 13.04
5	$Ti(OEt)_4$	6.23	6.35	$Ti(OEt)_2(meac)_2$ (10.4)	2.45	2.46 (2 moles)	12.98	13.04	159–160°/5 mm Found: Ti, 12.46 Calc. for $Ti(OEt)_2(meac)_2$ Ti, 13.04
6	$Ti(OPr^i)_4$	4.33	3.86	$Ti(OPr^i)_2(meac)_2$ Reddish yellow liquid (5.97)			12.07	12.13	
7	$Ti(OBu^n)_4$	5.25	3.67	$Ti(OBu^n)_2(meac)_2$ Yellow–orange liquid (6.51)			11.05	11.34	220–225°/15 mm Found: Ti, 10.95 Calc. for $Ti(OBu^n)_2(meac)_2$ Ti, 11.34

Reaction between titanium trialkoxy monomethyl acetoacetate and higher alcohols in benzene

Various amounts of higher alcohols were added to titanium trialkoxy monomethyl acetoacetate in benzene solution. No heat was evolved and no change in colour occurred. After refluxing the reaction mixture for 2–3 h, the azeotrope was fractionally distilled off. The solution was cooled and dried under reduced pressure at a bath temperature of 40°C. The compound obtained was analysed and the alcohol in the azeotrope estimated. The results of the above reactions are given (1–5) in Table II.

TABLE II

REACTIONS BETWEEN TITANIUM TRIALKOXY MONOMETHYL ACETOACETATE AND TITANIUM DIALKOXY DIMETHYL ACETOACETATE AND HIGHER ALCOHOLS

No.	Reactants	Amount (g)	Product (g)	Analysis (% Ti) Found	Calc.	(Amt. alc.) Found	Calc.
1	$Ti(OEt)_3(meac)$ isopropanol	1.4 1.06	$Ti(OPr^i)_3(meac)$ (1.49)	14.37	14.10	0.58	0.64
2	$Ti(OEt)_3(meac)$ *n*-butanol	0.82 0.71	$Ti(OBu^n)_3(meac)$ (1.00)	12.75	12.56		
3	$Ti(OEt)_3(meac)$ *tert*-butanol	2.07 1.90	$Ti(OBu^t)_3(meac)$ (2.60)	12.74	12.56	0.88	0.93
4	$Ti(OPr^i)_3(meac)$ *n*-butanol	0.77 0.53	$Ti(OBu^n)_3(meac)$ (0.84)	12.53	12.56		
5	$Ti(OPr^i)_3(meac)$ phenol	3.92 3.26	$Ti(OPh)_3(meac)$ Yellow–orange solid	10.48	10.64		
6	$Ti(OEt)_2(meac)_2$ Isopropanol	2.59 0.86	$Ti(OPr^i)_2(meac)_2$ (2.60)	12.36	12.13	0.63	0.63
7	$Ti(OEt)_2(meac)_2$ *n*-butanol	2.24 0.91	$Ti(OBu^n)_2(meac)_2$ (2.30)	11.7	11.34	0.55	0.54
8	$Ti(OEt)_2(meac)_2$ *tert*-butanol	3.50 1.45	$Ti(OBu^t)_2(meac)_2$ (3.91)	11.39	11.34	0.81	0.85
9	$Ti(OPr^i)_2(meac)_2$ *n*-butanol	2.97 1.14	$Ti(OBu^n)_2(meac)_2$ (3.15)	11.29	11.34		

TABLE III

MOLECULAR WEIGHTS OF COMPOUNDS IN 15 ml BENZENE

Compound	Amount of substance used (g)	Observed mol. wt.		Av. mol. wt.	Calc. mol. wt.
$Ti(OEt)_2(meac)_2$	0.2124–0.7265	437.2, 425.3, 423.5	440.1, 430.6,	431.5	368.0
$Ti(OPr^i)_2(meac)_2$	0.1749–0.8286	409.2, 412.2, 399.8	413.9, 404.2,	407.8	396.0
$Ti(OBu^n)_2(meac)_2$	0.1920–1.0307	449.5, 454.2, 455.6	446.2, 457.8,	452.6	424.0
$Ti(OEt)_3(meac)$	0.1356–0.4182	359.6, 369.9	365.8,	365.1	298.0
$Ti(OPr^i)_3(meac)$	0.0801–0.3036	345.0, 347.8,	348.4, 374.4	353.9	340.0

Reaction between titanium dialkoxy di-methyl acetoacetate and higher alcohols in benzene

The higher alcohol was added to titanium dialkoxy dimethyl acetoacetate in benzene solution. No heat or colour change was observed. The mixture was refluxed and the azeotrope removed by fractionation. After cooling the solution, it was dried under reduced pressure. The compound obtained was analysed and the alcohol in the azeotrope was estimated. The results of the above reactions are given (6–9) in Table II.

REFERENCES

1 F. SCHMIDT, *Angew. Chem.*, 64 (1952) 536.
2 R. E. REEVES AND L. W. MAZZENO JR., *J. Am. Chem. Soc.*, 76 (1954) 2533.
3 A. YAMAMOTO AND S. KAMBARA, *J. Am. Chem. Soc.*, 79 (1957) 4344.
4 TOSHIO ISHINO AND SHINICHI MINAMI, *Tech. Repts. Osaka Univ.*, 7 (1957) 439.
5 I. D. VARMA AND R. C. MEHROTRA, *J. Chem. Soc.*, (1960) 2966.
6 D. C. BRADLEY, R. C. MEHROTRA AND W. WARDLAW, *J. Chem. Soc.*, (1952) 2027, 4204.
7 D. C. BRADLEY, R. C. MEHROTRA AND W. WARDLAW, *J. Chem. Soc.*, (1952) 5020.
8 D. C. BRADLEY, R. C. MEHROTRA, J. D. SWANWICK AND W. WARDLAW, *J. Chem. Soc.*, (1953) 2025.
9 D. M. PURI AND R. C. MEHROTRA, *J. Less-Common Metals*, 3 (1961) 247.
10 D. C. BRADLEY AND W. WARDLAW, *J. Chem. Soc.*, (1950) 3450.

GRAVIMETRIC DETERMINATION OF CERIUM(IV) AND ITS SEPARATION FROM RARE EARTHS USING 3-ACETYL-4-HYDROXYCOUMARIN

A. N. BHAT AND B. D. JAIN

Department of Chemistry, University of Delhi (India)

(Received March 1st, 1961)

SUMMARY

3-Acetyl-4-hydroxycoumarin has been used for the gravimetric determination of cerium(IV) between pH 4.0 and 8.5. Since the reagent does not form any complexes with other trivalent rare earths, estimations of ceric salts can be readily carried out even when these are present in large quantities.

A number of organic reagents[1-4] have been recommended for the gravimetric determination of cerium(IV), but there is none that can be used effectively for its separation from other trivalent rare earths. The iodate method[5] is generally used for the separation of cerium from other rare earths as well as for its determination, but it involves a large number of operations[6].

3-Acetyl-4-hydroxycoumarin has been used for the gravimetric determination of zirconium and titanium[7]. This reagent has also been employed for the separation and determination of uranium and thorium based on the marked difference in the solubility in ethanol of their complexes; it may be used in the presence of cerium(III) and lanthanum but the presence of cerium(IV) seriously interferes[8]. This led us to study the reaction of cerium(IV) ions with 3-acetyl-4-hydroxycoumarin. It has now been found that when an alcoholic solution of the coumarin is added to an aqueous solution of cerium (IV) salt, a pale yellow complex of cerium(IV)-3-acetyl-4-hydroxycoumarin is formed immediately. The metal ion is precipitated quantitatively between pH 4.0 and 8.5, and under these conditions quantities as low as 4.6 mg of CeO_2 have been estimated. Since the reagent does not form any complexes with the trivalent rare earths, it can be used for the estimation and separation of cerium(IV) from large quantities of lanthanum, yttrium and gadolinium, chosen as typical rare earths.

EXPERIMENTAL

Reagent

2% ethanolic solution of 3-acetyl-4-hydroxycoumarin, prepared as previously described[8] was used.

Metallic salts used were either of A.R. or Pro-analysi quality. Gadolinium nitrate solution was made by dissolving Gd_2O_3 (Johnson Mathey) in dil. nitric acid.

Dilute hydrochloric acid, ammonium acetate and ammonium hydroxide were used for adjustment of pH.

The pH measurements were made with a Beckmann pH-meter Model H 2 and a glass electrode.

Determination of cerium(IV) with 3-acetyl-4-hydroxycoumarin

To an aliquot solution (about 150 ml) of cerium(IV) ammonium nitrate (pH adjusted to 4.0–7.0) containing about 25 mg of CeO_2, 10 ml of 2% ethanolic solution of 3-acetyl-4-hydroxycoumarin was added slowly with constant stirring. A pale yellow precipitate of the cerium complex was produced. The precipitate was allowed to stand for about 10 minutes at room temperature. It was filtered through Whatman filter paper No. 42, dried and ignited to CeO_2. The results obtained are given in Table I.

TABLE I

Sample no.	*Wt. of CeO_2 taken (mg) (oxine method)*	*Wt. of CeO_2 found (mg) (using this reagent)*
1	4.60	4.60
2	8.25	8.25
3	8.70	8.70
4	13.80	13.75
5	16.95	17.00
6	25.20	25.25
7	26.10	26.00
8	41.40	41.40
9	82.50	82.55

Effect of pH on the formation of the ceric complex

The effect of pH on the precipitation of the complex was studied by using ammonium acetate–ammonium hydroxide for higher pH and dil. HCl for low pH. It was found that precipitation of the ceric complex starts at low pH and is complete only between pH 4.0 and 8.5 (Table II).

TABLE II

Wt. of CeO_2 taken = 16.95 mg

Wt of CeO_2 found (mg)	15.75	16.0	17.0	16.90	16.90	16.95	16.95
pH	2.50	3.00	4.0	5.0	6.0	7.0	8.5

Determination of cerium(IV) in the presence of the rare earths

Since the reagent does not form any complexes with the trivalent rare earths, the procedure for the determination of cerium(IV) in the presence of these is the same as for the determination of cerium(IV) alone. The precipitate of the ceric complex was thoroughly washed with water before final ignition. It has been found that ceric salts can be separated from large amounts of the rare earths as Tables III-V show.

TABLE III

ESTIMATION OF CERIUM(IV) IN PRESENCE OF LANTHANUM (pH 4.0–7.0)

Sample no.	*Wt. of CeO_2 taken (mg)*	*Wt. of La_2O_3 added (mg)*	*Wt. of CeO_2 found (mg)*
1	25.20	27.50	25.25
2	13.80	55.00	13.75
3	13.80	110.00	13.75
4	13.80	165.00	13.85
5	13.80	275.00	13.85
6	13.80	385.00	13.85

TABLE IV

ESTIMATION OF CERIUM(IV) IN PRESENCE OF YTTRIUM (pH 4.0–7.0)

Sample no.	*Wt. of CeO_2 taken (mg)*	*Wt. of Y_2O_3 added (mg)*	*Wt. of CeO_2 found (mg)*
1	13.80	20.0	13.80
2	13.80	40.00	13.80
3	13.80	80.0	13.85
4	13.80	160.0	13.80
5	13.80	200.0	13.75
6	13.80	240.0	13.85

TABLE V

ESTIMATION OF CERIUM(IV) IN PRESENCE OF GADOLINIUM (pH 4.0–7.0)

Sample no.	*Wt. of CeO_2 taken (mg)*	*Wt. of Gd_2O_3 added (mg)*	*Wt. of CeO_2 found (mg)*
1	13.80	106.00	13.75
2	13.80	209.30	13.80
3	13.80	307.50	13.85
4	13.80	433.45	13.85

ACKNOWLEDGEMENT

Authors are grateful to Prof. T. R. SESHADRI for his keen interest and helpful discussions, and to the Department of Atomic Energy, Govt. of India, for financial assistance.

REFERENCES

1 S. KRISHNA AND H. SINGH, *J. Am. Chem. Soc.*, 50 (1928) 792; *C.A.*, 22 (1928) 1325.
2 A. M. JEFFERSON, *J. Am. Chem. Soc.*, 24 (1902) 540.
3 T. PIRTEA, *Bull. chim. soc. roumaine chim.*, 39 (1937) 83; *C.A.*, 34 (1940) 2277.
4 B. D. JAIN AND S. P. SINGHAL, *J. Sci. Ind. Research, (India), 19B* (1960) 494.
5 P. H. M. P. BRINTON AND C. JAMES, *J. Am. Chem. Soc.*, 41 (1919) 1080.
6 W. R. SCHOELLER AND A. R. POWELL, *The Analysis of Minerals and Ores of the Rarer Elements*, 3rd edn., Charles Griffin & Co. Ltd., London, 1955, p. 101.
7 A. N. BHAT AND B. D. JAIN, *Proc. Indian Acad. Sci.*, 53 A (1961) 147.
8 A. N. BHAT AND B. D. JAIN, *Talanta*, 4 (1960) 13.

Short Communication

Polymeric hydrocyanic acid — a means for the separation of the salts of the noble metals

A detailed report on the polymerisation of hydrocyanic acid and the structure of the reaction products formed has been published recently[1]. According to this, the polymerisation follows an anionic mechanism through a dimer (iminoacetonitrile) to a polymer having the form of a chain which undergoes stabilisation by ring closure.

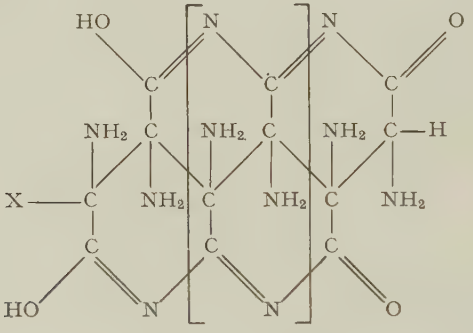

The observation of ZIMA that the insoluble polymer shows, to a high degree[2], the ability to add on salts of the noble metals as well as the fact that these salts can be eluted again[3] is of practical interest. ZIMA *et al.* have shown[4,5] that this reaction is typical for all high polymers containing $\rangle C{=}N$-groups.

The action of moderately concentrated solutions of silver or gold salts on polymeric hydrocyanic acid yields an uptake during a period of 24 h of 500–630 mg of silver and 650–2100 mg of gold respectively (based on noble metal)[1] per g of the polymer.

Fixation of salts of the noble metals does not follow a stoichiometric law but depends on the physical properties of the polymer and on whether it is easily wettable. It is not an ion-exchange mechanism since the pH-value of the solution treated remains unchanged. A rise in temperature causes the rate of addition to increase.

In practice the polymeric hydrocyanic acid is mostly used in a granulated form. The properties of the granulated material are such that heat, chemical agents, particularly mineral acids, as well as friction do not cause any decomposition. In this form the polymer may be used to fill ion-exchange columns and it may also be used in continuous processes producing salts of the noble metals. It is equally suitable for binding salts of the noble metals from concentrated as well as from strongly diluted solutions.

EXPERIMENTAL

A column (600 mm high, 26 mm diameter) was filled with 135 g of the granulated resin, the average diameter of the resin particles being 1–3 mm. A temperature of

50°C was maintained by circulating hot water through the heating mantle of the column. 1000 ml of a 1% solution of $H_2(PtCl/)$ in water was passed through the column during 280 min. Spectral analysis showed that the platinum content of the effluent was less than 10^{-5}%, an almost quantitative fixation of the noble metal having therefore been achieved.

Certain salts of the noble metals can be exchanged from the charged polymer by other stronger and faster binding ones. This phenomenon offers a possibility of employing polymeric hydrocyanic acid for the separation of mixtures of salts of the noble metals[6]. A crude separation of salts of the noble metals is also possible using uncharged granulated polymers.

In this case the polymer reacts preferably with the more strongly bound salt and thus the other salts in solution are correspondingly concentrated. In this way one can preferentially remove the salts of platinum from solutions of platinum and rhodium salts. By a similar procedure it is possible to enrich salts of palladium in a mixed solution of platinum and palladium salts.

Research Laboratory,
Röhm & Haas G.m.b.H.,
Darmstadt (West Germany)

TH. VÖLKER

[1] TH. VÖLKER, *Angew. Chem.*, 72 (1960) 379.
[2] H. ZIMA, *DBP 965,635* (1955), identical with *Brit. Pat. 813,202*, Röhm & Haas G.m.b.H., Darmstadt.
[3] H. ZIMA, *DBP 1,028,551* (1955), identical with *Brit. Pat. 824,6–1*, Röhm & Haas G.m.b.H., Darmstadt.
[4] TH. VÖLKER AND H. ZIMA, *DBP 1,020,320* (1956), identical with *Brit. Pat. 845,124*, Röhm & Haas G.m.b.H., Darmstadt.
[5] TH. VÖLKER, *DBP 1,069,130* (1958), Röhm & Haas G.m.b.H., Darmstadt.
[6] H. ZIMA, *DBP 1,053,482* (1957), Röhm & Haas G.m.b.H., Darmstadt; *cf.* also *Platinum Metals Rev.*, 4 (1960) 39.

Received February 6th, 1961

J. Less-Common Metals, 3 (1961) 262–263

Book Review

Atomic Theory for Students of Metallurgy, by WILLIAM HUME-ROTHERY, The Institute of Metals, London, 1960, 427 pages, £2 10s, $ 7.50.

This is a revised and considerably enlarged edition of the author's previous monograph bearing the same title which was published in 1946. During these past fourteen years considerable advances have been made in the field of nuclear physics and in other branches of the science with which this book is concerned, and the time was thus opportune for revision. The author has now produced a book that is a very worthy successor to the original volume and no doubt it will prove equally popular.

After dealing with the general background of atomic theory, the author elaborates and expands his subject until ultimately he is able to consider specific groups of metals. The intervening ground covers the structure of the free atom, assemblies of atoms, the free-electron theory of metals and the Brillouin zone theory of metals, and one is taken over it step by step with a clarity of exposition that is most commendable. The book is of course written by one who is a master of his subject. This is evident in the general excellence of the presentation of the data with which it abounds and in the care that has been bestowed on its planning. No other book treats the subject so appositely from the viewpoint of the student of metallurgy and no such student should be without it. It represents excellent value, and can be strongly recommended to all who may be interested in the fundamentals of metallurgy.

J.W.C.

J. Less-Common Metals, 3 (1961) 264

CONTENTS

Ammonolysis of molybdenum(V) chloride
by D. A. EDWARDS AND G. W. A. FOWLES (Southampton) 181

Bromide alkoxides of zirconium
by R. N. KAPOOR AND R. C. MEHROTRA (Gorakhpur, India) 188

Solid solubility of In_2Se_3 in some compounds of zinc blende structure
by J. C. WOOLLEY AND P. N. KEATING (Nottingham) 194

The thermal and electrical conductivities of zirconium and of some zirconium alloys
by R. W. POWELL AND R. P. TYE (Teddington, Middx.) 202

Hardening of molybdenum–zirconium alloy by nitride dispersions
by A. K. MUKHERJEE AND J. W. MARTIN (Oxford) 216

The solid solubility of tantalum in chromium
by J. H. AULD AND N. E. RYAN (Melbourne) 221

The thermal and electrical conductivity of titanium and its alloys
by R. W. POWELL AND R. P. TYE (Teddington, Middx.) 226

Scaling of chromium in a hot gas stream
by G. R. WILMS AND T. W. REA (Marybyrnong, Victoria, Australia) 234

Oxidation of uranium alloys in carbon dioxide and air
by J. E. ANTILL AND K. A. PEAKALL (Harwell, Berks.) 239

Derivatives of titanium with compounds having bidentate ligands.
I. Reactions of titanium tetrachloride
by D. M. PURI AND R. C. MEHROTRA (Gorakhpur, India) 247

II. Reactions of titanium alkoxides with methyl acetoacetate
by D. M. PURI AND R. C. MEHROTRA (Gorakhpur, India) 253

Gravimetric determination of cerium(IV) and its separation from rare earths using 3-acetyl-4-hydroxycoumarin
by A. N. BHAT AND B. D. JAIN (Delhi) 259

Short Communications

Polymeric hydrocyanic acid – a means for the separation of the salts of the noble metals
by TH. VÖLKER (Darmstadt, W. Germany) 262

Book Review 264

All rights reserved

ELSEVIER PUBLISHING COMPANY, AMSTERDAM

Printed in The Netherlands by

NEDERLANDSE BOEKDRUK INRICHTING N.V., 'S-HERTOGENBOSCH

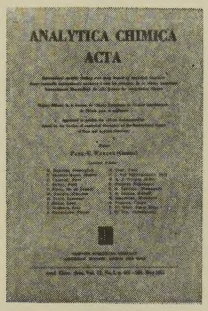

SOME ELSEVIER SCIENTIFIC JOURNALS

Analytica Chimica Acta

Journal of Chromatography

Journal of Electroanalytical Chemistry

Abstracts Section of the Journal of Electroanalytical Chemistry

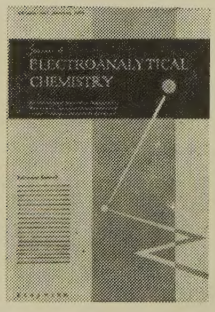

ICSU Review

Journal of the Less-Common Metals

Wear - Usure - Verschleiss

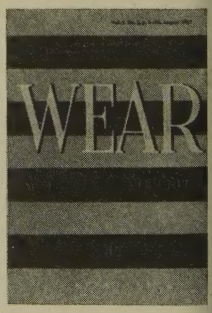

ELSEVIER PUBLISHING COMPANY

AMSTERDAM

221 E